

Journal Pre-proof

A diffusion-like process accommodates new crypts during clonal expansion in human colonic epithelium

Cora Olpe, Doran Khamis, Maria Chukanova, Nefeli Skoufou-Papoutsaki, Richard Kemp, Kate Marks, Cerys Tatton, Cecilia Lindskog, Anna Nicholson, Roxanne Brunton-Sim, Shalini Malhotra, Rogier ten Hoopen, Rachael Stanley, Douglas J. Winton, Edward Morrissey

PII: S0016-5085(21)00659-4
DOI: <https://doi.org/10.1053/j.gastro.2021.04.035>
Reference: YGAST 64292

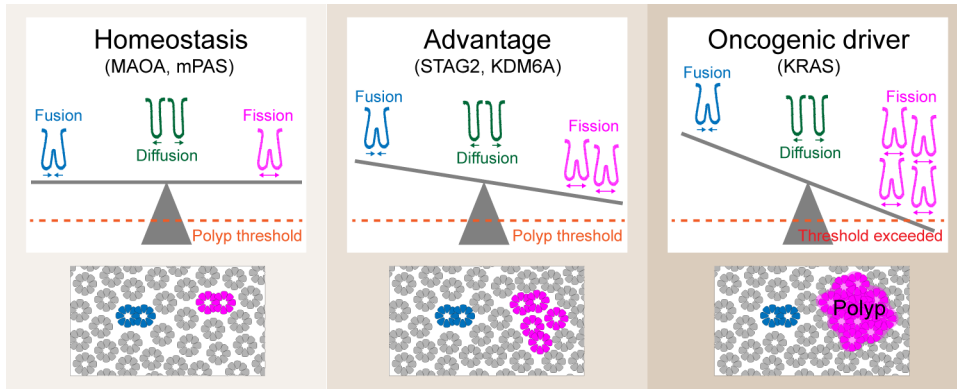
To appear in: *Gastroenterology*
Accepted Date: 13 April 2021

Please cite this article as: Olpe C, Khamis D, Chukanova M, Skoufou-Papoutsaki N, Kemp R, Marks K, Tatton C, Lindskog C, Nicholson A, Brunton-Sim R, Malhotra S, Hoopen Rt, Stanley R, Winton DJ, Morrissey E, A diffusion-like process accommodates new crypts during clonal expansion in human colonic epithelium, *Gastroenterology* (2021), doi: <https://doi.org/10.1053/j.gastro.2021.04.035>.

This is a PDF file of an article that has undergone enhancements after acceptance, such as the addition of a cover page and metadata, and formatting for readability, but it is not yet the definitive version of record. This version will undergo additional copyediting, typesetting and review before it is published in its final form, but we are providing this version to give early visibility of the article. Please note that, during the production process, errors may be discovered which could affect the content, and all legal disclaimers that apply to the journal pertain.

© 2021 by the AGA Institute





Journal Pre-proof

**Title: A diffusion-like process accommodates new crypts during clonal expansion
in human colonic epithelium**

Short title: Accommodation of new crypts by diffusion

Authors: Cora Olpe^{(1),1,2}, Doran Khamis^{(1),7}, Maria Chukanova¹, Nefeli Skoufou-Papoutsaki^{1,2}, Richard Kemp¹, Kate Marks⁴, Cerys Tatton¹, Cecilia Lindskog⁶, Anna Nicholson¹, Roxanne Brunton-Sim³, Shalini Malhotra⁵, Rogier ten Hoopen⁵, Rachael Stanley³, Douglas J Winton^{*1,2}, Edward Morrissey^{*7}

(1) These authors contributed equally.

¹Cancer Research-UK Cambridge Institute, Li Ka Shing Centre, Robinson Way, Cambridge, CB2 0RE, UK

²Wellcome Trust-Medical Research Council, Cambridge Stem Cell Institute, Cambridge, UK

³Norwich Research Park BioRepository. James Watson Road, Norwich, NR4 7UQ, UK

⁴Pathology & Data Analytics, Level 4, Wellcome Trust Brenner Building, St James's University Hospital, Beckett Street, Leeds, LS9 7TF, UK

⁵Department of Oncology, Box 231, University of Cambridge, Cambridge, CB2 2QQ, UK

⁶Department of Immunology, Genetics and Pathology, Science for Life Laboratory, Rudbeck Laboratory, Uppsala University, Uppsala, SE 751 85, Sweden

⁷MRC Weatherall Institute of Molecular Medicine, University of Oxford, John Radcliffe Hospital, Headington, Oxford OX3 9DS, UK.

Grant support: Wellcome Trust Grant (103805), Wellcome Trust PhD studentship (109141/Z/15/Z), MRC Computational Biology Fellowship (MC_UU_12025), CRUK Cambridge Institute core funding (A24456).

Abbreviations: ΔC_{fix} (slope of accumulation of fixed clones), C_{part} (frequency of partial clones), CRC (colorectal cancer), FFPE (formalin-fixed paraffin-embedded), FUF1 (crypt fusion or fission form), χ (contribution of mutant FUFIs to fusions), LCM (laser capture microdissection); MAF (mutant allele frequency), M/M (mutant/mutant), M/W (mutant/wild type), PPC (partially populated crypt), P_R (probability of replacement), WPC (wholly populated crypt)

Correspondence: *¹Doug Winton: doug.winton@cruk.cam.ac.uk, *⁷Edward Morrissey: edward.morrissey@imm.ox.ac.uk

Disclosures: The authors do not have any potential conflicts to declare.

Sequencing data: NCBI BioProject PRJNA449344

(<https://www.ncbi.nlm.nih.gov/bioproject/?term=PRJNA449344>)

Preprint server DOI: <https://doi.org/10.1101/2020.07.10.193748>

Author contributions: Conceptualisation: D.W & E.W.; Resources: C.L., R.B-S., R.S. S.M., K.M., R.t.H.; Methodology: D.K., CO., R.K., K.M.; Investigation: C.O., D.K., M.C., C.T., N.S-P.; Formal analysis: D.K., R.K., E.M., C.O.; Writing – original draft: C.O., D.W., D.K., E.M.; Writing – review & editing: C.O., D.W., D.K., R.t.H, N.S-P., A.N., E.W.

Acknowledgments

The authors thank the Biobanking, Histology and Genomics cores at the CRUK Cambridge Institute for technical support. The authors acknowledge the contribution and support to this project provided by the Norwich Research Park BioRepository (Human Tissue Authority licence number 11208) a facility supported by the BBSRC, the Norfolk and Norwich University Hospitals NHS Foundation Trust and the University of East Anglia. Equally, the authors acknowledge contribution and support provided by the Addenbrooke's Human Research Tissue Bank that is supported by the NIHR Cambridge Biomedical Research Centre.

Abstract

Background & Aims: Colorectal cancer (CRC) is thought to arise when the cumulative mutational burden within colonic crypts exceeds a certain threshold that leads to clonal expansion and ultimately neoplastic transformation. Therefore, quantification of the fixation and subsequent expansion of somatic mutations in normal epithelium is key to understanding colorectal cancer initiation. The aim of the present study was to understand how advantaged expansions can be accommodated in the human colon.

Methods: We used immunohistochemistry to visualise loss of the cancer driver KDM6A in formalin-fixed paraffin embedded (FFPE) normal human colonic epithelium. Using microscopy combined with neural network-based image analysis we determined the frequencies of KDM6A-mutant crypts as well as the expansion of clones into large areas by fission and fusion. We then used mathematical modelling to define the dynamics of fixation and expansion.

Results: Interpretation of the age-related behaviour of KDM6A-negative clones revealed significant competitive advantage in intra-crypt dynamics as well as a 5-fold increase in crypt fission rate. This was not accompanied by an increase in crypt fusion. Using mathematical modelling of crypt spacing we present evidence for a crypt diffusion process. We define the threshold fission rate at which diffusion fails to accommodate new crypts, which can be exceeded by KRAS activating mutations.

Conclusions: Advantaged gene mutations in KDM6A expand dramatically by crypt fission but not fusion. The crypt diffusion process enables accommodation of the additional crypts up to a threshold value, beyond which polyp growth may occur. The fission rate associated with *KRAS* mutations offers a potential explanation for *KRAS*-initiated polyps.

Keywords: colorectal cancer initiation; intestinal crypt; crypt fission; crypt fusion

Introduction

It is widely recognised that many renewing epithelia acquire a substantial burden of cancer driver mutations while remaining apparently normal¹⁻³. In the human colon, development of neoplastic disease is thought to be driven by elevated rates of gland replication or fission. Most notably loss of the tumour suppressor gene APC generates adenomas in this way⁴⁻⁷. Yet throughout life normal crypts also undergo crypt replication at a low rate, which can be elevated by advantaged mutations⁸⁻¹⁷.

There does not appear to be an increase in the net density of crypts, or of colonic epithelial area, with age¹⁸. This raises the question: how are local clonal expansions arising from elevated fission rates accommodated? One explanation might lie in crypt fusion. This process has recently been described and could counteract the consequences of fission^{19,20}. However, it remains unclear if fusion is an independent stochastic process or if it is locally co-regulated with fission. The latter possibility may be particularly relevant to pro-oncogenic mutations as fusions at the edge of mutant patches could enable effective local invasion of wildtype crypts with a high probability of subsequent displacement of wildtype cells.

KDM6A (UTX) is an X-linked gene encoding a histone demethylase that specifically targets di- and trimethyl groups on lysine 27 of histone H3. Inactivating mutations and deletions of *KDM6A* have been identified in a variety of human cancers including colon, bladder, prostate, oesophageal cancer²¹⁻²⁴. *KDM6A* featured among the 127 significantly mutated genes in The Cancer Genome Atlas study that analysed 3281 tumours derived from 12 cancer types²⁵. *KDM6A* mutations are infrequent in CRCs (<4% of all tumours, COSMIC database).

Here, in seeking additional cancer driver events that can be visualised as somatic clones, we identify loss of *KDM6A* as possessing advantage in both intra-crypt fixation and subsequent expansion. The large multicrypt clones resulting from elevated rates of crypt fission are investigated to study the impact of expansion on crypt packing and the role of crypt fusion in relieving overcrowding. The increased fission rate within *KDM6A*⁻ clones is not accompanied by an increase in crypt fusion, suggesting the two processes are driven by independent mechanisms and that fusion does not act to relieve local

overcrowding. Instead, it is demonstrated that new crypts generated by fission can be accommodated by localised crypt diffusion up to a threshold beyond which hyperplastic and neoplastic lesions may form.

Materials and Methods

Human tissue

Normal colon tissue samples were obtained from Addenbrooke's Hospital Cambridge and Norfolk and Norwich University Hospital under full local research ethical committee approval (Documents 15/WA/0131 & 17/EE/0265 and 06/Q0108/307 & 08/H0304/85, respectively) according to UK Home Office regulations. The study included 273 individuals aged 13–93 years. Colectomy specimens were fixed in 10% neutral buffered formalin. From areas without macroscopically visible disease mucosal sheets were removed and embedded *en face* in paraffin blocks. Sections were cut at 5 µm thickness onto charged glass slides.

Histochemistry

mPAS staining

This was performed as previously published²⁶.

Immunohistochemistry

Antibodies are listed in Table S1. For standard sections immunohistochemistry was performed as previously published²⁶. For laser capture microdissection (LCM) tissue was cut at 10 µm thickness onto UV-irradiated PEN membrane slides (ZEISS). Heat induced epitope retrieval was performed in citrate buffer in a water bath at 76 °C for 16 hours. Counterstaining with Mayer's Haematoxylin was performed manually for 15 seconds followed by blueing in tap water for 1 minute.

Experimental pathology

Data acquisition

Clones were scored by brightfield microscopy, followed by scanning of sections using a Leica Aperio AT2 scanner. The DeCryptICS image analysis tool developed by Edward Morrissey and Doran Khamis (<https://github.com/MorrisseyLab/DeCryptICS>) was used to count total number of crypts as well as Fusion

or Fission (FUFI) forms per section. This was followed by manual QC using QuPath²⁷ including classification of FUFIs into mutant/mutant (M/M), mutant/wildtype (M/W) or entirely wild type.

Quality control

Within the dataset two individuals aged 37 years with extreme average patch sizes were identified as outliers with respect to that measure and not included in subsequent analyses of patch sizes, fusion rates and newly generated crypts.

DNA extraction from FFPE tissue

LCM

Crypts were harvested into lids of 0.2 mm radius PCR tubes using a Leica LMD7000 Laser Microdissection System. 10 µl of Proteinase K solution from the Arcturus® PicoPure® DNA Extraction Kit (ThermoFisher) were added followed by lysis at 65 °C for 3 h and inactivation at 95 °C for 10 min.

Extraction from sections for KRAS sequencing

The QIAmp DNA FFPE Tissue Kit (QIAGEN) was used according to the supplier's protocol.

Library preparation and sequencing

Primers, PCR reaction components, cycling conditions and processing for amplification are described in tables S2-S6. Samples were barcoded using the Fast Start High Fidelity PCR System (Roche) according to the supplier's protocol. After pooling and purification by Clean & Concentrator Kit (Zymo Research) and size selection by PippinBlue (Sage Science), samples were sequenced using 150 bp paired-end sequencing with 10% PhiX in-house on the Illumina MiSeq platform.

Sequencing data analysis

Scripts are available under: <https://github.com/kemp05/>

KDM6A

Amplicons were extracted by starting, finishing and containing the expected sequence in the middle. Then, at every nucleotide position excluding the primer, the number of reads corresponding to the reference genome as well as those containing a base change were recorded. This enabled calculation of the noise at every position. Candidate mutations were identified when the mutant allele frequency (MAF)

was either >4x the mean of the noise at that position or >3.29 x the standard deviation at that position ($p \leq 0.001$). True mutations were called if present in all samples originating from the same patch in serial sections but absent in all wild-type samples from the same sections.

KRAS

Corresponding forward and reverse reads were combined using PANDAseq 2.11 with default options²⁸. Amplicons were extracted by beginning and ending with the expected primer sequence and correct overall length (+/- 3bp tolerance).

For codon 12 and 13 mutation calling, reads containing the sequences corresponding to wild type as well as all possible mutations (Table S8) were extracted. This yielded a MAF for every possible mutation in all four amplicons for every sample and revealed the noise. KRAS mutations were called if 1) >1000 reads were obtained for both KRAS amplicons and at least one mimic amplicon and 2) the MAF in both KRAS amplicons was > 0.1% (corresponding to at least 10 mutant reads) but found at background levels in the mimic amplicons. These criteria correspond to ≥ 1.96 standard deviations or a p-value of < 0.025 for the noisiest nucleotide position (G12D). The actual MAF for a particular mutation was calculated by subtracting the mean allele frequency (noise).

Mathematical modelling

Stem cell dynamics and crypt fission

The stem cell dynamics and fission rate associated with loss of KDM6A were mathematically modelled as previously described²⁶.

Crypt fusion and diffusion

Crypt fusion was modelled as a process parallel to fission, with the same duration. Therefore, the following applied:

$$\frac{\text{number of fission events}}{\text{number of fusion events}} \sim \frac{\text{fission rate}}{\text{fusion rate}}$$

All M/W FUFIs were considered fusions, but M/M FUFIs could be fissions or fusions. Therefore, the number of fission events and fusion events required for the above equation were not directly measurable. However, they were calculable by sampling FUFIs from the edge of mutant patches, which enabled calculation of the proportion of M/M FUFIs that are fusions (termed χ ; χ) by accounting for the

distribution of the mutational state of neighbouring crypts. (See supplemental materials for mathematical details.)

In order to infer a diffusion coefficient, growth of a patch through initial mutation and subsequent fissions was modelled as a stochastically firing point source of mass at the clone centroid. Potential trajectories from mutation hit to patch of size 10 (that is, stochastic event times) were simulated and an ensemble diffusion coefficient was inferred by randomly drawing paths from the set of simulated potential trajectories. The inferred diffusion coefficient was then used in a theoretical study of patch expansion. (See supplemental materials for mathematical details.)

KRAS expansion

The data obtained here was combined with our previously published dataset and analysed as described there²⁶.

Results

KDM6A-negative clones are advantaged in stem cell competition

We have previously used visualisation of loss of X-linked genes as clonal marks to quantify human colonic stem cell dynamics²⁶. In attempting to expand this methodology to X-linked genes with cancer association, clonal loss of KDM6A was identified by immunohistochemistry with two independent antibodies on normal human colonic epithelia (Figure S1A & B). Intra-crypt dynamics that describe the accumulation of clones comprising wholly populating entire crypts (WPC) from partly populated (PPC) transition forms were determined for KDM6A⁻ clones using colonic FFPE sections from 120 patients aged 21–93 as previously described²⁶ (Figure 1A & B). This revealed that loss of KDM6A confers a competitive advantage to affected stem cells shown as a decrease in the fraction of PPC supporting the accumulation of WPC (Figure 1C).

KDM6A-negative clones expand by 5-fold increased crypt fission

KDM6A⁻ crypts remain rare across ages, supporting their clonal origin. Expansion of individual KDM6A⁻ clones was recognisable as large patches that frequently exceeded 10 crypts (Figure 1D). To further

confirm the clonal origin of such patches, we used laser capture microdissection followed by targeted sequencing that covered 3.6 kb of exonic and flanking intronic sequence of *KDM6A* (24 amplicons), including sites frequently mutated in human cancers. No patch was found to carry more than one *KDM6A* mutation and mutant allele frequencies were in line with predictions from patient sex and stromal content, supporting clonality (Figure 1E, Figure S1C-E & Table S7).

The age-related size distribution of multicrypt clones was analysed to infer the fission rate associated with *KDM6A* loss and compare it to those previously described for neutral (MAOA and mPAS) and advantaged clonal marks (STAG2)²⁶. This revealed an age-related increase in the frequency of large clones (≥ 10 crypts/patch) for STAG2⁻ and *KDM6A*⁻ but not for neutral marks (Figure 2A). Loss of *KDM6A* generates a higher proportion of large patches than the other clonal marks while STAG2 loss results in more clones due to a higher event rate (Figure 2B and C). From these patch size distributions, the crypt fission rate associated with loss of *KDM6A* was calculated to be 3.6% per year (95% CI: 3.2-4.1), approximately 5-fold higher than the background homeostatic rate previously derived from neutral clonal marks (Figure 2D). Consequently, in individuals over 80 years of age 13.5% of *KDM6A*⁻ clones are found as patches comprising more than 5 crypts compared to 4.8% for STAG2, 1.7% for mPAS and 0.8% for MAOA.

***KDM6A*⁻ and STAG2⁻ patches lack significant local overcrowding**

Expanding clones are more likely to undergo additional fissions as the probability scales with the number of crypts present. Consequently, the interval between fissions decreases rapidly with increasing patch size. For example, mathematical modelling of the expansion of *KDM6A*⁻ crypts indicates the median time taken to grow from 1 to 2 crypts is 19 years, but only 2 years to grow from 10 to 11 (Figure 2E). Therefore, recently formed larger patches might be expected to demonstrate overcrowding.

To test if larger patches are more densely packed, the area occupied by crypts and their surrounding stroma was determined for 24 STAG2⁻ and 20 *KDM6A*⁻ clones containing ten crypts, the largest size for which sufficient data could be obtained (Figure 2F and G). The fraction of each patch occupied by stroma

was then calculated. Adjacent to each mutant clone three random groups of 10 crypts were defined as control 'patches' and similarly analysed (totalling 72 control patches for STAG2 and 60 control patches for KDM6A). Comparing the fraction of each patch occupied by stroma to adjacent wildtype groupings indicated a slight trend towards increased packing density for STAG2⁻ as well as KDM6A⁻ crypts that failed to reach significance (Figure 2G). Considering that a lack of overcrowding may stem from a decrease in crypt size, the areas of crypts were measured. This revealed that KDM6A⁻ crypt sections are around x1.3 the size of adjacent wildtype crypts (p-value <0.001) (Figure S2). No difference was found between STAG2⁻ crypts and their wildtype neighbours (Figure S2). Therefore, lack of overcrowding cannot be attributed to reduced crypt size for either STAG2 or KDM6A loss. We also considered the possibility of accommodation of clonal expansions by 'squashing' of neighbouring crypts. However, analysis of crypt eccentricities provided no evidence for the predicted flattening of crypt architecture that would result (Figures S3-S5).

Together these observations suggest that crypts even within relatively recent clonal expansions avoid overcrowding to largely achieve ambient density.

Evidence for crypt fusion

The lack of overcrowding in KDM6A⁻ clones suggests a mechanism counteracting the localised increase in fission. An opposing process of crypt fusion has been recognised in mouse intestine¹⁹. A homeostatic human fusion rate has been estimated by assuming equivalence in the rate of both fission and fusion²⁰. On a tissue wide basis such a balance of rates could act to maintain constant crypt density. However, local advantaged expansions can only be balanced if fission and fusion are locally coordinated.

We first sought confirmation that fusion occurs. The evidence in human epithelium is based on identification of branched crypts within which clonal loss of mitochondrial CCO activity is restricted to one branch. These are interpreted as transition intermediates in an active fusion process²⁰. Analysis of *en face* tissue sections stained to visualise mPAS positivity confirmed the existence of rare heterotypic branched forms in normal human colonic epithelium. Analysis of over 2×10^6 crypts in sections from 80

individuals containing mPAS⁺ clones identified 32 candidate mPAS⁺ branched forms that were either mixed (mutant and wild type, M/W) or fully mutant (M/M) (Figure 3A). Of the 13 M/W forms the positive epithelium was always restricted to one branch.

An alternative interpretation is that branched crypts are intermediate fission forms whereby heterotypic staining arises due to mutations occurring or segregating into a single branch (Figure 3B). We formally considered this possibility using the fusion duration estimate derived by Baker and colleagues as well as our previous estimates of *de novo* mutation probability and clone fixation rates that together determine the frequency of monoclonal crypts present in individuals of different age²⁶. Within the relatively small number of branched crypts present none are predicted to contain monoclonal crypt branches by either mechanism (Figure 3C). This suggests that heterotypic forms represent genuine intermediates in an active fusion process. Since the bulk of branched crypts are unstained and can represent intermediates in either fusion or fission we propose the agnostic term FUFIs (Fusion or Fission) to describe these transition forms (Figure S6).

Crypt fusion and fission are regulated independently

To calculate crypt fusion rates heterotypic and homotypic FUFIs were also evaluated for STAG2 and KDM6A loss by scoring around 3.9×10^6 and 1.8×10^6 crypts from 53 and 102 individuals, respectively. In total, over 28,000 FUFIs were evaluated. This identified 151 and 63 FUFIs with STAG2 (18,928 clones analysed) and KDM6A loss (5,353 clones analysed) respectively (Figure 3D). These could be found as single events or within multicrypt clones (Figure 3E).

Assuming equal duration for fission and fusion (i.e. the time window during which FUFIs are detectable), the fusion rate is accessible by proportionality. Specifically, the ratio of the frequency of observed fission FUFIs to the fission rate (independently calculated from the patch size distribution) would equal the ratio of the frequency of observed fusion FUFIs to the fusion rate. However, while all M/W FUFIs are considered fusions, M/M FUFIs can be either fissions or fusions. Therefore, to exploit this proportionality, the relative contribution of M/M FUFIs events to the total number of fusions (termed chi; χ) needs to be

determined. The value for χ is calculable on the basis that M/M FUFIs have a probability of being a fusion event that depends on the number of M and W neighbours present at the onset of the event. Therefore, the status of crypts neighbouring FUFIs at the patch border of multicrypt clones were scored as W or M (totalling 4, 121 and 49 for mPAS, STAG2 and KDM6A, respectively) (Figure 3 F and G). Single FUFIs had W neighbours only. Averaging the M and W neighbours of M/M FUFIs revealed χ to be 0.03 for mPAS. As neutral marks such as mPAS generate mostly small clones, most fusion events are W/M leading to low values of χ . At the edge of larger expansions generated by advantaged marks, M/M fusions occur more readily. Correspondingly the χ values for STAG2 and KDM6A are 0.26 and 0.35, respectively (Figure 3H). Rates of fusion using these values of χ were then estimated using the proportionality described above (see supplemental information for details).

This analysis indicates similar crypt fusion rates for mPAS, STAG2 and KDM6A of 0.3% per year (95% CI: 0.1-0.6), 0.4% (95% CI: 0.3-0.7) and 0.7% (95% CI 0.3-1.4) (Figure 3I). Comparison of mPAS fission (0.7% per year; 95% CI: 0.5-0.9) and fusion rates show that these closely correspond. This suggests that in homeostasis the rates of the two processes are balanced and will act together to maintain constant crypt numbers across the tissue as has been suggested previously²⁰. However, for mutations causing elevated fission rates there appears to be no evidence for a compensatory increase of the fusion rate. These analyses suggest that fission and fusion are independent processes and not coordinately regulated.

Crypt diffusion accommodates new crypts throughout life

A striking feature of larger patches is that mutant crypts have over decades populated the territory initially occupied by multiple independent crypts without a significant increase in crypt density. In the absence of appreciable crypt fusion this suggests local adjustments to disperse crypts from the growing focus. With this rationale we considered the possibility of random crypt movement in the form of a diffusion process.

In the colonic epithelium it is the crypts that are being diffused in the 'space' of the surrounding stroma (Figure 4A). The diffusion coefficient (change in area per unit time) can be estimated based on crypt packing (measured in terms of crypt area per unit area of mucosa) and consideration of all possible sequences of fission events generating a patch of 10 mutant crypts, constrained by the patient age and calculated using the mutation and fission rates.

To find evidence supporting a diffusion type process we revisited the STAG2- and KDM6A-negative patches of ten crypts and surrounding control patches. For each mutant clone (24 for STAG2 and 20 for KDM6A) and the corresponding three arbitrary control groups of ten adjacent wildtype crypts, each crypt was spatially mapped in X/Y coordinates. Total patch areas were divided in crypt domains that were defined as the area occupied by a crypt and its share of surrounding stroma (Figure 4B). Areas of individual crypts as well as total patch area were measured and the distance between mutant clones and wild type patch centroids, r , was determined (Figure 4C).

Using known mutation and fission rates the potential trajectories from initial mutation to ten-crypt mutant clones were simulated and the most likely trajectories were used to calculate the age of the clone (Figures S7 and S8). The diffusion coefficient was inferred to define an overall tissue process that best fits the differences in stromal densities between mutant and control patches. It describes how the burden of decreased stromal fraction resulting from a mutant clone is dispersed into the surrounding tissue over time. For older clones we expect the system to be close to the ambient density while for younger clones the perturbation to the local stromal fraction may still be evident. Examples of both presumptive young and old clones were readily detectable in our samples (Figure 4D and Figures S9 and S10).

For a subset of 7 patches (4 for KDM6A, 3 for STAG2) a more detailed rolling window analysis was performed in which the above approach was applied but where fields of ten crypts were moved outwards from the mutant clone. Again, evidence of a reduction in stromal fraction consistent with perturbation in younger clones was observed (Figure 4E and Figures S9 and S10). The diffusion coefficient was found to be 1.05 crypt domain areas/year (95% CI: 0.339 – 9.70) (Figure 4F). Reassuringly, testing a null

hypothesis, that there is no diffusion-type process and therefore no radial dependence in crypt packing, by considering neighbourhood ambient densities of crypts across all patches (mutant, wildtype or mixed), generated a significantly worse fit than the experimental comparisons (Figure S11). Of note this confirmation of radial dependence in packing argues against other possible alleviators of crypt density such as changes in the size or shape of crypts within mutant clones.

The inferred diffusion process can be used to define the number of crypt domains impacted to accommodate a new clonal expansion. For example, the model suggests that patches of ten KDM6A⁻ crypts would require 264 crypt domains to undergo a 1% reduction in their spacing, while a 5% reduction would only require 53 crypt domains (Figure 4G, H).

Defining a homeostatic threshold

Limited evidence suggests that there are no significant age-related changes in colon length and crypt density¹⁸. With respect just to STAG2 and KDM6A mutations the relatively few new crypts arising during life could be easily accommodated by crypt movement. By the time individuals exceed 75 years of age, for every 10⁵ crypts, fission has added only approximately 200 and 290 new STAG2⁻ and KDM6A⁻ crypts, respectively (Figure 4I). However, it seems highly probable that additional genetic variants will also promote fission to different degrees. The potential for diffusion to locally balance this process as fission rate increases was investigated.

Simulations were performed escalating the homeostatic fission rate of 0.7% per year (Figure S12). When fission rates remain below approximately 12-fold that of homeostasis, diffusion can generate enough space to accommodate newly generated crypts (Figure 4J). Higher fission rates result in a proportion of clones reaching a threshold of maximum packing density within which crypts are directly touching. This suggests a potential boundary for polyp growth, that is dependent on the physical processes of fission and diffusion. We have previously used targeted sequencing of FFPE sections to infer the effect of KRAS activating mutations on crypt fission²⁶. Here, in expanding on that initial dataset (see methods) KRAS activating mutations were found in 35 (22 new) of 256 individuals (130 new) in the age range 20-91 years,

corresponding to 13.7% of the cohort (Figure S13). Mutant allele frequencies in the range of 0.12% - 2.35% combined with total crypt numbers per section enabled estimation of clone size (Figure S13). Subsequent mathematical inference indicates that a 17-fold increase in crypt fission rate to 12% (95% CI: 10.8-13.7) per year best fits with the data. Around 1% of *KRAS* activating mutations are predicted to breach the threshold for lesion growth after 50 years (Figure 4J). A therapeutic intervention inhibiting crypt fission for any 10 years could reduce this to approximately 0.01% (Figure 4K).

Discussion

Several studies have identified large mutant expansions in seemingly normal epithelia^{1,2,26}. In the adult colon this occurs by increased crypt fission rate, whereby biased mutations can generate large clones that are appropriately distributed within the tissue²⁶. In contrast, elevated glandular fission rates are also known to drive the overgrowth of adenomas and CRCs suggesting that differences in the rate of fission or the response to it must differ between normal and neoplastic tissues⁴⁻⁷.

In considering the epithelial responses that compensate for elevated fission rates we first validated a new advantaged clonal mark, KDM6A that together with STAG2 provided two gene-specific assays with 5- and 3-fold increased fission rates respectively. Comparing the configuration of the size and frequency of clones for the two genes demonstrates the different strategies by which age-related mutational burden can be achieved. STAG2 has the higher mutation rate and generates many relatively small clones while KDM6A generates fewer but larger expansions. A corollary of the exponential growth of patches as their size increases is that larger patches will tend to be the most recent and therefore most likely to contain evidence of local adaptation to accommodate new crypts.

The recently recognised process of crypt fusion offers a potential mechanism to compensate for fission¹⁹. Occurring at equal rates in homeostasis they could effectively balance crypt numbers on a population basis²⁰. In considering fusion as a mechanism to accommodate new crypts, a baseline estimate was first established here and found to approximate that for fission. However, no upregulation of fusion

accompanying the local expansions resulting from STAG2 and KDM6A mutation was found. Conceivably other mutations may impact fusion to ease local packing but it does not appear necessary to do so.

Multicrypt clones that form over decades populate the territory previously occupied by multiple independent crypts. Aiming to understand this dispersal we sought and found evidence of a diffusion-type process in a subset of clones. These are consistent with a recent expansion 'caught in the act' of being restored to an ambient crypt density. The behaviour captured probably reflects a passive dispersal mechanism rather than actual diffusion and must be accompanied by some level of stromal turnover.

The diffusion coefficient defines the rate of movement of crypt domains and the size of the larger impacted zone that is required to absorb new crypts. Parameterising the process allows testing of the robustness of the tissue to deal with localised accelerated growth conferred by biased mutations. From this analysis the homeostatic dispersal mechanism seems able to accommodate increased fission rates of more than 10-fold above baseline. Even for mutations that generate higher crypt fission rates only the fastest growing clones would overgrow the available space. For example, around 5% of clones carrying a gene mutation that confers a 19-fold increase in fission rate would reach a threshold where they lack a stromal domain between crypts and overgrow the available space after 50 years.

The actual threshold at which clonal expansions become recognisable as pathologies may be lower than the extreme one applied here. However, the implication remains that the distinction between phenotypically normal clones and those forming overt pathologies may be determined solely by a probabilistic process in which a recent succession of fission events overwhelms homeostatic dispersal mechanisms.

Activating mutations of KRAS have been described in normal colonic epithelium. The revised estimate of a 17-fold increase for the fission rate conferred by KRAS activating mutations is higher than that previously inferred (10-fold) and is based on analysis of many more patients²⁶. It is intriguing that activating mutations of KRAS breach the extreme threshold defined here. KRAS is commonly mutated in

a broad spectrum of benign and premalignant pathologies such as serrated lesions and adenomas that may arise at least in part due to the dispersal threshold being reached²⁹⁻³³.

These findings have clinical significance with respect to bowel cancer screening programmes with the implication that clonal expansions with a high malignant potential are not all contained within visible lesions such as sessile serrated adenomas despite having a comparable tissue footprint. Further, it is known that a proportion of adenomas spontaneously regress when observed in longitudinal studies³⁴⁻³⁶. One plausible explanation for such phenomena is that these lesions first develop due to reaching the threshold resulting in local overcrowding but are transient because of ongoing crypt dispersal.

Loss of function mutations affecting the APC tumour suppressor gene are also initiated and expanded by glandular fission⁴⁻⁷. Mutation of both APC and KRAS is frequent in CRCs. The two pathways are known to interact at the molecular level³⁷. It is likely their combined activation will also synergise to further elevate gland fission rate and promote overgrowth as fully neoplastic CRCs develop.

Obesity, a known risk factor for CRC, is known to be accompanied by increased crypt fission rate³⁸. Furthermore, diets deficient for methyl donors are known to reduce crypt fission rates in the mouse³⁹. An implication of the colon having the capacity to absorb many more new crypts is that modest time limited reductions in fission rates may not only slow the growth of lesions but prevent them from forming at all.

References

1. Martincorena, I., Roshan, A., Gerstung, M., *et al.* Tumor evolution. High burden and pervasive positive selection of somatic mutations in normal human skin. *Science* **348**, 880–886 (2015).
2. **Martincorena, I., Fowler, J. C., Wabik, A., *et al.*** Somatic mutant clones colonize the human esophagus with age. *Science* **362**, 911–917 (2018).
3. Lee-Six, H., Olafsson, S., Ellis, P., *et al.* The landscape of somatic mutation in normal colorectal epithelial cells. *Nature* **574**, 532–537 (2019).
4. Wasan, H. S., Park, H.-S., Liu, K. C., *et al.* APC in the regulation of intestinal crypt fission. *J. Pathol.* **185**, 246–255 (1998).
5. Wong, W.-M., Mandir, N., Goodlad, R. A., *et al.* Histogenesis of human colorectal adenomas and hyperplastic polyps: the role of cell proliferation and crypt fission. *Gut* **50**, 212 LP – 217 (2002).
6. Preston, S. L., Wong, W.-M., Chan, A. O.-O., *et al.* Bottom-up Histogenesis of Colorectal Adenomas. *Cancer Res.* **63**, 3819–3825 (2003).
7. van den Brink, G. R. & Offerhaus, G. J. The morphogenetic code and colon cancer development. *Cancer Cell* **11**, 109–117 (2007).
8. Kim, K.-M. & Shibata, D. Methylation reveals a niche: stem cell succession in human colon crypts. *Oncogene* **21**, 5441–5449 (2002).
9. Kim, K.-M. & Shibata, D. Tracing ancestry with methylation patterns: most crypts

- appear distantly related in normal adult human colon. *BMC Gastroenterol.* **4**, 8 (2004).
10. **Greaves, L. C., Preston, S. L.,** Tadrous, P. J., *et al.* Mitochondrial DNA mutations are established in human colonic stem cells, and mutated clones expand by crypt fission. *Proc. Natl. Acad. Sci. U. S. A.* **103**, 714–719 (2006).
 11. Clarke, R. M. The effect of growth and of fasting on the number of villi and crypts in the small intestine of the albino rat. *J. Anat.* **112**, 27–33 (1972).
 12. Cairnie, A. B. & Millen, B. H. Fission of crypts in the small intestine of the irradiated mouse. *Cell Tissue Kinet.* **8**, 189–96 (1975).
 13. Maskens, A. Histogenesis of colon glands during postnatal growth. *Acta Anat (Basel).* **100**, 17–26 (1978).
 14. Maskens, A. P. & Duhardin-Loits, R. M. Kinetics of tissue proliferation in colorectal mucosa during post-natal growth. *Cell Tissue Kinet.* **14**, 467–77 (1981).
 15. Wright, N. A. & Al-Nafussi, A. The kinetics of villus cell populations in the mouse small intestine. II. Studies on growth control after death of proliferative cells induced by cytosine arabinoside, with special reference to negative feedback mechanisms. *Cell Tissue Kinet.* **15**, 611–21 (1982).
 16. Cheng, H., McCulloch, C. & Bjerknes, M. Effects of 30% intestinal resection on whole population cell kinetics of mouse intestinal epithelium. *Anat. Rec.* **215**, 35–41 (1986).
 17. Clair, W. H. S. & Osborne, J. W. Crypt fission in the small intestine of the rat. *Br. J. Cancer. Suppl.* **7**, 39–41 (1986).
 18. Hounnou, G., Destrieux, C., Desme, J., *et al.* Anatomical study of the length of the

- human intestine. *Surg. Radiol. Anat.* **24**, 290–294 (2002).
19. Bruens, L., Ellenbroek, S. I. J., van Rheenen, J., *et al.* In Vivo Imaging Reveals Existence of Crypt Fission and Fusion in Adult Mouse Intestine. *Gastroenterology* **153**, 674-677.e3 (2017).
 20. Baker, A.-M., Gabbutt, C., Williams, M. J., *et al.* Crypt fusion as a homeostatic mechanism in the human colon. *Gut* **68**, 1986–1993 (2019).
 21. Zhou, Z., Zhang, H.-S., Liu, Y., *et al.* Loss of TET1 facilitates DLD1 colon cancer cell migration via H3K27me3-mediated down-regulation of E-cadherin. *J. Cell. Physiol.* **233**, 1359–1369 (2018).
 22. Nickerson, M. L., Dancik, G. M., Im, K. M., *et al.* Concurrent alterations in TERT, KDM6A, and the BRCA pathway in bladder cancer. *Clin. cancer Res. an Off. J. Am. Assoc. Cancer Res.* **20**, 4935–4948 (2014).
 23. **Suvà, M. L., Riggi, N. & Bernstein, B. E.** Epigenetic reprogramming in cancer. *Science* **339**, 1567–1570 (2013).
 24. **van Haften, G., Dalglish, G. L., Davies, H., et al.** Somatic mutations of the histone H3K27 demethylase gene UTX in human cancer. *Nat. Genet.* **41**, 521–523 (2009).
 25. Kandoth, C., McLellan, M. D., Vandin, F., *et al.* Mutational landscape and significance across 12 major cancer types. *Nature* **502**, 333–339 (2013).
 26. Nicholson, A. M., Olpe, C., Hoyle, A., *et al.* Fixation and Spread of Somatic Mutations in Adult Human Colonic Epithelium. *Cell Stem Cell* **22**, 909-918.e8 (2018).
 27. Bankhead, P., Loughrey, M. B., Fernández, J. A., *et al.* QuPath: Open source

- software for digital pathology image analysis. *Sci. Rep.* **7**, 16878 (2017).
28. Masella, A. P., Bartram, A. K., Truszkowski, J. M., *et al.* PANDAseq: paired-end assembler for illumina sequences. *BMC Bioinformatics* **13**, 31 (2012).
 29. Zauber, P., Marotta, S. & Sabbath-Solitare, M. KRAS gene mutations are more common in colorectal villous adenomas and in situ carcinomas than in carcinomas. *Int. J. Mol. Epidemiol. Genet.* **4**, 1–10 (2013).
 30. Juárez, M., Egoavil, C., Rodríguez-Soler, M., *et al.* KRAS and BRAF somatic mutations in colonic polyps and the risk of metachronous neoplasia. *PLoS One* **12**, e0184937 (2017).
 31. Hashimoto, T., Tanaka, Y., Ogawa, R., *et al.* Superficially serrated adenoma: a proposal for a novel subtype of colorectal serrated lesion. *Mod. Pathol.* **31**, 1588–1598 (2018).
 32. McCarthy, A. J., Serra, S. & Chetty, R. Traditional serrated adenoma: an overview of pathology and emphasis on molecular pathogenesis. *BMJ open Gastroenterol.* **6**, e000317–e000317 (2019).
 33. De Palma, F. D. E., D'Argenio, V., Pol, J., *et al.* The Molecular Hallmarks of the Serrated Pathway in Colorectal Cancer. *Cancers (Basel)*. **11**, (2019).
 34. Knoernschild, H. Growth rate and malignant potential of colonic polyps: Early results. *Surg. Forum* **14**, 137–138 (1963).
 35. Hoff, G., Foerster, A., Vatn, M. H., *et al.* Epidemiology of Polyps in the Rectum and Colon: Recovery and Evaluation of Unresected Polyps 2 Years after Detection. *Scand. J. Gastroenterol.* **21**, 853–862 (1986).
 36. Loeve, F., Boer, R., Zauber, A. G., *et al.* National Polyp Study data: evidence for

- regression of adenomas. *Int. J. cancer* **111**, 633–639 (2004).
37. Jeong, W.-J., Ro, E. J. & Choi, K.-Y. Interaction between Wnt/ β -catenin and RAS-ERK pathways and an anti-cancer strategy via degradations of β -catenin and RAS by targeting the Wnt/ β -catenin pathway. *npj Precis. Oncol.* **2**, 5 (2018).
38. Sainsbury, A., Goodlad, R. A., Perry, S. L., *et al.* Increased Colorectal Epithelial Cell Proliferation and Crypt Fission Associated with Obesity and Roux-en-Y Gastric Bypass. *Cancer Epidemiol. Biomarkers Prev.* **17**, 1401–1410 (2008).
39. Hanley, M. P., Kadaveru, K., Perret, C., *et al.* Dietary Methyl Donor Depletion Suppresses Intestinal Adenoma Development. *Cancer Prev. Res.* **9**, 812–820 (2016).

Author names in bold designate shared co-first authorship.

Figure legends

Figure 1. Detection of clonal loss of KDM6A in normal human colon

(A) Representative images of KDM6A⁻ WPC (i) and PPC (ii). (B) Top panel: Frequency plot showing age-related behaviours of KDM6A⁻ WPC (circles, darker) and PPC (squares, lighter). Red line: regression analysis showing accumulation of WPC (ΔC_{fix} : 6.04×10^{-6} per year) and 95% CI in grey. Bottom panel: PPC only on expanded y-axis. (C) Plot showing increased ratio of $\Delta C_{fix}/C_{part}$ for KDM6A (0.23, 95% CI: 0.16–0.34) as compared to the neutral marks mPAS and MAOA (replotted from²⁶). Error bars = 95% CI. (D) Representative image of large KDM6A⁻ multicrypt patch highlighted by dashed line. (E) KDM6A cDNA structure annotated with sequenced areas (yellow), mutations found in COSMIC and mutations identified in KDM6A⁻ patches (red).

Figure 2. KDM6A⁻ patches lack significant overcrowding despite increased fission

(A) Plot showing mean frequency of large (≥ 10 crypts) patches for age groups shown. (B) Histogram showing the frequency of different patch sizes for mPAS, MAOA, KDM6A and STAG2 across all ages. Inset shows patch size ≥ 2 crypts on expanded y-axis. (C) Dot plot of mean clone frequency plotted against mean average patch size for multicrypt clones in age groups shown for mPAS, MAOA, STAG2 and KDM6A. (D) Plot showing inferred fission rate/crypt/year for KDM6A compared to mPAS, MAOA and STAG2 (data replotted from²⁶). Error bars = 95% CI. (E) Simulation data showing the time in years taken for transitions between patch sizes 1-2 and 10-11 for (i) mPAS, (ii) STAG2 and (iii) KDM6A. Insets show 10-11 transition on expanded y-axis. (F) Image showing patch selection for assessment of crypt packing density within KDM6A⁻ (blue) and adjacent wildtype crypts (brown). Inset indicates placement of borders between crypts. (G) Dot plots showing stromal fraction for STAG2⁻ and KDM6A⁻ and adjacent wildtype patches comprising 10 crypts.

Figure 3. Crypt fission and fusion are independently regulated processes

(A) Schematic and representative mPAS-stained images of three types of fusion or fission forms. (B) Schematic representation of alternative origins of M/W forms. Hypothesis 1 (Hyp1): stem cell mutation in

one branch of intermediate fission form followed by monoclonal conversion. Hypothesis 2 (Hyp 2): fission of a pre-existing partially populated crypt with segregation of mutant and wild type epithelium into each branch, followed by monoclonal conversion. (C) Comparison of M/W event frequencies simulated for hypotheses described in (B) and the observed frequency. Error bars = 95% CI. (D) Bar graphs showing numbers of FUFIs scored for (i) mPAS, (ii) STAG2, (iii) KDM6A. (E) Representative images of FUFIs at patch borders: (i) KDM6A M/M FUFIs, (ii) STAG2 M/W FUFIs. Insets show enlarged FUFIs. (F) Schematic showing scoring of FUFIs neighbours used for calculation of χ . (G) Dot plot showing neighbouring crypt status of patch border FUFIs (M/M or M/W) for mPAS, STAG2 and KDM6A. Each dot represents one or more FUFIs for which neighbours were scored. (H) Plot comparing the value of χ for mPAS, STAG2 and KDM6A. (I) Plot comparing the derived fission and fusion rates for mPAS, STAG2 and KDM6A. mPAS and STAG2 fission rates correspond to data from²⁶, replotted. Error bars = 95% CI.

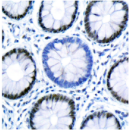
Figure 4. Evidence for a crypt diffusion process

(A) Representation of the proposed crypt diffusion process. Fission generates higher local density which is relieved by diffusion. (B) Schematic showing crypt cross section with area of surrounding stroma defining a crypt domain. (C) Representation of areas measured to assess packing of mutant patch and surrounding crypts in rolling windows placed at different distances (r) from centroid of mutant patch. (D) Examples of radial variation in crypt packing in patches of 10 crypts when moving from mutant clone to three adjacent control groupings for (i) STAG2 (ii) KDM6A. Points are data derived, the black line (grey ribbon) is the median (95% CI) theoretical stromal fraction as fitted from the diffusion model. Dashed line shows the average of the 25 most likely trajectories from initial mutation to clone of size 10, based on population average diffusion and neighbourhood ambient stromal fraction. (E) As (D) but with rolling window data. (F) Density plot of values obtained for the diffusion coefficient in human colonic epithelium. (G) Representation of area of crypts affected if space is decreased by 1% or 5% surrounding a mutant patch of 10. (Crypt numbers not to scale). (H) Boxplot showing simulated numbers of crypts affected if spacing is decreased by 1% or 5% respectively by addition of a patch of 10 mutant crypts. (I) Dot plot showing median frequency of newly generated crypts for mPAS, MAOA, STAG2 and KDM6A across four age bins. (J) Line graphs showing the stromal fraction resulting from crypt diffusion and crypt fission rates

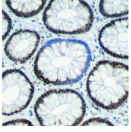
corresponding to the homeostatic (WT) rate as well as those associated with STAG2, KDM6A and KRAS and multiples of 11 and 12 of the WT rate. Dotted line = whitespace fraction calculated from optimal hexagonal packing of circles. r = distance from centroid of patch in crypt domains. (K) Line graph showing results from simulations to calculate the cumulative probability of a clone developing into a lesion, defined as reaching the whitespace fraction for hexagonal packing shown in (J), over time. Plots using the fission rate associated with KRAS (17x WT, none) are shown alongside those including therapeutic crypt fission inhibition applied for a decade either immediately after mutation acquisition (0-10), after 10 years (10-20) or 20 years (20-30).

Journal Pre-proof

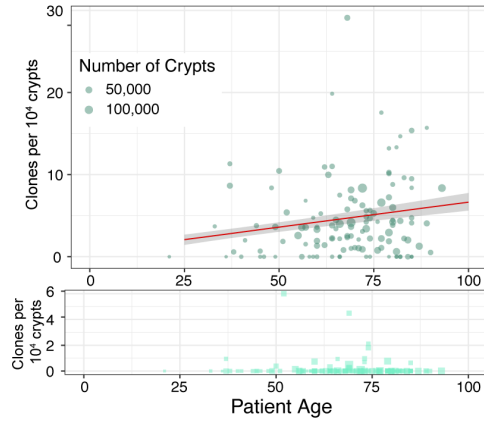
Ai



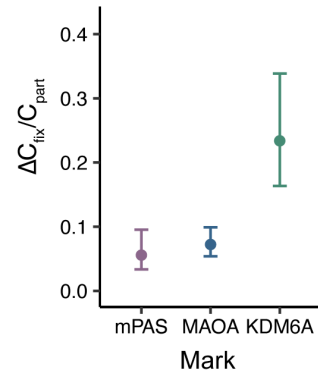
Aii



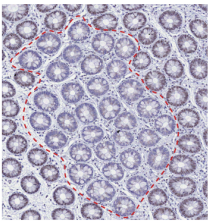
B



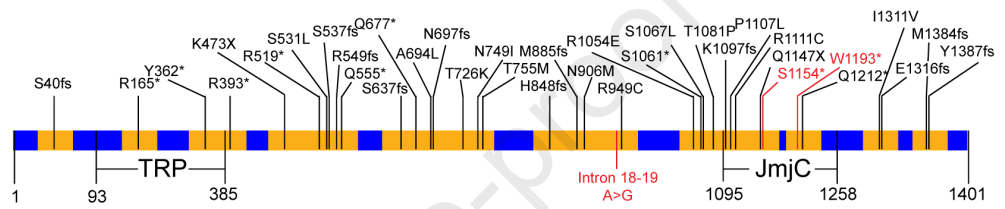
C

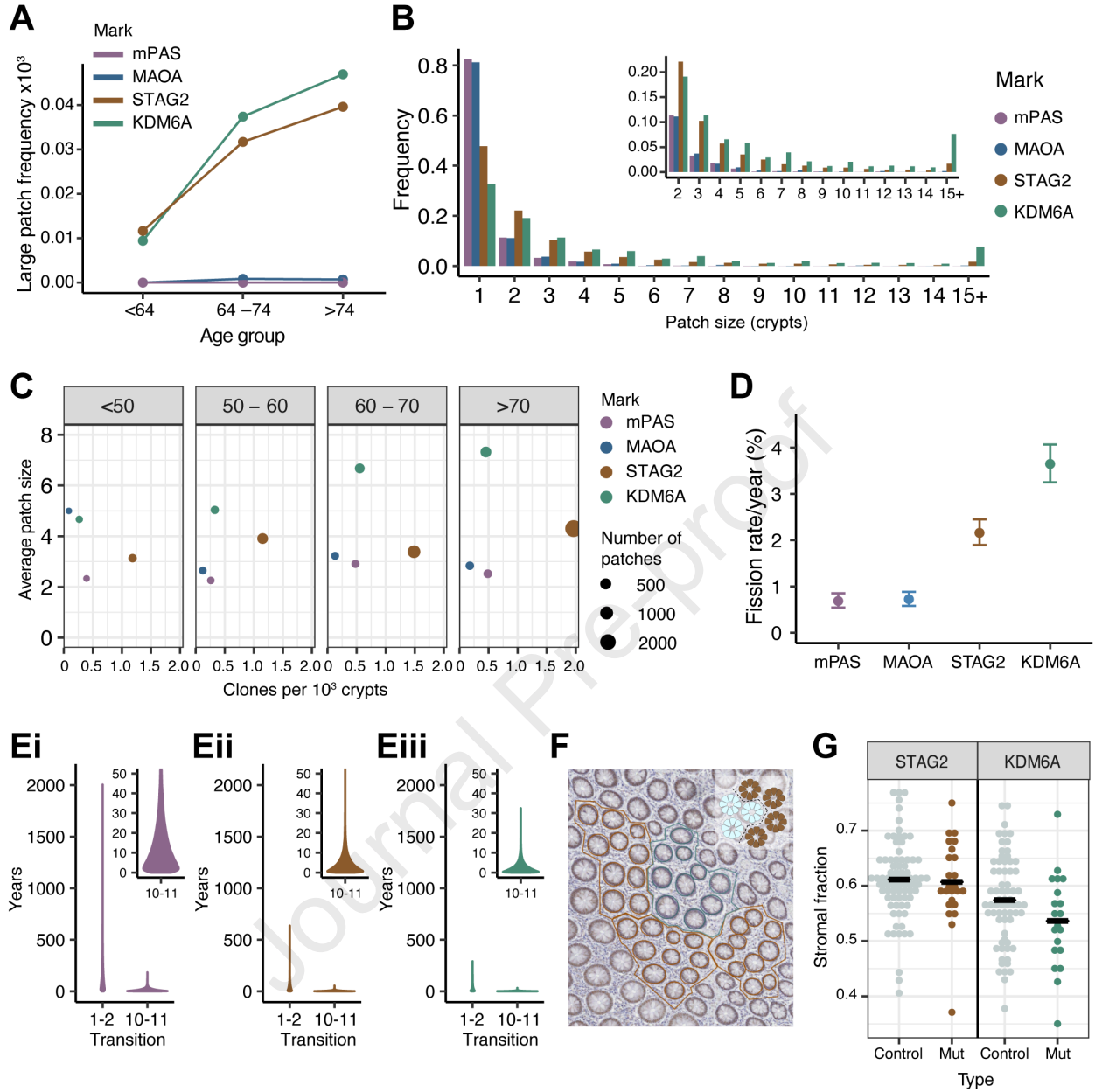


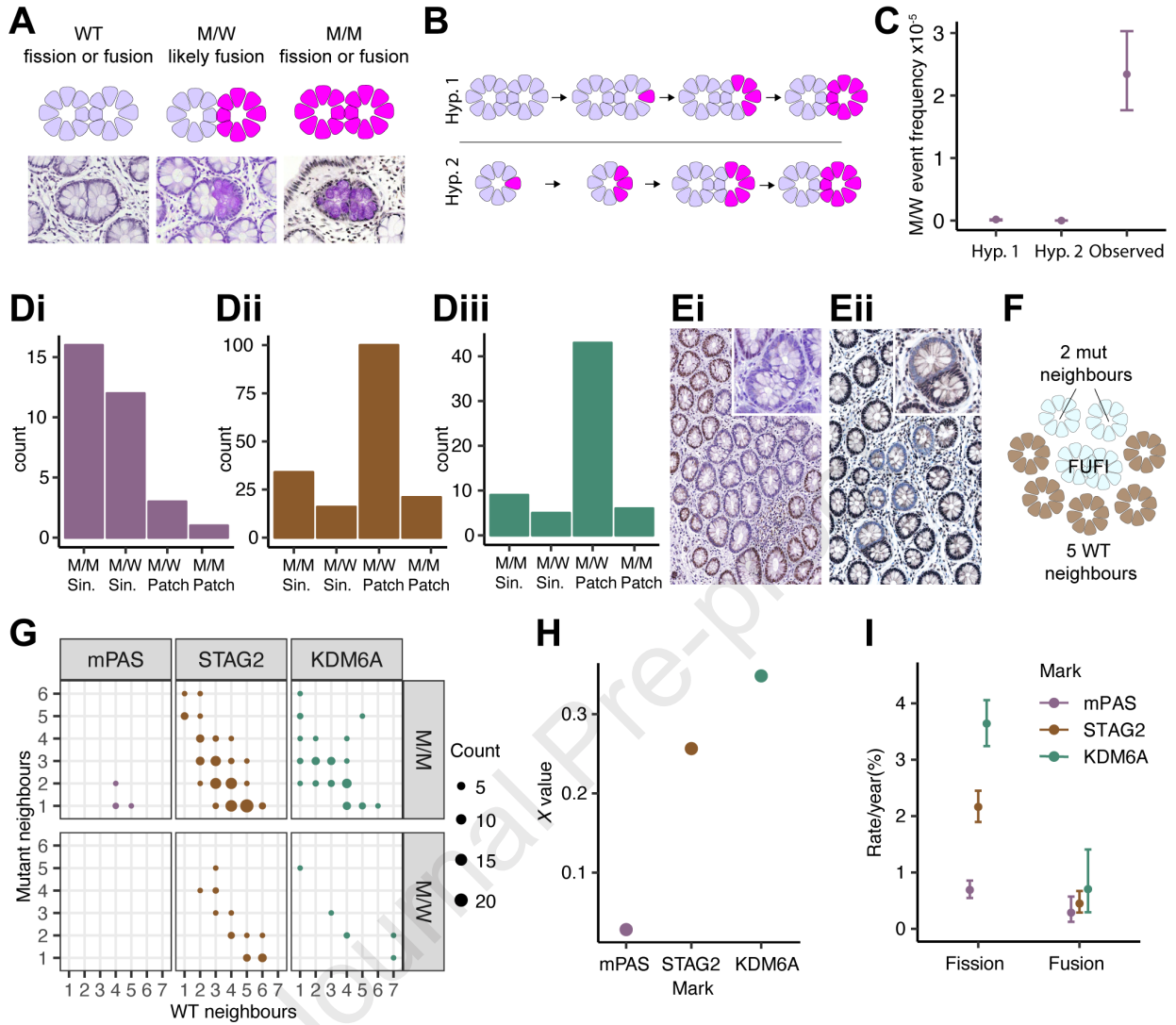
D

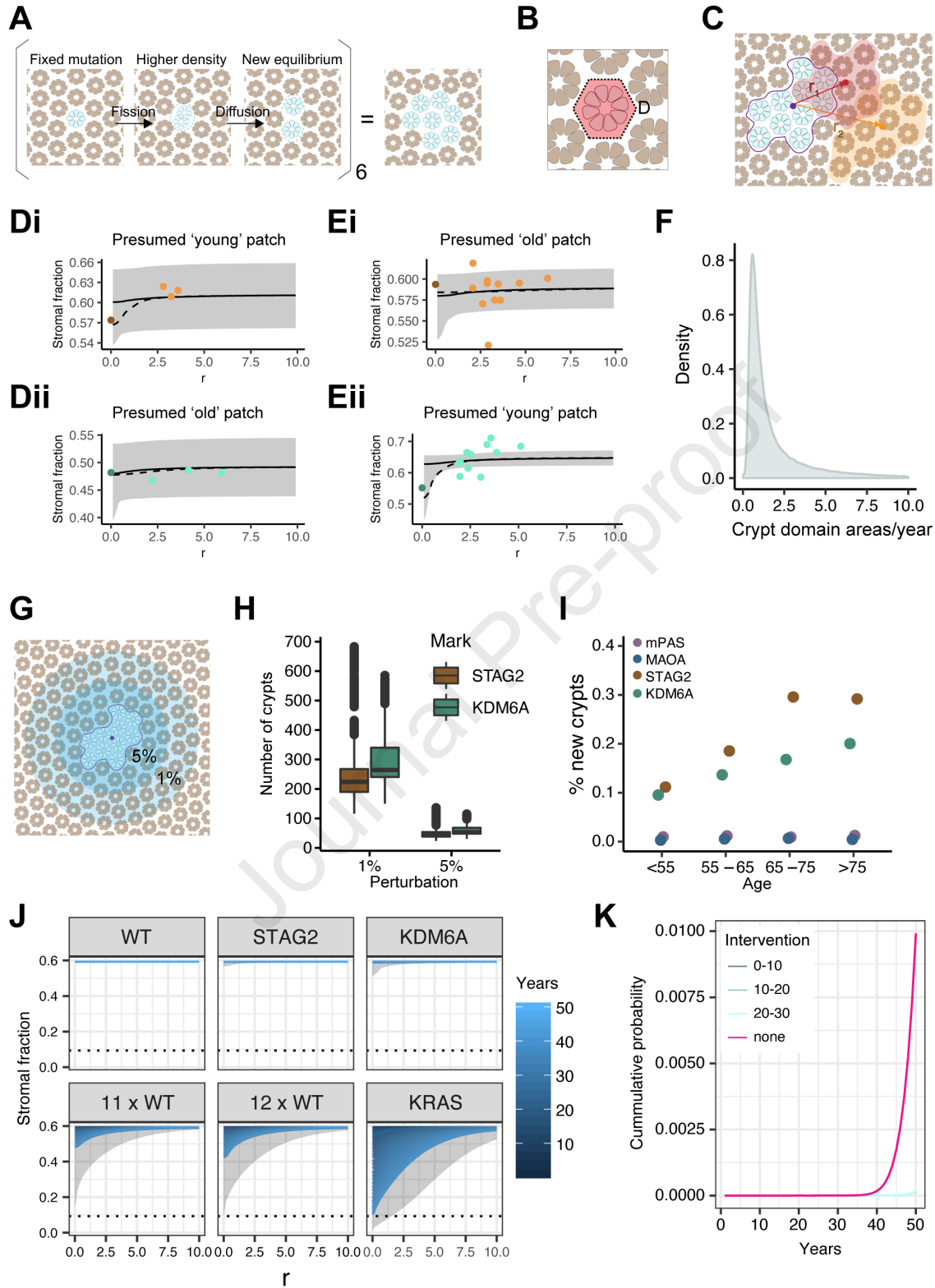


E









DW.Patient.n Age	SEX	num_crypts	PPC	WPC	full	fullx2	fullx3	fullx4	fullx5	fullx6	fullx7	fullx8	fullx9	fullx10	fullxmore10	tot_mut_cryp	freq_mono	freq_part
CDA_00002	59 M	2718		0	0	0	0	0	0	0	0	0	0	0	0	0	0	0
CDA_00003	85 F	2411		0	0	0	0	0	0	0	0	0	0	0	0	0	0	0
CDA_00016	66 F	2487		0	0	0	0	0	0	0	0	0	0	0	0	0	0	0
CDA_00074	79 M	502		0	0	0	0	0	0	0	0	0	0	0	0	0	0	0
CDA_00076	81 M	2251		0	3	2	0	1	0	0	0	0	0	0	0	0	5	0.00133274
CDA_00080	64 M	4497		0	1	1	0	0	0	0	0	0	0	0	0	0	1	2.22E-04
CDA_00087	79 F	4545		0	6	3	0	0	1	1	0	0	1	0	0	0	20	0.00132013
CDA_00088	41 F	5001		0	1	0	0	1	0	0	0	0	0	0	0	0	3	2.00E-04
CDA_00089	82 F	2727		0	4	1	1	0	1	1	0	0	0	0	0	0	12	0.00146681
CDA_00097	77 F	3988		0	7	0	2	2	2	1	0	0	0	0	0	0	23	0.00175527
CRA_00117	73 M	14172		0	6	3	1	1	0	0	0	0	0	0	1	0	18	4.23E-04
CRA_00125	74 M	27784		5	13	5	2	1	0	0	3	1	0	0	0	1	68	4.68E-04
CRA_00126	70 M	18118		0	2	1	0	1	0	0	0	0	0	0	0	0	4	1.10E-04
CRA_00127	85 M	14577		0	6	3	2	0	1	0	0	0	0	0	0	0	11	4.12E-04
CRA_00128	69 F	35633		1	13	3	2	1	4	2	0	0	0	0	1	0	46	3.65E-04
CRA_00129	93 M	80140		0	67	16	5	5	3	4	7	3	0	0	3	21	708	8.36E-04
CRA_00130	55 F	69742		1	18	11	3	1	2	1	0	0	0	0	0	0	33	2.58E-04
CRA_00131	62 M	28254		0	4	0	2	0	0	1	0	0	1	0	0	0	17	1.42E-04
CRA_00134	64 F	35781		0	8	4	2	0	1	0	0	1	0	0	0	0	19	2.24E-04
CRA_00294	89 M	31996		0	13	6	2	2	1	0	0	1	1	0	0	0	35	4.06E-04
CRA_00295	85 F	16875		0	8	3	4	0	0	0	0	0	1	0	0	0	19	4.74E-04
CRA_00297	50 M	25842		1	27	5	9	6	1	2	0	1	1	1	0	1	90	0.00104481
CRA_00298	76 F	51554		0	4	4	0	0	0	0	0	0	0	0	0	0	4	7.76E-05
CRA_00299	37 F	10600		1	12	3	1	0	0	0	1	0	2	1	0	4	193	0.00113208
CRA_00300	60 F	7349		0	0	0	0	0	0	0	0	0	0	0	0	0	0	0
CRA_00301	69 M	50372		1	41	9	8	4	5	3	0	3	2	0	1	6	285	8.14E-04
CRA_00302	83 M	22528		0	5	4	1	0	0	0	0	0	0	0	0	0	6	2.22E-04
CRA_00303	57 F	44802		0	16	6	1	4	1	2	1	1	0	0	0	0	77	3.57E-04
CRA_00304	60 M	29962		0	4	1	0	1	0	0	0	0	0	1	0	1	47	1.34E-04
CRA_00305	51 M	16097		0	3	0	0	1	1	0	1	0	0	0	0	0	13	1.86E-04
CRA_00306	76 F	4694		0	2	1	0	0	0	0	0	1	0	0	0	0	28	4.26E-04
CRA_00307	62 F	17379		0	19	8	2	6	0	1	1	0	0	0	0	1	69	0.00109327
CRA_00308	73 F	14249		1	8	3	2	1	0	1	0	0	0	0	0	1	55	5.61E-04
CRA_00309	80 F	18214		0	7	6	0	1	0	0	0	0	0	0	0	0	9	3.84E-04
CRA_00312	67 M	24383		0	2	1	0	0	0	1	0	0	0	0	0	0	6	8.20E-05
CRA_00313	57 M	1465		0	1	0	1	0	0	0	0	0	0	0	0	0	2	6.83E-04
CRA_00314	89 M	1911		0	3	1	2	0	0	0	0	0	0	0	0	0	5	0.00156986
CRA_00315	60 F	13910		0	5	1	0	1	0	1	0	1	0	0	0	1	52	3.59E-04
CRA_00316	85 M	20167		0	31	8	7	2	6	0	1	1	0	1	1	4	219	0.00153716
CRA_00317	69 M	26736		12	19	9	2	0	0	1	1	0	0	0	2	4	172	7.11E-04
CRA_00318	48 M	8347		0	7	5	2	0	0	0	0	0	0	0	0	0	9	8.39E-04
CRA_00347	68 M	24249		0	14	4	6	1	0	1	0	2	0	0	0	0	38	5.77E-04
CRA_00348	56 F	64606		0	23	9	10	3	0	0	0	0	1	0	0	0	46	3.56E-04
CRA_00349	37 M	31217		0	27	3	2	1	1	2	2	1	0	1	1	13	352	8.65E-04
CRA_00350	70 M	21979		0	15	5	3	4	1	2	0	0	0	0	0	0	37	6.82E-04
CRA_00351	68 F	27683		0	7	4	1	2	0	0	0	0	0	0	0	0	12	2.53E-04
CRA_00357	79 M	31900		0	6	1	2	3	0	0	0	0	0	0	0	0	14	1.88E-04
CRA_00358	87 F	62422		0	8	6	1	0	0	0	1	0	0	0	0	0	14	1.28E-04
CRA_00359	68 M	21274		0	5	2	0	0	0	2	0	0	0	0	1	0	22	2.35E-04
CRA_00360	65 F	44582		0	20	4	1	1	1	0	0	0	0	1	0	12	421	4.49E-04
CRA_00361	65 F	11729		0	4	1	2	1	0	0	0	0	0	0	0	0	8	3.41E-04
CRA_00362	85 F	934		0	0	0	0	0	0	0	0	0	0	0	0	0	0	0
CRA_00363	72 M	28745		0	18	5	3	6	0	1	0	0	0	0	1	2	67	6.26E-04
CRA_00364	74 M	14158		3	8	5	0	0	0	1	0	0	1	0	0	1	55	5.65E-04

NDX_00394	73 F	3284	0	0	0	0	0	0	0	0	0	0	0	0	0	0	0	0
NDX_00403	64 M	2015	0	4	3	0	0	0	1	0	0	0	0	0	0	8	0.00198511	0
NDX_00404	81 F/M	3427	0	0	0	0	0	0	0	0	0	0	0	0	0	0	0	0
NDX_00405	59 M	2103	0	1	1	0	0	0	0	0	0	0	0	0	0	1	4.76E-04	0
NDX_00406	74 M	2397	0	0	0	0	0	0	0	0	0	0	0	0	0	0	0	0
NRA_00345	72 F	44358	0	4	0	1	0	1	0	0	0	0	0	0	2	29	9.02E-05	0
NRA_00346	49 F	38575	0	14	4	4	2	1	0	0	1	1	0	1	0	47	3.63E-04	0
NRA_00368	79 F	78156	6	23	14	5	4	0	0	0	0	0	0	0	0	36	2.94E-04	7.68E-05
NRA_00369	72 F	9724	0	3	3	0	0	0	0	0	0	0	0	0	0	25	3.09E-04	0
NRA_00416	77 F	27778	0	3	1	1	0	1	0	0	0	0	0	0	0	7	1.08E-04	0
NRA_00417	46 F	4298	0	0	0	0	0	0	0	0	0	0	0	0	0	0	0	0

Journal Pre-proof

Block_ID	section	Slide_ID	DW.Patient.nAge	Sex	Mark	Patch	Type	crypt	x_um	y_um	size_um2	Total_area_um2	
114394	5	619028	CRA_00301	69 M	KDM6A		1 mut		1	4580	10566	4852	87747
114394	5	619028	CRA_00301	69 M	KDM6A		1 mut		2	4566	10660	3009	87747
114394	5	619028	CRA_00301	69 M	KDM6A		1 mut		3	4654	10637	3369	87747
114394	5	619028	CRA_00301	69 M	KDM6A		1 mut		4	4703	10701	3112	87747
114394	5	619028	CRA_00301	69 M	KDM6A		1 mut		5	4716	10595	3948	87747
114394	5	619028	CRA_00301	69 M	KDM6A		1 mut		6	4785	10562	3206	87747
114394	5	619028	CRA_00301	69 M	KDM6A		1 mut		7	4863	10542	2589	87747
114394	5	619028	CRA_00301	69 M	KDM6A		1 mut		8	4847	10623	3230	87747
114394	5	619028	CRA_00301	69 M	KDM6A		1 mut		9	4865	10709	3778	87747
114394	5	619028	CRA_00301	69 M	KDM6A		1 mut		10	4975	10699	3094	87747
114394	5	619028	CRA_00301	69 M	KDM6A		2 WT		1	4950	10515	2297	84805
114394	5	619028	CRA_00301	69 M	KDM6A		2 WT		2	4958	10592	2552	84805
114394	5	619028	CRA_00301	69 M	KDM6A		2 WT		3	5055	10590	2526	84805
114394	5	619028	CRA_00301	69 M	KDM6A		2 WT		4	5074	10677	2683	84805
114394	5	619028	CRA_00301	69 M	KDM6A		2 WT		5	5041	10517	2709	84805
114394	5	619028	CRA_00301	69 M	KDM6A		2 WT		6	5139	10498	3021	84805
114394	5	619028	CRA_00301	69 M	KDM6A		2 WT		7	5174	10577	3232	84805
114394	5	619028	CRA_00301	69 M	KDM6A		2 WT		8	5234	10512	3116	84805
114394	5	619028	CRA_00301	69 M	KDM6A		2 WT		9	5301	10447	2775	84805
114394	5	619028	CRA_00301	69 M	KDM6A		2 WT		10	5187	10658	3751	84805
114394	5	619028	CRA_00301	69 M	KDM6A		3 WT		1	5333	9883	3924	70531
114394	5	619028	CRA_00301	69 M	KDM6A		3 WT		2	5426	9886	3777	70531
114394	5	619028	CRA_00301	69 M	KDM6A		3 WT		3	5391	9794	3266	70531
114394	5	619028	CRA_00301	69 M	KDM6A		3 WT		4	5481	9809	3085	70531
114394	5	619028	CRA_00301	69 M	KDM6A		3 WT		5	5515	9877	2945	70531
114394	5	619028	CRA_00301	69 M	KDM6A		3 WT		6	5481	9949	3201	70531
114394	5	619028	CRA_00301	69 M	KDM6A		3 WT		7	5397	9981	2845	70531
114394	5	619028	CRA_00301	69 M	KDM6A		3 WT		8	5320	9966	2985	70531
114394	5	619028	CRA_00301	69 M	KDM6A		3 WT		9	5276	9824	3406	70531
114394	5	619028	CRA_00301	69 M	KDM6A		3 WT		10	5569	9931	2577	70531
114394	5	619028	CRA_00301	69 M	KDM6A		4 WT		1	5694	10320	3495	84212
114394	5	619028	CRA_00301	69 M	KDM6A		4 WT		2	5745	10385	3900	84212
114394	5	619028	CRA_00301	69 M	KDM6A		4 WT		3	5826	10337	3488	84212
114394	5	619028	CRA_00301	69 M	KDM6A		4 WT		4	5868	10411	3710	84212
114394	5	619028	CRA_00301	69 M	KDM6A		4 WT		5	5764	10460	3760	84212
114394	5	619028	CRA_00301	69 M	KDM6A		4 WT		6	5658	10450	4244	84212
114394	5	619028	CRA_00301	69 M	KDM6A		4 WT		7	5642	10376	3557	84212
114394	5	619028	CRA_00301	69 M	KDM6A		4 WT		8	5886	10496	3950	84212
114394	5	619028	CRA_00301	69 M	KDM6A		4 WT		9	5721	10539	4600	84212
114394	5	619028	CRA_00301	69 M	KDM6A		4 WT		10	5591	10303	3843	84212

114394	5	619028 CRA_00301	69 M	KDM6A	5 WT	1	5830	10911	2961	91602
114394	5	619028 CRA_00301	69 M	KDM6A	5 WT	2	5865	10999	4065	91602
114394	5	619028 CRA_00301	69 M	KDM6A	5 WT	3	5761	11008	3227	91602
114394	5	619028 CRA_00301	69 M	KDM6A	5 WT	4	5976	11006	3787	91602
114394	5	619028 CRA_00301	69 M	KDM6A	5 WT	5	5762	10887	2815	91602
114394	5	619028 CRA_00301	69 M	KDM6A	5 WT	6	5702	10934	2747	91602
114394	5	619028 CRA_00301	69 M	KDM6A	5 WT	7	5671	11003	3473	91602
114394	5	619028 CRA_00301	69 M	KDM6A	5 WT	8	5761	11111	3019	91602
114394	5	619028 CRA_00301	69 M	KDM6A	5 WT	9	5849	11098	3485	91602
114394	5	619028 CRA_00301	69 M	KDM6A	5 WT	10	5938	11119	3410	91602
114394	5	627731 CRA_00301	69 M	KDM6A	78 mut	1	4453	10704	5019	93775
114394	5	627731 CRA_00301	69 M	KDM6A	78 mut	2	4438	10797	3321	93775
114394	5	627731 CRA_00301	69 M	KDM6A	78 mut	3	4526	10777	4054	93775
114394	5	627731 CRA_00301	69 M	KDM6A	78 mut	4	4575	10838	3193	93775
114394	5	627731 CRA_00301	69 M	KDM6A	78 mut	5	4584	10733	3938	93775
114394	5	627731 CRA_00301	69 M	KDM6A	78 mut	6	4657	10700	3470	93775
114394	5	627731 CRA_00301	69 M	KDM6A	78 mut	7	4735	10680	2890	93775
114394	5	627731 CRA_00301	69 M	KDM6A	78 mut	8	4717	10761	3222	93775
114394	5	627731 CRA_00301	69 M	KDM6A	78 mut	9	4738	10847	3823	93775
114394	5	627731 CRA_00301	69 M	KDM6A	78 mut	10	4846	10837	3219	93775
114394	5	627731 CRA_00301	69 M	KDM6A	79 mut3_WT7	1	4453	10704	5019	101099
114394	5	627731 CRA_00301	69 M	KDM6A	79 mut3_WT7	2	4438	10797	3321	101099
114394	5	627731 CRA_00301	69 M	KDM6A	79 mut3_WT7	3	4526	10777	4054	101099
114394	5	627731 CRA_00301	69 M	KDM6A	79 mut3_WT7	4	4452	10608	4197	101099
114394	5	627731 CRA_00301	69 M	KDM6A	79 mut3_WT7	5	4353	10669	4289	101099
114394	5	627731 CRA_00301	69 M	KDM6A	79 mut3_WT7	6	4409	10523	2990	101099
114394	5	627731 CRA_00301	69 M	KDM6A	79 mut3_WT7	7	4311	10569	3443	101099
114394	5	627731 CRA_00301	69 M	KDM6A	79 mut3_WT7	8	4239	10648	4472	101099
114394	5	627731 CRA_00301	69 M	KDM6A	79 mut3_WT7	9	4293	10760	4218	101099
114394	5	627731 CRA_00301	69 M	KDM6A	79 mut3_WT7	10	4342	10827	3817	101099
114394	5	627731 CRA_00301	69 M	KDM6A	80 mut3_WT7	1	4717	10761	3222	95087
114394	5	627731 CRA_00301	69 M	KDM6A	80 mut3_WT7	2	4738	10847	3823	95087
114394	5	627731 CRA_00301	69 M	KDM6A	80 mut3_WT7	3	4846	10837	3219	95087
114394	5	627731 CRA_00301	69 M	KDM6A	80 mut3_WT7	4	4706	10926	2913	95087
114394	5	627731 CRA_00301	69 M	KDM6A	80 mut3_WT7	5	4828	10922	2856	95087
114394	5	627731 CRA_00301	69 M	KDM6A	80 mut3_WT7	6	4924	10904	2862	95087
114394	5	627731 CRA_00301	69 M	KDM6A	80 mut3_WT7	7	4942	10815	2512	95087
114394	5	627731 CRA_00301	69 M	KDM6A	80 mut3_WT7	8	4828	10728	2512	95087
114394	5	627731 CRA_00301	69 M	KDM6A	80 mut3_WT7	9	4925	10726	2344	95087
114394	5	627731 CRA_00301	69 M	KDM6A	80 mut3_WT7	10	5018	10885	4289	95087
114394	5	627731 CRA_00301	69 M	KDM6A	81 mut2_WT8	1	4657	10700	3470	80749

114394	5	627731 CRA_00301	69 M	KDM6A	81 mut2_WT8	2	4735	10680	2890	80749
114394	5	627731 CRA_00301	69 M	KDM6A	81 mut2_WT8	3	4828	10728	2512	80749
114394	5	627731 CRA_00301	69 M	KDM6A	81 mut2_WT8	4	4925	10726	2344	80749
114394	5	627731 CRA_00301	69 M	KDM6A	81 mut2_WT8	5	4671	10599	4092	80749
114394	5	627731 CRA_00301	69 M	KDM6A	81 mut2_WT8	6	4788	10589	3039	80749
114394	5	627731 CRA_00301	69 M	KDM6A	81 mut2_WT8	7	4823	10652	2428	80749
114394	5	627731 CRA_00301	69 M	KDM6A	81 mut2_WT8	8	4912	10654	2495	80749
114394	5	627731 CRA_00301	69 M	KDM6A	81 mut2_WT8	9	4927	10574	3029	80749
114394	5	627731 CRA_00301	69 M	KDM6A	81 mut2_WT8	10	5007	10634	3227	80749
114394	5	627731 CRA_00301	69 M	KDM6A	82 mut2_WT8	1	4846	10837	3219	90646
114394	5	627731 CRA_00301	69 M	KDM6A	82 mut2_WT8	2	4738	10847	3823	90646
114394	5	627731 CRA_00301	69 M	KDM6A	82 mut2_WT8	3	4706	10926	2913	90646
114394	5	627731 CRA_00301	69 M	KDM6A	82 mut2_WT8	4	4828	10922	2856	90646
114394	5	627731 CRA_00301	69 M	KDM6A	82 mut2_WT8	5	4924	10904	2862	90646
114394	5	627731 CRA_00301	69 M	KDM6A	82 mut2_WT8	6	4942	10815	2512	90646
114394	5	627731 CRA_00301	69 M	KDM6A	82 mut2_WT8	7	4925	10726	2344	90646
114394	5	627731 CRA_00301	69 M	KDM6A	82 mut2_WT8	8	4828	10728	2512	90646
114394	5	627731 CRA_00301	69 M	KDM6A	82 mut2_WT8	9	5045	10715	3368	90646
114394	5	627731 CRA_00301	69 M	KDM6A	82 mut2_WT8	10	5060	10796	4069	90646
114394	5	627731 CRA_00301	69 M	KDM6A	83 mut1_WT9	1	4453	10704	5019	101476
114394	5	627731 CRA_00301	69 M	KDM6A	83 mut1_WT9	2	4342	10827	3817	101476
114394	5	627731 CRA_00301	69 M	KDM6A	83 mut1_WT9	3	4293	10760	4218	101476
114394	5	627731 CRA_00301	69 M	KDM6A	83 mut1_WT9	4	4353	10669	4289	101476
114394	5	627731 CRA_00301	69 M	KDM6A	83 mut1_WT9	5	4239	10648	4472	101476
114394	5	627731 CRA_00301	69 M	KDM6A	83 mut1_WT9	6	4311	10569	3443	101476
114394	5	627731 CRA_00301	69 M	KDM6A	83 mut1_WT9	7	4452	10608	4197	101476
114394	5	627731 CRA_00301	69 M	KDM6A	83 mut1_WT9	8	4409	10523	2990	101476
114394	5	627731 CRA_00301	69 M	KDM6A	83 mut1_WT9	9	4311	10478	3372	101476
114394	5	627731 CRA_00301	69 M	KDM6A	83 mut1_WT9	10	4218	10560	2878	101476
114394	5	627731 CRA_00301	69 M	KDM6A	84 mut1_WT9	1	4846	10837	3219	93945
114394	5	627731 CRA_00301	69 M	KDM6A	84 mut1_WT9	2	4828	10922	2856	93945
114394	5	627731 CRA_00301	69 M	KDM6A	84 mut1_WT9	3	4924	10904	2862	93945
114394	5	627731 CRA_00301	69 M	KDM6A	84 mut1_WT9	4	5018	10885	4289	93945
114394	5	627731 CRA_00301	69 M	KDM6A	84 mut1_WT9	5	4942	10815	2512	93945
114394	5	627731 CRA_00301	69 M	KDM6A	84 mut1_WT9	6	5060	10796	4069	93945
114394	5	627731 CRA_00301	69 M	KDM6A	84 mut1_WT9	7	5045	10715	3368	93945
114394	5	627731 CRA_00301	69 M	KDM6A	84 mut1_WT9	8	4925	10726	2344	93945
114394	5	627731 CRA_00301	69 M	KDM6A	84 mut1_WT9	9	4828	10728	2512	93945
114394	5	627731 CRA_00301	69 M	KDM6A	84 mut1_WT9	10	5007	10634	3227	93945
114394	5	627731 CRA_00301	69 M	KDM6A	85 WT	1	4924	10904	2862	96402
114394	5	627731 CRA_00301	69 M	KDM6A	85 WT	2	5018	10885	4289	96402

114394	5	627731 CRA_00301	69 M	KDM6A	85 WT	3	4942	10815	2512	96402
114394	5	627731 CRA_00301	69 M	KDM6A	85 WT	4	5060	10796	4069	96402
114394	5	627731 CRA_00301	69 M	KDM6A	85 WT	5	5045	10715	3368	96402
114394	5	627731 CRA_00301	69 M	KDM6A	85 WT	6	4925	10726	2344	96402
114394	5	627731 CRA_00301	69 M	KDM6A	85 WT	7	5007	10634	3227	96402
114394	5	627731 CRA_00301	69 M	KDM6A	85 WT	8	5107	10650	3048	96402
114394	5	627731 CRA_00301	69 M	KDM6A	85 WT	9	5160	10775	3053	96402
114394	5	627731 CRA_00301	69 M	KDM6A	85 WT	10	5215	10709	2540	96402
114394	5	627731 CRA_00301	69 M	KDM6A	86 WT	1	5060	10796	4069	89774
114394	5	627731 CRA_00301	69 M	KDM6A	86 WT	2	5160	10775	3053	89774
114394	5	627731 CRA_00301	69 M	KDM6A	86 WT	3	5045	10715	3368	89774
114394	5	627731 CRA_00301	69 M	KDM6A	86 WT	4	5215	10709	2540	89774
114394	5	627731 CRA_00301	69 M	KDM6A	86 WT	5	5107	10650	3048	89774
114394	5	627731 CRA_00301	69 M	KDM6A	86 WT	6	5176	10585	2851	89774
114394	5	627731 CRA_00301	69 M	KDM6A	86 WT	7	5267	10640	3507	89774
114394	5	627731 CRA_00301	69 M	KDM6A	86 WT	8	5274	10553	2080	89774
114394	5	627731 CRA_00301	69 M	KDM6A	86 WT	9	5350	10577	4095	89774
114394	5	627731 CRA_00301	69 M	KDM6A	86 WT	10	5241	10496	2686	89774
114394	5	627731 CRA_00301	69 M	KDM6A	87 WT	1	4353	10669	4289	98793
114394	5	627731 CRA_00301	69 M	KDM6A	87 WT	2	4452	10608	4197	98793
114394	5	627731 CRA_00301	69 M	KDM6A	87 WT	3	4311	10569	3443	98793
114394	5	627731 CRA_00301	69 M	KDM6A	87 WT	4	4409	10523	2990	98793
114394	5	627731 CRA_00301	69 M	KDM6A	87 WT	5	4311	10478	3372	98793
114394	5	627731 CRA_00301	69 M	KDM6A	87 WT	6	4563	10620	5594	98793
114394	5	627731 CRA_00301	69 M	KDM6A	87 WT	7	4511	10523	3719	98793
114394	5	627731 CRA_00301	69 M	KDM6A	87 WT	8	4594	10481	5117	98793
114394	5	627731 CRA_00301	69 M	KDM6A	87 WT	9	4493	10421	4063	98793
114394	5	627731 CRA_00301	69 M	KDM6A	87 WT	10	4397	10434	2280	98793
114394	5	627731 CRA_00301	69 M	KDM6A	88 WT	1	4594	10481	5117	93009
114394	5	627731 CRA_00301	69 M	KDM6A	88 WT	2	4511	10523	3719	93009
114394	5	627731 CRA_00301	69 M	KDM6A	88 WT	3	4409	10523	2990	93009
114394	5	627731 CRA_00301	69 M	KDM6A	88 WT	4	4493	10421	4063	93009
114394	5	627731 CRA_00301	69 M	KDM6A	88 WT	5	4397	10434	2280	93009
114394	5	627731 CRA_00301	69 M	KDM6A	88 WT	6	4311	10478	3372	93009
114394	5	627731 CRA_00301	69 M	KDM6A	88 WT	7	4603	10370	3862	93009
114394	5	627731 CRA_00301	69 M	KDM6A	88 WT	8	4524	10288	3369	93009
114394	5	627731 CRA_00301	69 M	KDM6A	88 WT	9	4446	10327	2863	93009
114394	5	627731 CRA_00301	69 M	KDM6A	88 WT	10	4346	10349	2860	93009
114394	5	627731 CRA_00301	69 M	KDM6A	89 WT	1	4493	10421	4063	87959
114394	5	627731 CRA_00301	69 M	KDM6A	89 WT	2	4603	10370	3862	87959
114394	5	627731 CRA_00301	69 M	KDM6A	89 WT	3	4524	10288	3369	87959

114394	5	627731 CRA_00301	69 M	KDM6A	89 WT	4	4446	10327	2863	87959
114394	5	627731 CRA_00301	69 M	KDM6A	89 WT	5	4346	10349	2860	87959
114394	5	627731 CRA_00301	69 M	KDM6A	89 WT	6	4641	10286	3418	87959
114394	5	627731 CRA_00301	69 M	KDM6A	89 WT	7	4589	10213	2376	87959
114394	5	627731 CRA_00301	69 M	KDM6A	89 WT	8	4507	10194	2455	87959
114394	5	627731 CRA_00301	69 M	KDM6A	89 WT	9	4402	10192	2899	87959
114394	5	627731 CRA_00301	69 M	KDM6A	89 WT	10	4393	10274	2719	87959
99385	5	627738 CRA_00129	93 M	KDM6A	58 mut	1	5174	13388	1266	66352
99385	5	627738 CRA_00129	93 M	KDM6A	58 mut	1	5174	13388	1266	66352
99385	5	627738 CRA_00129	93 M	KDM6A	58 mut	1	5174	13388	1266	66352
99385	5	627738 CRA_00129	93 M	KDM6A	58 mut	2	5224	13415	1213	66352
99385	5	627738 CRA_00129	93 M	KDM6A	58 mut	2	5224	13415	1213	66352
99385	5	627738 CRA_00129	93 M	KDM6A	58 mut	2	5224	13415	1213	66352
99385	5	627738 CRA_00129	93 M	KDM6A	58 mut	3	5307	13374	4564	66352
99385	5	627738 CRA_00129	93 M	KDM6A	58 mut	3	5307	13374	4564	66352
99385	5	627738 CRA_00129	93 M	KDM6A	58 mut	3	5307	13374	4564	66352
99385	5	627738 CRA_00129	93 M	KDM6A	58 mut	4	5340	13442	4231	66352
99385	5	627738 CRA_00129	93 M	KDM6A	58 mut	4	5340	13442	4231	66352
99385	5	627738 CRA_00129	93 M	KDM6A	58 mut	4	5340	13442	4231	66352
99385	5	627738 CRA_00129	93 M	KDM6A	58 mut	5	5277	13483	5206	66352
99385	5	627738 CRA_00129	93 M	KDM6A	58 mut	5	5277	13483	5206	66352
99385	5	627738 CRA_00129	93 M	KDM6A	58 mut	5	5277	13483	5206	66352
99385	5	627738 CRA_00129	93 M	KDM6A	58 mut	6	5389	13360	3575	66352
99385	5	627738 CRA_00129	93 M	KDM6A	58 mut	6	5389	13360	3575	66352
99385	5	627738 CRA_00129	93 M	KDM6A	58 mut	6	5389	13360	3575	66352
99385	5	627738 CRA_00129	93 M	KDM6A	58 mut	7	5425	13457	3308	66352
99385	5	627738 CRA_00129	93 M	KDM6A	58 mut	7	5425	13457	3308	66352
99385	5	627738 CRA_00129	93 M	KDM6A	58 mut	7	5425	13457	3308	66352
99385	5	627738 CRA_00129	93 M	KDM6A	58 mut	8	5453	13385	2368	66352
99385	5	627738 CRA_00129	93 M	KDM6A	58 mut	8	5453	13385	2368	66352
99385	5	627738 CRA_00129	93 M	KDM6A	58 mut	8	5453	13385	2368	66352
99385	5	627738 CRA_00129	93 M	KDM6A	58 mut	9	5428	13532	3945	66352
99385	5	627738 CRA_00129	93 M	KDM6A	58 mut	9	5428	13532	3945	66352
99385	5	627738 CRA_00129	93 M	KDM6A	58 mut	9	5428	13532	3945	66352
99385	5	627738 CRA_00129	93 M	KDM6A	58 mut	10	5355	13551	4707	66352
99385	5	627738 CRA_00129	93 M	KDM6A	58 mut	10	5355	13551	4707	66352
99385	5	627738 CRA_00129	93 M	KDM6A	58 mut	10	5355	13551	4707	66352
99385	5	627738 CRA_00129	93 M	KDM6A	59 WT	1	5202	13521	3127	64713
99385	5	627738 CRA_00129	93 M	KDM6A	59 WT	1	5202	13521	3127	64713
99385	5	627738 CRA_00129	93 M	KDM6A	59 WT	1	5202	13521	3127	64713
99385	5	627738 CRA_00129	93 M	KDM6A	59 WT	2	5279	13565	2704	64713

99385	5	627738 CRA_00129	93 M	KDM6A	59 WT	2	5279	13565	2704	64713
99385	5	627738 CRA_00129	93 M	KDM6A	59 WT	2	5279	13565	2704	64713
99385	5	627738 CRA_00129	93 M	KDM6A	59 WT	3	5356	13628	3739	64713
99385	5	627738 CRA_00129	93 M	KDM6A	59 WT	3	5356	13628	3739	64713
99385	5	627738 CRA_00129	93 M	KDM6A	59 WT	3	5356	13628	3739	64713
99385	5	627738 CRA_00129	93 M	KDM6A	59 WT	4	5207	13598	3868	64713
99385	5	627738 CRA_00129	93 M	KDM6A	59 WT	4	5207	13598	3868	64713
99385	5	627738 CRA_00129	93 M	KDM6A	59 WT	4	5207	13598	3868	64713
99385	5	627738 CRA_00129	93 M	KDM6A	59 WT	5	5280	13661	3780	64713
99385	5	627738 CRA_00129	93 M	KDM6A	59 WT	5	5280	13661	3780	64713
99385	5	627738 CRA_00129	93 M	KDM6A	59 WT	5	5280	13661	3780	64713
99385	5	627738 CRA_00129	93 M	KDM6A	59 WT	6	5365	13719	3006	64713
99385	5	627738 CRA_00129	93 M	KDM6A	59 WT	6	5365	13719	3006	64713
99385	5	627738 CRA_00129	93 M	KDM6A	59 WT	6	5365	13719	3006	64713
99385	5	627738 CRA_00129	93 M	KDM6A	59 WT	7	5215	13712	4228	64713
99385	5	627738 CRA_00129	93 M	KDM6A	59 WT	7	5215	13712	4228	64713
99385	5	627738 CRA_00129	93 M	KDM6A	59 WT	7	5215	13712	4228	64713
99385	5	627738 CRA_00129	93 M	KDM6A	59 WT	8	5305	13749	3660	64713
99385	5	627738 CRA_00129	93 M	KDM6A	59 WT	8	5305	13749	3660	64713
99385	5	627738 CRA_00129	93 M	KDM6A	59 WT	8	5305	13749	3660	64713
99385	5	627738 CRA_00129	93 M	KDM6A	59 WT	9	5140	13629	3888	64713
99385	5	627738 CRA_00129	93 M	KDM6A	59 WT	9	5140	13629	3888	64713
99385	5	627738 CRA_00129	93 M	KDM6A	59 WT	9	5140	13629	3888	64713
99385	5	627738 CRA_00129	93 M	KDM6A	59 WT	10	5364	13800	2447	64713
99385	5	627738 CRA_00129	93 M	KDM6A	59 WT	10	5364	13800	2447	64713
99385	5	627738 CRA_00129	93 M	KDM6A	59 WT	10	5364	13800	2447	64713
99385	5	627738 CRA_00129	93 M	KDM6A	60 WT	1	5471	13623	3490	64602
99385	5	627738 CRA_00129	93 M	KDM6A	60 WT	1	5471	13623	3490	64602
99385	5	627738 CRA_00129	93 M	KDM6A	60 WT	1	5471	13623	3490	64602
99385	5	627738 CRA_00129	93 M	KDM6A	60 WT	2	5427	13673	3043	64602
99385	5	627738 CRA_00129	93 M	KDM6A	60 WT	2	5427	13673	3043	64602
99385	5	627738 CRA_00129	93 M	KDM6A	60 WT	2	5427	13673	3043	64602
99385	5	627738 CRA_00129	93 M	KDM6A	60 WT	3	5428	13740	2585	64602
99385	5	627738 CRA_00129	93 M	KDM6A	60 WT	3	5428	13740	2585	64602
99385	5	627738 CRA_00129	93 M	KDM6A	60 WT	3	5428	13740	2585	64602
99385	5	627738 CRA_00129	93 M	KDM6A	60 WT	4	5519	13693	2682	64602
99385	5	627738 CRA_00129	93 M	KDM6A	60 WT	4	5519	13693	2682	64602
99385	5	627738 CRA_00129	93 M	KDM6A	60 WT	4	5519	13693	2682	64602
99385	5	627738 CRA_00129	93 M	KDM6A	60 WT	5	5503	13761	2866	64602
99385	5	627738 CRA_00129	93 M	KDM6A	60 WT	5	5503	13761	2866	64602
99385	5	627738 CRA_00129	93 M	KDM6A	60 WT	5	5503	13761	2866	64602

99385	5	627738 CRA_00129	93 M	KDM6A	60 WT	6	5459	13827	4810	64602
99385	5	627738 CRA_00129	93 M	KDM6A	60 WT	6	5459	13827	4810	64602
99385	5	627738 CRA_00129	93 M	KDM6A	60 WT	6	5459	13827	4810	64602
99385	5	627738 CRA_00129	93 M	KDM6A	60 WT	7	5557	13634	2159	64602
99385	5	627738 CRA_00129	93 M	KDM6A	60 WT	7	5557	13634	2159	64602
99385	5	627738 CRA_00129	93 M	KDM6A	60 WT	7	5557	13634	2159	64602
99385	5	627738 CRA_00129	93 M	KDM6A	60 WT	8	5614	13685	2598	64602
99385	5	627738 CRA_00129	93 M	KDM6A	60 WT	8	5614	13685	2598	64602
99385	5	627738 CRA_00129	93 M	KDM6A	60 WT	8	5614	13685	2598	64602
99385	5	627738 CRA_00129	93 M	KDM6A	60 WT	9	5612	14826	4826	64602
99385	5	627738 CRA_00129	93 M	KDM6A	60 WT	9	5612	14826	4826	64602
99385	5	627738 CRA_00129	93 M	KDM6A	60 WT	9	5612	14826	4826	64602
99385	5	627738 CRA_00129	93 M	KDM6A	60 WT	10	5591	13839	4134	64602
99385	5	627738 CRA_00129	93 M	KDM6A	60 WT	10	5591	13839	4134	64602
99385	5	627738 CRA_00129	93 M	KDM6A	60 WT	10	5591	13839	4134	64602
99385	5	627738 CRA_00129	93 M	KDM6A	61 WT	1	5807	13829	3450	56518
99385	5	627738 CRA_00129	93 M	KDM6A	61 WT	1	5807	13829	3450	56518
99385	5	627738 CRA_00129	93 M	KDM6A	61 WT	1	5807	13829	3450	56518
99385	5	627738 CRA_00129	93 M	KDM6A	61 WT	2	5746	13785	2923	56518
99385	5	627738 CRA_00129	93 M	KDM6A	61 WT	2	5746	13785	2923	56518
99385	5	627738 CRA_00129	93 M	KDM6A	61 WT	2	5746	13785	2923	56518
99385	5	627738 CRA_00129	93 M	KDM6A	61 WT	3	5743	13878	4088	56518
99385	5	627738 CRA_00129	93 M	KDM6A	61 WT	3	5743	13878	4088	56518
99385	5	627738 CRA_00129	93 M	KDM6A	61 WT	3	5743	13878	4088	56518
99385	5	627738 CRA_00129	93 M	KDM6A	61 WT	4	5798	13745	1609	56518
99385	5	627738 CRA_00129	93 M	KDM6A	61 WT	4	5798	13745	1609	56518
99385	5	627738 CRA_00129	93 M	KDM6A	61 WT	4	5798	13745	1609	56518
99385	5	627738 CRA_00129	93 M	KDM6A	61 WT	5	5860	13792	1807	56518
99385	5	627738 CRA_00129	93 M	KDM6A	61 WT	5	5860	13792	1807	56518
99385	5	627738 CRA_00129	93 M	KDM6A	61 WT	5	5860	13792	1807	56518
99385	5	627738 CRA_00129	93 M	KDM6A	61 WT	6	5877	13729	3032	56518
99385	5	627738 CRA_00129	93 M	KDM6A	61 WT	6	5877	13729	3032	56518
99385	5	627738 CRA_00129	93 M	KDM6A	61 WT	6	5877	13729	3032	56518
99385	5	627738 CRA_00129	93 M	KDM6A	61 WT	7	5807	13686	1717	56518
99385	5	627738 CRA_00129	93 M	KDM6A	61 WT	7	5807	13686	1717	56518
99385	5	627738 CRA_00129	93 M	KDM6A	61 WT	7	5807	13686	1717	56518
99385	5	627738 CRA_00129	93 M	KDM6A	61 WT	8	5941	13777	2965	56518
99385	5	627738 CRA_00129	93 M	KDM6A	61 WT	8	5941	13777	2965	56518
99385	5	627738 CRA_00129	93 M	KDM6A	61 WT	8	5941	13777	2965	56518
99385	5	627738 CRA_00129	93 M	KDM6A	61 WT	9	5928	13841	3809	56518
99385	5	627738 CRA_00129	93 M	KDM6A	61 WT	9	5928	13841	3809	56518

99385	5	627738 CRA_00129	93 M	KDM6A	61 WT	9	5928	13841	3809	56518
99385	5	627738 CRA_00129	93 M	KDM6A	61 WT	10	5877	13892	3900	56518
99385	5	627738 CRA_00129	93 M	KDM6A	61 WT	10	5877	13892	3900	56518
99385	5	627738 CRA_00129	93 M	KDM6A	61 WT	10	5877	13892	3900	56518
99385	5	627738 CRA_00129	93 M	KDM6A	62 mut	1	11329	6790	3052	62163
99385	5	627738 CRA_00129	93 M	KDM6A	62 mut	1	11329	6790	3052	62163
99385	5	627738 CRA_00129	93 M	KDM6A	62 mut	1	11329	6790	3052	62163
99385	5	627738 CRA_00129	93 M	KDM6A	62 mut	2	11430	6795	3925	62163
99385	5	627738 CRA_00129	93 M	KDM6A	62 mut	2	11430	6795	3925	62163
99385	5	627738 CRA_00129	93 M	KDM6A	62 mut	2	11430	6795	3925	62163
99385	5	627738 CRA_00129	93 M	KDM6A	62 mut	3	11380	6864	3099	62163
99385	5	627738 CRA_00129	93 M	KDM6A	62 mut	3	11380	6864	3099	62163
99385	5	627738 CRA_00129	93 M	KDM6A	62 mut	3	11380	6864	3099	62163
99385	5	627738 CRA_00129	93 M	KDM6A	62 mut	4	11468	6876	2599	62163
99385	5	627738 CRA_00129	93 M	KDM6A	62 mut	4	11468	6876	2599	62163
99385	5	627738 CRA_00129	93 M	KDM6A	62 mut	4	11468	6876	2599	62163
99385	5	627738 CRA_00129	93 M	KDM6A	62 mut	5	11518	6812	3250	62163
99385	5	627738 CRA_00129	93 M	KDM6A	62 mut	5	11518	6812	3250	62163
99385	5	627738 CRA_00129	93 M	KDM6A	62 mut	5	11518	6812	3250	62163
99385	5	627738 CRA_00129	93 M	KDM6A	62 mut	6	11525	6918	2325	62163
99385	5	627738 CRA_00129	93 M	KDM6A	62 mut	6	11525	6918	2325	62163
99385	5	627738 CRA_00129	93 M	KDM6A	62 mut	6	11525	6918	2325	62163
99385	5	627738 CRA_00129	93 M	KDM6A	62 mut	7	11420	6951	2773	62163
99385	5	627738 CRA_00129	93 M	KDM6A	62 mut	7	11420	6951	2773	62163
99385	5	627738 CRA_00129	93 M	KDM6A	62 mut	7	11420	6951	2773	62163
99385	5	627738 CRA_00129	93 M	KDM6A	62 mut	8	11483	6983	1883	62163
99385	5	627738 CRA_00129	93 M	KDM6A	62 mut	8	11483	6983	1883	62163
99385	5	627738 CRA_00129	93 M	KDM6A	62 mut	8	11483	6983	1883	62163
99385	5	627738 CRA_00129	93 M	KDM6A	62 mut	9	11410	7023	2142	62163
99385	5	627738 CRA_00129	93 M	KDM6A	62 mut	9	11410	7023	2142	62163
99385	5	627738 CRA_00129	93 M	KDM6A	62 mut	9	11410	7023	2142	62163
99385	5	627738 CRA_00129	93 M	KDM6A	62 mut	10	11349	7057	3061	62163
99385	5	627738 CRA_00129	93 M	KDM6A	62 mut	10	11349	7057	3061	62163
99385	5	627738 CRA_00129	93 M	KDM6A	62 mut	10	11349	7057	3061	62163
99385	5	627738 CRA_00129	93 M	KDM6A	63 WT	1	11638	6708	1766	40255
99385	5	627738 CRA_00129	93 M	KDM6A	63 WT	1	11638	6708	1766	40255
99385	5	627738 CRA_00129	93 M	KDM6A	63 WT	1	11638	6708	1766	40255
99385	5	627738 CRA_00129	93 M	KDM6A	63 WT	2	11661	6750	1104	40255
99385	5	627738 CRA_00129	93 M	KDM6A	63 WT	2	11661	6750	1104	40255
99385	5	627738 CRA_00129	93 M	KDM6A	63 WT	2	11661	6750	1104	40255
99385	5	627738 CRA_00129	93 M	KDM6A	63 WT	3	11698	6783	1129	40255

99385	5	627738 CRA_00129	93 M	KDM6A	63 WT	3	11698	6783	1129	40255
99385	5	627738 CRA_00129	93 M	KDM6A	63 WT	3	11698	6783	1129	40255
99385	5	627738 CRA_00129	93 M	KDM6A	63 WT	4	11734	6731	2574	40255
99385	5	627738 CRA_00129	93 M	KDM6A	63 WT	4	11734	6731	2574	40255
99385	5	627738 CRA_00129	93 M	KDM6A	63 WT	4	11734	6731	2574	40255
99385	5	627738 CRA_00129	93 M	KDM6A	63 WT	5	11769	6793	2039	40255
99385	5	627738 CRA_00129	93 M	KDM6A	63 WT	5	11769	6793	2039	40255
99385	5	627738 CRA_00129	93 M	KDM6A	63 WT	5	11769	6793	2039	40255
99385	5	627738 CRA_00129	93 M	KDM6A	63 WT	6	11733	6846	1459	40255
99385	5	627738 CRA_00129	93 M	KDM6A	63 WT	6	11733	6846	1459	40255
99385	5	627738 CRA_00129	93 M	KDM6A	63 WT	6	11733	6846	1459	40255
99385	5	627738 CRA_00129	93 M	KDM6A	63 WT	7	11667	6834	1408	40255
99385	5	627738 CRA_00129	93 M	KDM6A	63 WT	7	11667	6834	1408	40255
99385	5	627738 CRA_00129	93 M	KDM6A	63 WT	7	11667	6834	1408	40255
99385	5	627738 CRA_00129	93 M	KDM6A	63 WT	8	11693	6895	1932	40255
99385	5	627738 CRA_00129	93 M	KDM6A	63 WT	8	11693	6895	1932	40255
99385	5	627738 CRA_00129	93 M	KDM6A	63 WT	8	11693	6895	1932	40255
99385	5	627738 CRA_00129	93 M	KDM6A	63 WT	9	11820	6748	2826	40255
99385	5	627738 CRA_00129	93 M	KDM6A	63 WT	9	11820	6748	2826	40255
99385	5	627738 CRA_00129	93 M	KDM6A	63 WT	9	11820	6748	2826	40255
99385	5	627738 CRA_00129	93 M	KDM6A	63 WT	10	11629	6882	1222	40255
99385	5	627738 CRA_00129	93 M	KDM6A	63 WT	10	11629	6882	1222	40255
99385	5	627738 CRA_00129	93 M	KDM6A	63 WT	10	11629	6882	1222	40255
99385	5	627738 CRA_00129	93 M	KDM6A	64 WT	1	11278	7126	2889	48898
99385	5	627738 CRA_00129	93 M	KDM6A	64 WT	1	11278	7126	2889	48898
99385	5	627738 CRA_00129	93 M	KDM6A	64 WT	1	11278	7126	2889	48898
99385	5	627738 CRA_00129	93 M	KDM6A	64 WT	2	11351	7136	2308	48898
99385	5	627738 CRA_00129	93 M	KDM6A	64 WT	2	11351	7136	2308	48898
99385	5	627738 CRA_00129	93 M	KDM6A	64 WT	2	11351	7136	2308	48898
99385	5	627738 CRA_00129	93 M	KDM6A	64 WT	3	11386	7201	2644	48898
99385	5	627738 CRA_00129	93 M	KDM6A	64 WT	3	11386	7201	2644	48898
99385	5	627738 CRA_00129	93 M	KDM6A	64 WT	3	11386	7201	2644	48898
99385	5	627738 CRA_00129	93 M	KDM6A	64 WT	4	11291	7190	2121	48898
99385	5	627738 CRA_00129	93 M	KDM6A	64 WT	4	11291	7190	2121	48898
99385	5	627738 CRA_00129	93 M	KDM6A	64 WT	4	11291	7190	2121	48898
99385	5	627738 CRA_00129	93 M	KDM6A	64 WT	5	11342	7241	1013	48898
99385	5	627738 CRA_00129	93 M	KDM6A	64 WT	5	11342	7241	1013	48898
99385	5	627738 CRA_00129	93 M	KDM6A	64 WT	5	11342	7241	1013	48898
99385	5	627738 CRA_00129	93 M	KDM6A	64 WT	6	11469	7232	2423	48898
99385	5	627738 CRA_00129	93 M	KDM6A	64 WT	6	11469	7232	2423	48898
99385	5	627738 CRA_00129	93 M	KDM6A	64 WT	6	11469	7232	2423	48898

99385	5	627738 CRA_00129	93 M	KDM6A	64 WT	7	11410	7276	2121	48898
99385	5	627738 CRA_00129	93 M	KDM6A	64 WT	7	11410	7276	2121	48898
99385	5	627738 CRA_00129	93 M	KDM6A	64 WT	7	11410	7276	2121	48898
99385	5	627738 CRA_00129	93 M	KDM6A	64 WT	8	11317	7296	2318	48898
99385	5	627738 CRA_00129	93 M	KDM6A	64 WT	8	11317	7296	2318	48898
99385	5	627738 CRA_00129	93 M	KDM6A	64 WT	8	11317	7296	2318	48898
99385	5	627738 CRA_00129	93 M	KDM6A	64 WT	9	11383	7336	2308	48898
99385	5	627738 CRA_00129	93 M	KDM6A	64 WT	9	11383	7336	2308	48898
99385	5	627738 CRA_00129	93 M	KDM6A	64 WT	9	11383	7336	2308	48898
99385	5	627738 CRA_00129	93 M	KDM6A	64 WT	10	11478	7172	1672	48898
99385	5	627738 CRA_00129	93 M	KDM6A	64 WT	10	11478	7172	1672	48898
99385	5	627738 CRA_00129	93 M	KDM6A	64 WT	10	11478	7172	1672	48898
99385	5	627738 CRA_00129	93 M	KDM6A	65 WT	1	11113	6678	2405	68284
99385	5	627738 CRA_00129	93 M	KDM6A	65 WT	1	11113	6678	2405	68284
99385	5	627738 CRA_00129	93 M	KDM6A	65 WT	1	11113	6678	2405	68284
99385	5	627738 CRA_00129	93 M	KDM6A	65 WT	2	11108	6745	3217	68284
99385	5	627738 CRA_00129	93 M	KDM6A	65 WT	2	11108	6745	3217	68284
99385	5	627738 CRA_00129	93 M	KDM6A	65 WT	2	11108	6745	3217	68284
99385	5	627738 CRA_00129	93 M	KDM6A	65 WT	3	11023	6709	1914	68284
99385	5	627738 CRA_00129	93 M	KDM6A	65 WT	3	11023	6709	1914	68284
99385	5	627738 CRA_00129	93 M	KDM6A	65 WT	3	11023	6709	1914	68284
99385	5	627738 CRA_00129	93 M	KDM6A	65 WT	4	10937	6683	2969	68284
99385	5	627738 CRA_00129	93 M	KDM6A	65 WT	4	10937	6683	2969	68284
99385	5	627738 CRA_00129	93 M	KDM6A	65 WT	4	10937	6683	2969	68284
99385	5	627738 CRA_00129	93 M	KDM6A	65 WT	4	10937	6683	2969	68284
99385	5	627738 CRA_00129	93 M	KDM6A	65 WT	5	11030	6797	2669	68284
99385	5	627738 CRA_00129	93 M	KDM6A	65 WT	5	11030	6797	2669	68284
99385	5	627738 CRA_00129	93 M	KDM6A	65 WT	5	11030	6797	2669	68284
99385	5	627738 CRA_00129	93 M	KDM6A	65 WT	6	10959	6760	2484	68284
99385	5	627738 CRA_00129	93 M	KDM6A	65 WT	6	10959	6760	2484	68284
99385	5	627738 CRA_00129	93 M	KDM6A	65 WT	6	10959	6760	2484	68284
99385	5	627738 CRA_00129	93 M	KDM6A	65 WT	7	11174	6793	2947	68284
99385	5	627738 CRA_00129	93 M	KDM6A	65 WT	7	11174	6793	2947	68284
99385	5	627738 CRA_00129	93 M	KDM6A	65 WT	7	11174	6793	2947	68284
99385	5	627738 CRA_00129	93 M	KDM6A	65 WT	8	11067	6850	2702	68284
99385	5	627738 CRA_00129	93 M	KDM6A	65 WT	8	11067	6850	2702	68284
99385	5	627738 CRA_00129	93 M	KDM6A	65 WT	8	11067	6850	2702	68284
99385	5	627738 CRA_00129	93 M	KDM6A	65 WT	9	11039	6628	3220	68284
99385	5	627738 CRA_00129	93 M	KDM6A	65 WT	9	11039	6628	3220	68284
99385	5	627738 CRA_00129	93 M	KDM6A	65 WT	9	11039	6628	3220	68284
99385	5	627738 CRA_00129	93 M	KDM6A	65 WT	10	11204	6704	2839	68284
99385	5	627738 CRA_00129	93 M	KDM6A	65 WT	10	11204	6704	2839	68284

99385	5	627738 CRA_00129	93 M	KDM6A	65 WT	10	11204	6704	2839	68284
99385	5	627738 CRA_00129	93 M	KDM6A	66 mut	1	23165	20590	6384	81823
99385	5	627738 CRA_00129	93 M	KDM6A	66 mut	1	23165	20590	6384	81823
99385	5	627738 CRA_00129	93 M	KDM6A	66 mut	1	23165	20590	6384	81823
99385	5	627738 CRA_00129	93 M	KDM6A	66 mut	2	23159	20512	3585	81823
99385	5	627738 CRA_00129	93 M	KDM6A	66 mut	2	23159	20512	3585	81823
99385	5	627738 CRA_00129	93 M	KDM6A	66 mut	2	23159	20512	3585	81823
99385	5	627738 CRA_00129	93 M	KDM6A	66 mut	3	23047	20491	3703	81823
99385	5	627738 CRA_00129	93 M	KDM6A	66 mut	3	23047	20491	3703	81823
99385	5	627738 CRA_00129	93 M	KDM6A	66 mut	3	23047	20491	3703	81823
99385	5	627738 CRA_00129	93 M	KDM6A	66 mut	4	23002	20555	3703	81823
99385	5	627738 CRA_00129	93 M	KDM6A	66 mut	4	23002	20555	3703	81823
99385	5	627738 CRA_00129	93 M	KDM6A	66 mut	4	23002	20555	3703	81823
99385	5	627738 CRA_00129	93 M	KDM6A	66 mut	5	23156	20685	3919	81823
99385	5	627738 CRA_00129	93 M	KDM6A	66 mut	5	23156	20685	3919	81823
99385	5	627738 CRA_00129	93 M	KDM6A	66 mut	5	23156	20685	3919	81823
99385	5	627738 CRA_00129	93 M	KDM6A	66 mut	6	23280	20506	3294	81823
99385	5	627738 CRA_00129	93 M	KDM6A	66 mut	6	23280	20506	3294	81823
99385	5	627738 CRA_00129	93 M	KDM6A	66 mut	6	23280	20506	3294	81823
99385	5	627738 CRA_00129	93 M	KDM6A	66 mut	7	23278	20590	3541	81823
99385	5	627738 CRA_00129	93 M	KDM6A	66 mut	7	23278	20590	3541	81823
99385	5	627738 CRA_00129	93 M	KDM6A	66 mut	7	23278	20590	3541	81823
99385	5	627738 CRA_00129	93 M	KDM6A	66 mut	8	23395	20455	3092	81823
99385	5	627738 CRA_00129	93 M	KDM6A	66 mut	8	23395	20455	3092	81823
99385	5	627738 CRA_00129	93 M	KDM6A	66 mut	8	23395	20455	3092	81823
99385	5	627738 CRA_00129	93 M	KDM6A	66 mut	9	23363	20526	1829	81823
99385	5	627738 CRA_00129	93 M	KDM6A	66 mut	9	23363	20526	1829	81823
99385	5	627738 CRA_00129	93 M	KDM6A	66 mut	9	23363	20526	1829	81823
99385	5	627738 CRA_00129	93 M	KDM6A	66 mut	10	23353	20598	2685	81823
99385	5	627738 CRA_00129	93 M	KDM6A	66 mut	10	23353	20598	2685	81823
99385	5	627738 CRA_00129	93 M	KDM6A	66 mut	10	23353	20598	2685	81823
99385	5	627738 CRA_00129	93 M	KDM6A	67 WT	1	23084	20433	1702	62812
99385	5	627738 CRA_00129	93 M	KDM6A	67 WT	1	23084	20433	1702	62812
99385	5	627738 CRA_00129	93 M	KDM6A	67 WT	1	23084	20433	1702	62812
99385	5	627738 CRA_00129	93 M	KDM6A	67 WT	2	23067	20333	1645	62812
99385	5	627738 CRA_00129	93 M	KDM6A	67 WT	2	23067	20333	1645	62812
99385	5	627738 CRA_00129	93 M	KDM6A	67 WT	2	23067	20333	1645	62812
99385	5	627738 CRA_00129	93 M	KDM6A	67 WT	3	23087	20379	1744	62812
99385	5	627738 CRA_00129	93 M	KDM6A	67 WT	3	23087	20379	1744	62812
99385	5	627738 CRA_00129	93 M	KDM6A	67 WT	3	23087	20379	1744	62812
99385	5	627738 CRA_00129	93 M	KDM6A	67 WT	4	23181	20397	2097	62812

99385	5	627738 CRA_00129	93 M	KDM6A	67 WT	4	23181	20397	2097	62812
99385	5	627738 CRA_00129	93 M	KDM6A	67 WT	4	23181	20397	2097	62812
99385	5	627738 CRA_00129	93 M	KDM6A	67 WT	5	23194	20341	3784	62812
99385	5	627738 CRA_00129	93 M	KDM6A	67 WT	5	23194	20341	3784	62812
99385	5	627738 CRA_00129	93 M	KDM6A	67 WT	5	23194	20341	3784	62812
99385	5	627738 CRA_00129	93 M	KDM6A	67 WT	6	23242	20419	1849	62812
99385	5	627738 CRA_00129	93 M	KDM6A	67 WT	6	23242	20419	1849	62812
99385	5	627738 CRA_00129	93 M	KDM6A	67 WT	6	23242	20419	1849	62812
99385	5	627738 CRA_00129	93 M	KDM6A	67 WT	7	22978	20279	2307	62812
99385	5	627738 CRA_00129	93 M	KDM6A	67 WT	7	22978	20279	2307	62812
99385	5	627738 CRA_00129	93 M	KDM6A	67 WT	7	22978	20279	2307	62812
99385	5	627738 CRA_00129	93 M	KDM6A	67 WT	8	23088	20261	4135	62812
99385	5	627738 CRA_00129	93 M	KDM6A	67 WT	8	23088	20261	4135	62812
99385	5	627738 CRA_00129	93 M	KDM6A	67 WT	8	23088	20261	4135	62812
99385	5	627738 CRA_00129	93 M	KDM6A	67 WT	9	23306	20348	2203	62812
99385	5	627738 CRA_00129	93 M	KDM6A	67 WT	9	23306	20348	2203	62812
99385	5	627738 CRA_00129	93 M	KDM6A	67 WT	9	23306	20348	2203	62812
99385	5	627738 CRA_00129	93 M	KDM6A	67 WT	10	23196	20463	2011	62812
99385	5	627738 CRA_00129	93 M	KDM6A	67 WT	10	23196	20463	2011	62812
99385	5	627738 CRA_00129	93 M	KDM6A	67 WT	10	23196	20463	2011	62812
99385	5	627738 CRA_00129	93 M	KDM6A	68 WT	1	22887	20451	1824	44630
99385	5	627738 CRA_00129	93 M	KDM6A	68 WT	1	22887	20451	1824	44630
99385	5	627738 CRA_00129	93 M	KDM6A	68 WT	1	22887	20451	1824	44630
99385	5	627738 CRA_00129	93 M	KDM6A	68 WT	2	22815	20442	2213	44630
99385	5	627738 CRA_00129	93 M	KDM6A	68 WT	2	22815	20442	2213	44630
99385	5	627738 CRA_00129	93 M	KDM6A	68 WT	2	22815	20442	2213	44630
99385	5	627738 CRA_00129	93 M	KDM6A	68 WT	3	22865	20505	1675	44630
99385	5	627738 CRA_00129	93 M	KDM6A	68 WT	3	22865	20505	1675	44630
99385	5	627738 CRA_00129	93 M	KDM6A	68 WT	3	22865	20505	1675	44630
99385	5	627738 CRA_00129	93 M	KDM6A	68 WT	4	22821	20556	2111	44630
99385	5	627738 CRA_00129	93 M	KDM6A	68 WT	4	22821	20556	2111	44630
99385	5	627738 CRA_00129	93 M	KDM6A	68 WT	4	22821	20556	2111	44630
99385	5	627738 CRA_00129	93 M	KDM6A	68 WT	5	22946	20408	1249	44630
99385	5	627738 CRA_00129	93 M	KDM6A	68 WT	5	22946	20408	1249	44630
99385	5	627738 CRA_00129	93 M	KDM6A	68 WT	5	22946	20408	1249	44630
99385	5	627738 CRA_00129	93 M	KDM6A	68 WT	6	22977	20447	1359	44630
99385	5	627738 CRA_00129	93 M	KDM6A	68 WT	6	22977	20447	1359	44630
99385	5	627738 CRA_00129	93 M	KDM6A	68 WT	6	22977	20447	1359	44630
99385	5	627738 CRA_00129	93 M	KDM6A	68 WT	7	22879	20399	1641	44630
99385	5	627738 CRA_00129	93 M	KDM6A	68 WT	7	22879	20399	1641	44630
99385	5	627738 CRA_00129	93 M	KDM6A	68 WT	7	22879	20399	1641	44630

99385	5	627738 CRA_00129	93 M	KDM6A	68 WT	8	22959	20495	1354	44630
99385	5	627738 CRA_00129	93 M	KDM6A	68 WT	8	22959	20495	1354	44630
99385	5	627738 CRA_00129	93 M	KDM6A	68 WT	8	22959	20495	1354	44630
99385	5	627738 CRA_00129	93 M	KDM6A	68 WT	9	22910	20552	1877	44630
99385	5	627738 CRA_00129	93 M	KDM6A	68 WT	9	22910	20552	1877	44630
99385	5	627738 CRA_00129	93 M	KDM6A	68 WT	9	22910	20552	1877	44630
99385	5	627738 CRA_00129	93 M	KDM6A	68 WT	10	22793	20509	1575	44630
99385	5	627738 CRA_00129	93 M	KDM6A	68 WT	10	22793	20509	1575	44630
99385	5	627738 CRA_00129	93 M	KDM6A	68 WT	10	22793	20509	1575	44630
99385	5	627738 CRA_00129	93 M	KDM6A	69 WT	1	22979	19850	1213	36823
99385	5	627738 CRA_00129	93 M	KDM6A	69 WT	1	22979	19850	1213	36823
99385	5	627738 CRA_00129	93 M	KDM6A	69 WT	1	22979	19850	1213	36823
99385	5	627738 CRA_00129	93 M	KDM6A	69 WT	2	22905	19859	1227	36823
99385	5	627738 CRA_00129	93 M	KDM6A	69 WT	2	22905	19859	1227	36823
99385	5	627738 CRA_00129	93 M	KDM6A	69 WT	2	22905	19859	1227	36823
99385	5	627738 CRA_00129	93 M	KDM6A	69 WT	3	22899	19810	946	36823
99385	5	627738 CRA_00129	93 M	KDM6A	69 WT	3	22899	19810	946	36823
99385	5	627738 CRA_00129	93 M	KDM6A	69 WT	3	22899	19810	946	36823
99385	5	627738 CRA_00129	93 M	KDM6A	69 WT	4	23006	19895	1531	36823
99385	5	627738 CRA_00129	93 M	KDM6A	69 WT	4	23006	19895	1531	36823
99385	5	627738 CRA_00129	93 M	KDM6A	69 WT	4	23006	19895	1531	36823
99385	5	627738 CRA_00129	93 M	KDM6A	69 WT	5	22915	19900	1558	36823
99385	5	627738 CRA_00129	93 M	KDM6A	69 WT	5	22915	19900	1558	36823
99385	5	627738 CRA_00129	93 M	KDM6A	69 WT	5	22915	19900	1558	36823
99385	5	627738 CRA_00129	93 M	KDM6A	69 WT	6	22963	19811	1021	36823
99385	5	627738 CRA_00129	93 M	KDM6A	69 WT	6	22963	19811	1021	36823
99385	5	627738 CRA_00129	93 M	KDM6A	69 WT	6	22963	19811	1021	36823
99385	5	627738 CRA_00129	93 M	KDM6A	69 WT	7	23052	19839	1423	36823
99385	5	627738 CRA_00129	93 M	KDM6A	69 WT	7	23052	19839	1423	36823
99385	5	627738 CRA_00129	93 M	KDM6A	69 WT	7	23052	19839	1423	36823
99385	5	627738 CRA_00129	93 M	KDM6A	69 WT	8	22848	19850	778	36823
99385	5	627738 CRA_00129	93 M	KDM6A	69 WT	8	22848	19850	778	36823
99385	5	627738 CRA_00129	93 M	KDM6A	69 WT	8	22848	19850	778	36823
99385	5	627738 CRA_00129	93 M	KDM6A	69 WT	9	22909	19949	1461	36823
99385	5	627738 CRA_00129	93 M	KDM6A	69 WT	9	22909	19949	1461	36823
99385	5	627738 CRA_00129	93 M	KDM6A	69 WT	9	22909	19949	1461	36823
99385	5	627738 CRA_00129	93 M	KDM6A	69 WT	10	22972	19957	2054	36823
99385	5	627738 CRA_00129	93 M	KDM6A	69 WT	10	22972	19957	2054	36823
99385	5	627738 CRA_00129	93 M	KDM6A	69 WT	10	22972	19957	2054	36823
99385	5	627738 CRA_00129	93 M	KDM6A	90 mut3_WT7	1	23363	20526	1829	60279
99385	5	627738 CRA_00129	93 M	KDM6A	90 mut3_WT7	1	23363	20526	1829	60279

99385	5	627738 CRA_00129	93 M	KDM6A	94 mut1_WT9	2	23395	20455	3092	46741
99385	5	627738 CRA_00129	93 M	KDM6A	94 mut1_WT9	3	23413	20392	1663	46741
99385	5	627738 CRA_00129	93 M	KDM6A	94 mut1_WT9	3	23413	20392	1663	46741
99385	5	627738 CRA_00129	93 M	KDM6A	94 mut1_WT9	3	23413	20392	1663	46741
99385	5	627738 CRA_00129	93 M	KDM6A	94 mut1_WT9	4	23487	20389	2698	46741
99385	5	627738 CRA_00129	93 M	KDM6A	94 mut1_WT9	4	23487	20389	2698	46741
99385	5	627738 CRA_00129	93 M	KDM6A	94 mut1_WT9	4	23487	20389	2698	46741
99385	5	627738 CRA_00129	93 M	KDM6A	94 mut1_WT9	5	23477	20334	1192	46741
99385	5	627738 CRA_00129	93 M	KDM6A	94 mut1_WT9	5	23477	20334	1192	46741
99385	5	627738 CRA_00129	93 M	KDM6A	94 mut1_WT9	5	23477	20334	1192	46741
99385	5	627738 CRA_00129	93 M	KDM6A	94 mut1_WT9	6	23412	20325	1150	46741
99385	5	627738 CRA_00129	93 M	KDM6A	94 mut1_WT9	6	23412	20325	1150	46741
99385	5	627738 CRA_00129	93 M	KDM6A	94 mut1_WT9	6	23412	20325	1150	46741
99385	5	627738 CRA_00129	93 M	KDM6A	94 mut1_WT9	7	23442	20282	1818	46741
99385	5	627738 CRA_00129	93 M	KDM6A	94 mut1_WT9	7	23442	20282	1818	46741
99385	5	627738 CRA_00129	93 M	KDM6A	94 mut1_WT9	7	23442	20282	1818	46741
99385	5	627738 CRA_00129	93 M	KDM6A	94 mut1_WT9	8	23576	20373	2425	46741
99385	5	627738 CRA_00129	93 M	KDM6A	94 mut1_WT9	8	23576	20373	2425	46741
99385	5	627738 CRA_00129	93 M	KDM6A	94 mut1_WT9	8	23576	20373	2425	46741
99385	5	627738 CRA_00129	93 M	KDM6A	94 mut1_WT9	9	23535	20435	1692	46741
99385	5	627738 CRA_00129	93 M	KDM6A	94 mut1_WT9	9	23535	20435	1692	46741
99385	5	627738 CRA_00129	93 M	KDM6A	94 mut1_WT9	9	23535	20435	1692	46741
99385	5	627738 CRA_00129	93 M	KDM6A	94 mut1_WT9	10	23530	20489	2458	46741
99385	5	627738 CRA_00129	93 M	KDM6A	94 mut1_WT9	10	23530	20489	2458	46741
99385	5	627738 CRA_00129	93 M	KDM6A	94 mut1_WT9	10	23530	20489	2458	46741
99385	5	627738 CRA_00129	93 M	KDM6A	95 mut1_WT9	1	23047	20491	3703	46268
99385	5	627738 CRA_00129	93 M	KDM6A	95 mut1_WT9	1	23047	20491	3703	46268
99385	5	627738 CRA_00129	93 M	KDM6A	95 mut1_WT9	1	23047	20491	3703	46268
99385	5	627738 CRA_00129	93 M	KDM6A	95 mut1_WT9	2	22959	20495	1354	46268
99385	5	627738 CRA_00129	93 M	KDM6A	95 mut1_WT9	2	22959	20495	1354	46268
99385	5	627738 CRA_00129	93 M	KDM6A	95 mut1_WT9	2	22959	20495	1354	46268
99385	5	627738 CRA_00129	93 M	KDM6A	95 mut1_WT9	3	22977	20447	1359	46268
99385	5	627738 CRA_00129	93 M	KDM6A	95 mut1_WT9	3	22977	20447	1359	46268
99385	5	627738 CRA_00129	93 M	KDM6A	95 mut1_WT9	3	22977	20447	1359	46268
99385	5	627738 CRA_00129	93 M	KDM6A	95 mut1_WT9	4	22946	20408	1249	46268
99385	5	627738 CRA_00129	93 M	KDM6A	95 mut1_WT9	4	22946	20408	1249	46268
99385	5	627738 CRA_00129	93 M	KDM6A	95 mut1_WT9	4	22946	20408	1249	46268
99385	5	627738 CRA_00129	93 M	KDM6A	95 mut1_WT9	5	23084	20433	1702	46268
99385	5	627738 CRA_00129	93 M	KDM6A	95 mut1_WT9	5	23084	20433	1702	46268
99385	5	627738 CRA_00129	93 M	KDM6A	95 mut1_WT9	5	23084	20433	1702	46268
99385	5	627738 CRA_00129	93 M	KDM6A	95 mut1_WT9	6	23025	20406	1378	46268

99385	5	627738 CRA_00129	93 M	KDM6A	95 mut1_WT9	6	23025	20406	1378	46268
99385	5	627738 CRA_00129	93 M	KDM6A	95 mut1_WT9	6	23025	20406	1378	46268
99385	5	627738 CRA_00129	93 M	KDM6A	95 mut1_WT9	7	23087	20379	1744	46268
99385	5	627738 CRA_00129	93 M	KDM6A	95 mut1_WT9	7	23087	20379	1744	46268
99385	5	627738 CRA_00129	93 M	KDM6A	95 mut1_WT9	7	23087	20379	1744	46268
99385	5	627738 CRA_00129	93 M	KDM6A	95 mut1_WT9	8	23067	20333	1645	46268
99385	5	627738 CRA_00129	93 M	KDM6A	95 mut1_WT9	8	23067	20333	1645	46268
99385	5	627738 CRA_00129	93 M	KDM6A	95 mut1_WT9	8	23067	20333	1645	46268
99385	5	627738 CRA_00129	93 M	KDM6A	95 mut1_WT9	9	22982	20357	1973	46268
99385	5	627738 CRA_00129	93 M	KDM6A	95 mut1_WT9	9	22982	20357	1973	46268
99385	5	627738 CRA_00129	93 M	KDM6A	95 mut1_WT9	9	22982	20357	1973	46268
99385	5	627738 CRA_00129	93 M	KDM6A	95 mut1_WT9	10	22914	20347	1555	46268
99385	5	627738 CRA_00129	93 M	KDM6A	95 mut1_WT9	10	22914	20347	1555	46268
99385	5	627738 CRA_00129	93 M	KDM6A	95 mut1_WT9	10	22914	20347	1555	46268
99385	5	627738 CRA_00129	93 M	KDM6A	96 WT	1	23530	20489	2458	39502
99385	5	627738 CRA_00129	93 M	KDM6A	96 WT	1	23530	20489	2458	39502
99385	5	627738 CRA_00129	93 M	KDM6A	96 WT	1	23530	20489	2458	39502
99385	5	627738 CRA_00129	93 M	KDM6A	96 WT	2	23535	20435	1692	39502
99385	5	627738 CRA_00129	93 M	KDM6A	96 WT	2	23535	20435	1692	39502
99385	5	627738 CRA_00129	93 M	KDM6A	96 WT	2	23535	20435	1692	39502
99385	5	627738 CRA_00129	93 M	KDM6A	96 WT	3	23576	20373	2425	39502
99385	5	627738 CRA_00129	93 M	KDM6A	96 WT	3	23576	20373	2425	39502
99385	5	627738 CRA_00129	93 M	KDM6A	96 WT	3	23576	20373	2425	39502
99385	5	627738 CRA_00129	93 M	KDM6A	96 WT	4	23487	20389	2698	39502
99385	5	627738 CRA_00129	93 M	KDM6A	96 WT	4	23487	20389	2698	39502
99385	5	627738 CRA_00129	93 M	KDM6A	96 WT	4	23487	20389	2698	39502
99385	5	627738 CRA_00129	93 M	KDM6A	96 WT	5	23477	20334	1192	39502
99385	5	627738 CRA_00129	93 M	KDM6A	96 WT	5	23477	20334	1192	39502
99385	5	627738 CRA_00129	93 M	KDM6A	96 WT	5	23477	20334	1192	39502
99385	5	627738 CRA_00129	93 M	KDM6A	96 WT	6	23604	20479	2038	39502
99385	5	627738 CRA_00129	93 M	KDM6A	96 WT	6	23604	20479	2038	39502
99385	5	627738 CRA_00129	93 M	KDM6A	96 WT	6	23604	20479	2038	39502
99385	5	627738 CRA_00129	93 M	KDM6A	96 WT	7	23609	20426	1150	39502
99385	5	627738 CRA_00129	93 M	KDM6A	96 WT	7	23609	20426	1150	39502
99385	5	627738 CRA_00129	93 M	KDM6A	96 WT	7	23609	20426	1150	39502
99385	5	627738 CRA_00129	93 M	KDM6A	96 WT	8	23647	20384	1882	39502
99385	5	627738 CRA_00129	93 M	KDM6A	96 WT	8	23647	20384	1882	39502
99385	5	627738 CRA_00129	93 M	KDM6A	96 WT	8	23647	20384	1882	39502
99385	5	627738 CRA_00129	93 M	KDM6A	96 WT	9	23661	20340	1422	39502
99385	5	627738 CRA_00129	93 M	KDM6A	96 WT	9	23661	20340	1422	39502
99385	5	627738 CRA_00129	93 M	KDM6A	96 WT	9	23661	20340	1422	39502

99385	5	627738 CRA_00129	93 M	KDM6A	96 WT	10	23611	20309	975	39502
99385	5	627738 CRA_00129	93 M	KDM6A	96 WT	10	23611	20309	975	39502
99385	5	627738 CRA_00129	93 M	KDM6A	96 WT	10	23611	20309	975	39502
119329	5	627772 CRA_00316	85 M	KDM6A	74 mut	1	10365	13536	6049	115666
119329	5	627772 CRA_00316	85 M	KDM6A	74 mut	2	10447	13458	4902	115666
119329	5	627772 CRA_00316	85 M	KDM6A	74 mut	3	10446	13580	4100	115666
119329	5	627772 CRA_00316	85 M	KDM6A	74 mut	4	10480	13658	7397	115666
119329	5	627772 CRA_00316	85 M	KDM6A	74 mut	5	10506	13527	5425	115666
119329	5	627772 CRA_00316	85 M	KDM6A	74 mut	6	10588	13570	7412	115666
119329	5	627772 CRA_00316	85 M	KDM6A	74 mut	7	10575	13457	8309	115666
119329	5	627772 CRA_00316	85 M	KDM6A	74 mut	8	10674	13624	6974	115666
119329	5	627772 CRA_00316	85 M	KDM6A	74 mut	9	10728	13521	6292	115666
119329	5	627772 CRA_00316	85 M	KDM6A	74 mut	10	10707	13444	7124	115666
119329	5	627772 CRA_00316	85 M	KDM6A	75 WT	1	10799	13360	5868	90126
119329	5	627772 CRA_00316	85 M	KDM6A	75 WT	2	10838	13424	4917	90126
119329	5	627772 CRA_00316	85 M	KDM6A	75 WT	3	10886	13499	6039	90126
119329	5	627772 CRA_00316	85 M	KDM6A	75 WT	4	10938	13378	5006	90126
119329	5	627772 CRA_00316	85 M	KDM6A	75 WT	5	10989	13443	4358	90126
119329	5	627772 CRA_00316	85 M	KDM6A	75 WT	6	11032	13327	5026	90126
119329	5	627772 CRA_00316	85 M	KDM6A	75 WT	7	11073	13394	3254	90126
119329	5	627772 CRA_00316	85 M	KDM6A	75 WT	8	11095	13459	4109	90126
119329	5	627772 CRA_00316	85 M	KDM6A	75 WT	9	11144	13355	3136	90126
119329	5	627772 CRA_00316	85 M	KDM6A	75 WT	10	11197	13418	3964	90126
119329	5	627772 CRA_00316	85 M	KDM6A	76 WT	1	10248	14135	5156	86922
119329	5	627772 CRA_00316	85 M	KDM6A	76 WT	2	10338	14198	4167	86922
119329	5	627772 CRA_00316	85 M	KDM6A	76 WT	3	10371	14295	4029	86922
119329	5	627772 CRA_00316	85 M	KDM6A	76 WT	4	10347	14088	3906	86922
119329	5	627772 CRA_00316	85 M	KDM6A	76 WT	5	10415	14147	4597	86922
119329	5	627772 CRA_00316	85 M	KDM6A	76 WT	6	10436	14249	3289	86922
119329	5	627772 CRA_00316	85 M	KDM6A	76 WT	7	10427	14030	3605	86922
119329	5	627772 CRA_00316	85 M	KDM6A	76 WT	8	10495	14092	3700	86922
119329	5	627772 CRA_00316	85 M	KDM6A	76 WT	9	10492	14196	3746	86922
119329	5	627772 CRA_00316	85 M	KDM6A	76 WT	10	10566	14161	3812	86922
119329	5	627772 CRA_00316	85 M	KDM6A	77 WT	1	11138	14236	4582	70144
119329	5	627772 CRA_00316	85 M	KDM6A	77 WT	2	11197	14301	3819	70144
119329	5	627772 CRA_00316	85 M	KDM6A	77 WT	3	11147	14149	3114	70144
119329	5	627772 CRA_00316	85 M	KDM6A	77 WT	4	11230	14228	3142	70144
119329	5	627772 CRA_00316	85 M	KDM6A	77 WT	5	11286	14292	3562	70144
119329	5	627772 CRA_00316	85 M	KDM6A	77 WT	6	11196	14090	3265	70144
119329	5	627772 CRA_00316	85 M	KDM6A	77 WT	7	11249	14164	2760	70144
119329	5	627772 CRA_00316	85 M	KDM6A	77 WT	8	11329	14220	4625	70144

119329	5	627772 CRA_00316	85 M	KDM6A	77 WT	9	11270	14064	3523	70144
119329	5	627772 CRA_00316	85 M	KDM6A	77 WT	10	11325	14127	3468	70144
122238	5	642672 CRA_00349	37 M	KDM6A	14 mut	1	15172	12647	4236	90436
122238	5	642672 CRA_00349	37 M	KDM6A	14 mut	2	15243	12638	2794	90436
122238	5	642672 CRA_00349	37 M	KDM6A	14 mut	3	15236	12713	3555	90436
122238	5	642672 CRA_00349	37 M	KDM6A	14 mut	4	15334	12723	4508	90436
122238	5	642672 CRA_00349	37 M	KDM6A	14 mut	5	15303	12584	2594	90436
122238	5	642672 CRA_00349	37 M	KDM6A	14 mut	6	15364	12640	4677	90436
122238	5	642672 CRA_00349	37 M	KDM6A	14 mut	7	15354	12502	4773	90436
122238	5	642672 CRA_00349	37 M	KDM6A	14 mut	8	15442	12701	6021	90436
122238	5	642672 CRA_00349	37 M	KDM6A	14 mut	9	15489	12597	4829	90436
122238	5	642672 CRA_00349	37 M	KDM6A	14 mut	10	15434	12536	4988	90436
122238	5	642672 CRA_00349	37 M	KDM6A	15 WT	1	15571	12602	3415	78663
122238	5	642672 CRA_00349	37 M	KDM6A	15 WT	2	15557	12679	1971	78663
122238	5	642672 CRA_00349	37 M	KDM6A	15 WT	3	15520	12761	4192	78663
122238	5	642672 CRA_00349	37 M	KDM6A	15 WT	4	15642	12580	3333	78663
122238	5	642672 CRA_00349	37 M	KDM6A	15 WT	5	15631	12688	3406	78663
122238	5	642672 CRA_00349	37 M	KDM6A	15 WT	6	15608	12787	4792	78663
122238	5	642672 CRA_00349	37 M	KDM6A	15 WT	7	15698	12616	3415	78663
122238	5	642672 CRA_00349	37 M	KDM6A	15 WT	8	15695	12752	5068	78663
122238	5	642672 CRA_00349	37 M	KDM6A	15 WT	9	15758	12674	3814	78663
122238	5	642672 CRA_00349	37 M	KDM6A	15 WT	10	15526	12852	4827	78663
122238	5	642672 CRA_00349	37 M	KDM6A	16 WT	1	15244	12808	4540	88628
122238	5	642672 CRA_00349	37 M	KDM6A	16 WT	2	15330	12820	3987	88628
122238	5	642672 CRA_00349	37 M	KDM6A	16 WT	3	15433	12809	4442	88628
122238	5	642672 CRA_00349	37 M	KDM6A	16 WT	4	15319	12903	5765	88628
122238	5	642672 CRA_00349	37 M	KDM6A	16 WT	5	15421	12905	5444	88628
122238	5	642672 CRA_00349	37 M	KDM6A	16 WT	6	15197	12881	3933	88628
122238	5	642672 CRA_00349	37 M	KDM6A	16 WT	7	15162	12816	2197	88628
122238	5	642672 CRA_00349	37 M	KDM6A	16 WT	8	15116	12904	4409	88628
122238	5	642672 CRA_00349	37 M	KDM6A	16 WT	9	15207	12960	4851	88628
122238	5	642672 CRA_00349	37 M	KDM6A	16 WT	10	15099	13005	4461	88628
122238	5	642672 CRA_00349	37 M	KDM6A	17 WT	1	15604	12318	4709	70389
122238	5	642672 CRA_00349	37 M	KDM6A	17 WT	2	15531	12304	3603	70389
122238	5	642672 CRA_00349	37 M	KDM6A	17 WT	3	15654	12372	4105	70389
122238	5	642672 CRA_00349	37 M	KDM6A	17 WT	4	15678	12442	2751	70389
122238	5	642672 CRA_00349	37 M	KDM6A	17 WT	5	15484	12375	3364	70389
122238	5	642672 CRA_00349	37 M	KDM6A	17 WT	6	15531	12431	3896	70389
122238	5	642672 CRA_00349	37 M	KDM6A	17 WT	7	15579	12437	2560	70389
122238	5	642672 CRA_00349	37 M	KDM6A	17 WT	8	15610	12483	3196	70389
122238	5	642672 CRA_00349	37 M	KDM6A	17 WT	9	15719	12482	3475	70389

122238	5	642672 CRA_00349	37 M	KDM6A	17 WT	10	15743	12376	3468	70389
119338	5	642674 CRA_00317	69 M	KDM6A	6 mut	1	8607	17572	4056	90734
119338	5	642674 CRA_00317	69 M	KDM6A	6 mut	2	8671	17649	4957	90734
119338	5	642674 CRA_00317	69 M	KDM6A	6 mut	3	8720	17747	4561	90734
119338	5	642674 CRA_00317	69 M	KDM6A	6 mut	4	8746	17557	4058	90734
119338	5	642674 CRA_00317	69 M	KDM6A	6 mut	5	8762	17643	3579	90734
119338	5	642674 CRA_00317	69 M	KDM6A	6 mut	6	8788	17725	3806	90734
119338	5	642674 CRA_00317	69 M	KDM6A	6 mut	7	8800	17508	3269	90734
119338	5	642674 CRA_00317	69 M	KDM6A	6 mut	8	8884	17577	2994	90734
119338	5	642674 CRA_00317	69 M	KDM6A	6 mut	9	8861	17649	5296	90734
119338	5	642674 CRA_00317	69 M	KDM6A	6 mut	10	8880	17742	4106	90734
119338	5	642674 CRA_00317	69 M	KDM6A	7 WT	1	9040	17447	2723	90760
119338	5	642674 CRA_00317	69 M	KDM6A	7 WT	2	8992	17500	2924	90760
119338	5	642674 CRA_00317	69 M	KDM6A	7 WT	3	8997	17577	2884	90760
119338	5	642674 CRA_00317	69 M	KDM6A	7 WT	4	8974	17643	2447	90760
119338	5	642674 CRA_00317	69 M	KDM6A	7 WT	5	9110	17575	2605	90760
119338	5	642674 CRA_00317	69 M	KDM6A	7 WT	6	9108	17649	2799	90760
119338	5	642674 CRA_00317	69 M	KDM6A	7 WT	7	9142	17505	3095	90760
119338	5	642674 CRA_00317	69 M	KDM6A	7 WT	8	9201	17608	3010	90760
119338	5	642674 CRA_00317	69 M	KDM6A	7 WT	9	9265	17531	3137	90760
119338	5	642674 CRA_00317	69 M	KDM6A	7 WT	10	9301	17615	2488	90760
119338	5	642674 CRA_00317	69 M	KDM6A	8 WT	1	8894	17498	2844	93866
119338	5	642674 CRA_00317	69 M	KDM6A	8 WT	2	8864	17428	2761	93866
119338	5	642674 CRA_00317	69 M	KDM6A	8 WT	3	8909	17378	2848	93866
119338	5	642674 CRA_00317	69 M	KDM6A	8 WT	4	8994	17365	2848	93866
119338	5	642674 CRA_00317	69 M	KDM6A	8 WT	5	9067	17331	2804	93866
119338	5	642674 CRA_00317	69 M	KDM6A	8 WT	6	9195	17308	3299	93866
119338	5	642674 CRA_00317	69 M	KDM6A	8 WT	7	9147	17223	2984	93866
119338	5	642674 CRA_00317	69 M	KDM6A	8 WT	8	9035	17259	2243	93866
119338	5	642674 CRA_00317	69 M	KDM6A	8 WT	9	8941	17282	2145	93866
119338	5	642674 CRA_00317	69 M	KDM6A	8 WT	10	8846	17309	2344	93866
119338	5	642674 CRA_00317	69 M	KDM6A	9 WT	1	8586	17201	3333	94378
119338	5	642674 CRA_00317	69 M	KDM6A	9 WT	2	8563	17297	2747	94378
119338	5	642674 CRA_00317	69 M	KDM6A	9 WT	3	8570	17376	2909	94378
119338	5	642674 CRA_00317	69 M	KDM6A	9 WT	4	8650	17348	3246	94378
119338	5	642674 CRA_00317	69 M	KDM6A	9 WT	5	8663	17271	3555	94378
119338	5	642674 CRA_00317	69 M	KDM6A	9 WT	6	8760	17330	2439	94378
119338	5	642674 CRA_00317	69 M	KDM6A	9 WT	7	8766	17235	3742	94378
119338	5	642674 CRA_00317	69 M	KDM6A	9 WT	8	8697	17181	3379	94378
119338	5	642674 CRA_00317	69 M	KDM6A	9 WT	9	8498	17243	2630	94378
119338	5	642674 CRA_00317	69 M	KDM6A	9 WT	10	8654	17108	3650	94378

119338	5	642674 CRA_00317	69 M	KDM6A	97 mut3_WT7	1	8746	17557	4058	80301
119338	5	642674 CRA_00317	69 M	KDM6A	97 mut3_WT7	2	8800	17508	3269	80301
119338	5	642674 CRA_00317	69 M	KDM6A	97 mut3_WT7	3	8884	17577	2994	80301
119338	5	642674 CRA_00317	69 M	KDM6A	97 mut3_WT7	4	8894	17498	2844	80301
119338	5	642674 CRA_00317	69 M	KDM6A	97 mut3_WT7	5	8864	17428	2761	80301
119338	5	642674 CRA_00317	69 M	KDM6A	97 mut3_WT7	6	8909	17378	2848	80301
119338	5	642674 CRA_00317	69 M	KDM6A	97 mut3_WT7	7	8846	17309	2344	80301
119338	5	642674 CRA_00317	69 M	KDM6A	97 mut3_WT7	8	8760	17330	2439	80301
119338	5	642674 CRA_00317	69 M	KDM6A	97 mut3_WT7	9	8776	17418	2577	80301
119338	5	642674 CRA_00317	69 M	KDM6A	97 mut3_WT7	10	8696	17446	3528	80301
119338	5	642674 CRA_00317	69 M	KDM6A	98 mut3_WT7	1	8671	17649	4957	88471
119338	5	642674 CRA_00317	69 M	KDM6A	98 mut3_WT7	2	8607	17572	4056	88471
119338	5	642674 CRA_00317	69 M	KDM6A	98 mut3_WT7	3	8746	17557	4058	88471
119338	5	642674 CRA_00317	69 M	KDM6A	98 mut3_WT7	4	8696	17446	3528	88471
119338	5	642674 CRA_00317	69 M	KDM6A	98 mut3_WT7	5	8668	17526	2325	88471
119338	5	642674 CRA_00317	69 M	KDM6A	98 mut3_WT7	6	8613	17470	3686	88471
119338	5	642674 CRA_00317	69 M	KDM6A	98 mut3_WT7	7	8505	17417	3326	88471
119338	5	642674 CRA_00317	69 M	KDM6A	98 mut3_WT7	8	8460	17479	3470	88471
119338	5	642674 CRA_00317	69 M	KDM6A	98 mut3_WT7	9	8492	17559	3981	88471
119338	5	642674 CRA_00317	69 M	KDM6A	98 mut3_WT7	10	8532	17632	3065	88471
119338	5	642674 CRA_00317	69 M	KDM6A	99 mut2_WT8	1	8746	17557	4058	83280
119338	5	642674 CRA_00317	69 M	KDM6A	99 mut2_WT8	2	8800	17508	3269	83280
119338	5	642674 CRA_00317	69 M	KDM6A	99 mut2_WT8	3	8668	17526	2325	83280
119338	5	642674 CRA_00317	69 M	KDM6A	99 mut2_WT8	4	8613	17470	3686	83280
119338	5	642674 CRA_00317	69 M	KDM6A	99 mut2_WT8	5	8696	17446	3528	83280
119338	5	642674 CRA_00317	69 M	KDM6A	99 mut2_WT8	6	8776	17418	2577	83280
119338	5	642674 CRA_00317	69 M	KDM6A	99 mut2_WT8	7	8864	17428	2761	83280
119338	5	642674 CRA_00317	69 M	KDM6A	99 mut2_WT8	8	8846	17309	2344	83280
119338	5	642674 CRA_00317	69 M	KDM6A	99 mut2_WT8	9	8760	17330	2439	83280
119338	5	642674 CRA_00317	69 M	KDM6A	99 mut2_WT8	10	8650	17348	3246	83280
119338	5	642674 CRA_00317	69 M	KDM6A	100 mut2_WT8	1	8861	17649	5296	91253
119338	5	642674 CRA_00317	69 M	KDM6A	100 mut2_WT8	2	8884	17577	2994	91253
119338	5	642674 CRA_00317	69 M	KDM6A	100 mut2_WT8	3	8894	17498	2844	91253
119338	5	642674 CRA_00317	69 M	KDM6A	100 mut2_WT8	4	8974	17643	2447	91253
119338	5	642674 CRA_00317	69 M	KDM6A	100 mut2_WT8	5	8997	17577	2884	91253
119338	5	642674 CRA_00317	69 M	KDM6A	100 mut2_WT8	6	8992	17500	2924	91253
119338	5	642674 CRA_00317	69 M	KDM6A	100 mut2_WT8	7	9040	17447	2723	91253
119338	5	642674 CRA_00317	69 M	KDM6A	100 mut2_WT8	8	9108	17649	2799	91253
119338	5	642674 CRA_00317	69 M	KDM6A	100 mut2_WT8	9	9110	17575	2605	91253
119338	5	642674 CRA_00317	69 M	KDM6A	100 mut2_WT8	10	9142	17505	3095	91253
119338	5	642674 CRA_00317	69 M	KDM6A	101 mut1_WT9	1	8800	17508	3269	79941

119338	5	642674 CRA_00317	69 M	KDM6A	101 mut1_WT9	2	8894	17498	2844	79941
119338	5	642674 CRA_00317	69 M	KDM6A	101 mut1_WT9	3	8992	17500	2924	79941
119338	5	642674 CRA_00317	69 M	KDM6A	101 mut1_WT9	4	9040	17447	2723	79941
119338	5	642674 CRA_00317	69 M	KDM6A	101 mut1_WT9	5	8994	17365	2848	79941
119338	5	642674 CRA_00317	69 M	KDM6A	101 mut1_WT9	6	8941	17282	2145	79941
119338	5	642674 CRA_00317	69 M	KDM6A	101 mut1_WT9	7	8846	17309	2344	79941
119338	5	642674 CRA_00317	69 M	KDM6A	101 mut1_WT9	8	8776	17418	2577	79941
119338	5	642674 CRA_00317	69 M	KDM6A	101 mut1_WT9	9	8864	17428	2761	79941
119338	5	642674 CRA_00317	69 M	KDM6A	101 mut1_WT9	10	8909	17378	2848	79941
119338	5	642674 CRA_00317	69 M	KDM6A	102 mut1_WT9	1	8607	17572	4056	87180
119338	5	642674 CRA_00317	69 M	KDM6A	102 mut1_WT9	2	8532	17632	3065	87180
119338	5	642674 CRA_00317	69 M	KDM6A	102 mut1_WT9	3	8492	17559	3981	87180
119338	5	642674 CRA_00317	69 M	KDM6A	102 mut1_WT9	4	8460	17479	3470	87180
119338	5	642674 CRA_00317	69 M	KDM6A	102 mut1_WT9	5	8505	17417	3326	87180
119338	5	642674 CRA_00317	69 M	KDM6A	102 mut1_WT9	6	8668	17526	2325	87180
119338	5	642674 CRA_00317	69 M	KDM6A	102 mut1_WT9	7	8613	17470	3686	87180
119338	5	642674 CRA_00317	69 M	KDM6A	102 mut1_WT9	8	8696	17446	3528	87180
119338	5	642674 CRA_00317	69 M	KDM6A	102 mut1_WT9	9	8650	17348	3246	87180
119338	5	642674 CRA_00317	69 M	KDM6A	102 mut1_WT9	10	8570	17376	2909	87180
119338	5	642674 CRA_00317	69 M	KDM6A	103 WT	1	8941	17282	2145	88092
119338	5	642674 CRA_00317	69 M	KDM6A	103 WT	2	9035	17259	2243	88092
119338	5	642674 CRA_00317	69 M	KDM6A	103 WT	3	8863	17212	3663	88092
119338	5	642674 CRA_00317	69 M	KDM6A	103 WT	4	8966	17184	2900	88092
119338	5	642674 CRA_00317	69 M	KDM6A	103 WT	5	9081	17157	2442	88092
119338	5	642674 CRA_00317	69 M	KDM6A	103 WT	6	9011	17092	2840	88092
119338	5	642674 CRA_00317	69 M	KDM6A	103 WT	7	8854	17117	3595	88092
119338	5	642674 CRA_00317	69 M	KDM6A	103 WT	8	8936	17078	1827	88092
119338	5	642674 CRA_00317	69 M	KDM6A	103 WT	9	8882	17025	2275	88092
119338	5	642674 CRA_00317	69 M	KDM6A	103 WT	10	8977	16988	3856	88092
119338	5	642674 CRA_00317	69 M	KDM6A	104 WT	1	8492	17559	3981	99582
119338	5	642674 CRA_00317	69 M	KDM6A	104 WT	2	8532	17632	3065	99582
119338	5	642674 CRA_00317	69 M	KDM6A	104 WT	3	8600	17707	4098	99582
119338	5	642674 CRA_00317	69 M	KDM6A	104 WT	4	8495	17706	3759	99582
119338	5	642674 CRA_00317	69 M	KDM6A	104 WT	5	8394	17591	3473	99582
119338	5	642674 CRA_00317	69 M	KDM6A	104 WT	6	8386	17669	3334	99582
119338	5	642674 CRA_00317	69 M	KDM6A	104 WT	7	8423	17745	3615	99582
119338	5	642674 CRA_00317	69 M	KDM6A	104 WT	8	8548	17806	5880	99582
119338	5	642674 CRA_00317	69 M	KDM6A	104 WT	9	8449	17833	5537	99582
119338	5	642674 CRA_00317	69 M	KDM6A	104 WT	10	8339	17871	4516	99582
135741	5	642681 CRA_00414	72 F	KDM6A	42 mut	1	5055	9559	3968	77246
135741	5	642681 CRA_00414	72 F	KDM6A	42 mut	2	5055	9636	2974	77246

135741	5	642681 CRA_00414	72 F	KDM6A	42 mut	3	5147	9563	3062	77246
135741	5	642681 CRA_00414	72 F	KDM6A	42 mut	4	5176	9603	3915	77246
135741	5	642681 CRA_00414	72 F	KDM6A	42 mut	5	5263	9662	5220	77246
135741	5	642681 CRA_00414	72 F	KDM6A	42 mut	6	4977	9655	3093	77246
135741	5	642681 CRA_00414	72 F	KDM6A	42 mut	7	5082	9693	2849	77246
135741	5	642681 CRA_00414	72 F	KDM6A	42 mut	8	5141	9717	4270	77246
135741	5	642681 CRA_00414	72 F	KDM6A	42 mut	9	4907	9664	3790	77246
135741	5	642681 CRA_00414	72 F	KDM6A	42 mut	10	5005	9746	4224	77246
135741	5	642681 CRA_00414	72 F	KDM6A	43 WT	1	5147	9486	2697	58519
135741	5	642681 CRA_00414	72 F	KDM6A	43 WT	2	5102	9489	1892	58519
135741	5	642681 CRA_00414	72 F	KDM6A	43 WT	3	5168	9431	1883	58519
135741	5	642681 CRA_00414	72 F	KDM6A	43 WT	4	5085	9446	2224	58519
135741	5	642681 CRA_00414	72 F	KDM6A	43 WT	5	5080	9371	2634	58519
135741	5	642681 CRA_00414	72 F	KDM6A	43 WT	6	5184	9358	2947	58519
135741	5	642681 CRA_00414	72 F	KDM6A	43 WT	7	5251	9439	2354	58519
135741	5	642681 CRA_00414	72 F	KDM6A	43 WT	8	5259	9499	2016	58519
135741	5	642681 CRA_00414	72 F	KDM6A	43 WT	9	5240	9379	1069	58519
135741	5	642681 CRA_00414	72 F	KDM6A	43 WT	10	5261	9554	1878	58519
135741	5	642681 CRA_00414	72 F	KDM6A	44 WT	1	4943	9730	1379	51825
135741	5	642681 CRA_00414	72 F	KDM6A	44 WT	2	4869	9752	1808	51825
135741	5	642681 CRA_00414	72 F	KDM6A	44 WT	3	4905	9805	2393	51825
135741	5	642681 CRA_00414	72 F	KDM6A	44 WT	4	4843	9843	1611	51825
135741	5	642681 CRA_00414	72 F	KDM6A	44 WT	5	4812	9799	2052	51825
135741	5	642681 CRA_00414	72 F	KDM6A	44 WT	6	4799	9729	2476	51825
135741	5	642681 CRA_00414	72 F	KDM6A	44 WT	7	4800	9670	2222	51825
135741	5	642681 CRA_00414	72 F	KDM6A	44 WT	8	4892	9862	1869	51825
135741	5	642681 CRA_00414	72 F	KDM6A	44 WT	9	4950	9866	3166	51825
135741	5	642681 CRA_00414	72 F	KDM6A	44 WT	10	4741	9802	2040	51825
135741	5	642681 CRA_00414	72 F	KDM6A	45 WT	1	4757	9856	1234	55143
135741	5	642681 CRA_00414	72 F	KDM6A	45 WT	2	4806	9902	1923	55143
135741	5	642681 CRA_00414	72 F	KDM6A	45 WT	3	4739	9927	2770	55143
135741	5	642681 CRA_00414	72 F	KDM6A	45 WT	4	4685	9888	2787	55143
135741	5	642681 CRA_00414	72 F	KDM6A	45 WT	5	4830	9956	3435	55143
135741	5	642681 CRA_00414	72 F	KDM6A	45 WT	6	4736	10006	2520	55143
135741	5	642681 CRA_00414	72 F	KDM6A	45 WT	7	4675	9990	2215	55143
135741	5	642681 CRA_00414	72 F	KDM6A	45 WT	8	4610	9932	2840	55143
135741	5	642681 CRA_00414	72 F	KDM6A	45 WT	9	4815	10043	2613	55143
135741	5	642681 CRA_00414	72 F	KDM6A	45 WT	10	4745	10083	1839	55143
135734	5	642686 CRA_00413	65 F	KDM6A	30 mut	1	24149	4371	4521	87888
135734	5	642686 CRA_00413	65 F	KDM6A	30 mut	2	24121	4436	3630	87888
135734	5	642686 CRA_00413	65 F	KDM6A	30 mut	3	24127	4271	6017	87888

135734	5	642686 CRA_00413	65 F	KDM6A	30 mut	4	24074	4298	3192	87888
135734	5	642686 CRA_00413	65 F	KDM6A	30 mut	5	23989	4355	5173	87888
135734	5	642686 CRA_00413	65 F	KDM6A	30 mut	6	24059	4422	4022	87888
135734	5	642686 CRA_00413	65 F	KDM6A	30 mut	7	23987	4443	4015	87888
135734	5	642686 CRA_00413	65 F	KDM6A	30 mut	8	23891	4405	5610	87888
135734	5	642686 CRA_00413	65 F	KDM6A	30 mut	9	23919	4268	4369	87888
135734	5	642686 CRA_00413	65 F	KDM6A	30 mut	10	23960	4225	3463	87888
135734	5	642686 CRA_00413	65 F	KDM6A	31 WT	1	24072	4486	1954	47722
135734	5	642686 CRA_00413	65 F	KDM6A	31 WT	2	24013	4522	2456	47722
135734	5	642686 CRA_00413	65 F	KDM6A	31 WT	3	23946	4494	2668	47722
135734	5	642686 CRA_00413	65 F	KDM6A	31 WT	4	24125	4532	3040	47722
135734	5	642686 CRA_00413	65 F	KDM6A	31 WT	5	24069	4571	3527	47722
135734	5	642686 CRA_00413	65 F	KDM6A	31 WT	6	23981	4596	3510	47722
135734	5	642686 CRA_00413	65 F	KDM6A	31 WT	7	23930	4548	1283	47722
135734	5	642686 CRA_00413	65 F	KDM6A	31 WT	8	23877	4513	2584	47722
135734	5	642686 CRA_00413	65 F	KDM6A	31 WT	9	23878	4569	3152	47722
135734	5	642686 CRA_00413	65 F	KDM6A	31 WT	10	23902	4624	2411	47722
135734	5	642686 CRA_00413	65 F	KDM6A	32 WT	1	24030	4650	2909	53572
135734	5	642686 CRA_00413	65 F	KDM6A	32 WT	2	24110	4633	3518	53572
135734	5	642686 CRA_00413	65 F	KDM6A	32 WT	3	24183	4594	2796	53572
135734	5	642686 CRA_00413	65 F	KDM6A	32 WT	4	24188	4659	2931	53572
135734	5	642686 CRA_00413	65 F	KDM6A	32 WT	5	24124	4718	3120	53572
135734	5	642686 CRA_00413	65 F	KDM6A	32 WT	6	24049	4711	2958	53572
135734	5	642686 CRA_00413	65 F	KDM6A	32 WT	7	23944	4665	1463	53572
135734	5	642686 CRA_00413	65 F	KDM6A	32 WT	8	23939	4718	3238	53572
135734	5	642686 CRA_00413	65 F	KDM6A	32 WT	9	24016	4772	3470	53572
135734	5	642686 CRA_00413	65 F	KDM6A	32 WT	10	24100	4781	2278	53572
135734	5	642686 CRA_00413	65 F	KDM6A	33 WT	1	24232	4412	3931	57970
135734	5	642686 CRA_00413	65 F	KDM6A	33 WT	2	24198	4476	3141	57970
135734	5	642686 CRA_00413	65 F	KDM6A	33 WT	3	24215	4539	3315	57970
135734	5	642686 CRA_00413	65 F	KDM6A	33 WT	4	24277	4589	2501	57970
135734	5	642686 CRA_00413	65 F	KDM6A	33 WT	5	24288	4504	2907	57970
135734	5	642686 CRA_00413	65 F	KDM6A	33 WT	6	24322	4455	3176	57970
135734	5	642686 CRA_00413	65 F	KDM6A	33 WT	7	24350	4540	2783	57970
135734	5	642686 CRA_00413	65 F	KDM6A	33 WT	8	24302	4641	3632	57970
135734	5	642686 CRA_00413	65 F	KDM6A	33 WT	9	24387	4589	2864	57970
135734	5	642686 CRA_00413	65 F	KDM6A	33 WT	10	24414	4499	2824	57970
135743	5	642688 CRA_00414	72 F	KDM6A	46 mut	1	20726	20728	5700	91585
135743	5	642688 CRA_00414	72 F	KDM6A	46 mut	2	20826	20711	2184	91585
135743	5	642688 CRA_00414	72 F	KDM6A	46 mut	3	20854	20793	2943	91585
135743	5	642688 CRA_00414	72 F	KDM6A	46 mut	4	20930	20725	3653	91585

135743	5	642688 CRA_00414	72 F	KDM6A	46 mut	5	20746	20820	4069	91585
135743	5	642688 CRA_00414	72 F	KDM6A	46 mut	6	20817	20874	2243	91585
135743	5	642688 CRA_00414	72 F	KDM6A	46 mut	7	20763	20907	2692	91585
135743	5	642688 CRA_00414	72 F	KDM6A	46 mut	8	20934	20831	3410	91585
135743	5	642688 CRA_00414	72 F	KDM6A	46 mut	9	21036	20677	4572	91585
135743	5	642688 CRA_00414	72 F	KDM6A	46 mut	10	21018	20781	3769	91585
135743	5	642688 CRA_00414	72 F	KDM6A	47 WT	1	20917	20956	1946	70955
135743	5	642688 CRA_00414	72 F	KDM6A	47 WT	2	20847	20963	1980	70955
135743	5	642688 CRA_00414	72 F	KDM6A	47 WT	3	20847	21054	3138	70955
135743	5	642688 CRA_00414	72 F	KDM6A	47 WT	4	20909	21057	3021	70955
135743	5	642688 CRA_00414	72 F	KDM6A	47 WT	5	20973	21044	2510	70955
135743	5	642688 CRA_00414	72 F	KDM6A	47 WT	6	21033	21005	2824	70955
135743	5	642688 CRA_00414	72 F	KDM6A	47 WT	7	20946	21139	3532	70955
135743	5	642688 CRA_00414	72 F	KDM6A	47 WT	8	21017	21121	2157	70955
135743	5	642688 CRA_00414	72 F	KDM6A	47 WT	9	21083	21105	2157	70955
135743	5	642688 CRA_00414	72 F	KDM6A	47 WT	10	20966	20908	2049	70955
135743	5	642688 CRA_00414	72 F	KDM6A	48 WT	1	21145	21296	1519	54125
135743	5	642688 CRA_00414	72 F	KDM6A	48 WT	2	21079	21308	3029	54125
135743	5	642688 CRA_00414	72 F	KDM6A	48 WT	3	21115	21381	3241	54125
135743	5	642688 CRA_00414	72 F	KDM6A	48 WT	4	21185	21350	1401	54125
135743	5	642688 CRA_00414	72 F	KDM6A	48 WT	5	21045	21367	2298	54125
135743	5	642688 CRA_00414	72 F	KDM6A	48 WT	6	21958	21427	2447	54125
135743	5	642688 CRA_00414	72 F	KDM6A	48 WT	7	21130	21467	2386	54125
135743	5	642688 CRA_00414	72 F	KDM6A	48 WT	8	21188	21466	2324	54125
135743	5	642688 CRA_00414	72 F	KDM6A	48 WT	9	21207	21406	1271	54125
135743	5	642688 CRA_00414	72 F	KDM6A	48 WT	10	21258	21451	2039	54125
135743	5	642688 CRA_00414	72 F	KDM6A	49 WT	1	20889	21281	3646	75971
135743	5	642688 CRA_00414	72 F	KDM6A	49 WT	2	20857	21196	3146	75971
135743	5	642688 CRA_00414	72 F	KDM6A	49 WT	3	20925	21199	1893	75971
135743	5	642688 CRA_00414	72 F	KDM6A	49 WT	4	20987	21287	2257	75971
135743	5	642688 CRA_00414	72 F	KDM6A	49 WT	5	20956	21356	2395	75971
135743	5	642688 CRA_00414	72 F	KDM6A	49 WT	6	20793	21250	2504	75971
135743	5	642688 CRA_00414	72 F	KDM6A	49 WT	7	20781	21315	2343	75971
135743	5	642688 CRA_00414	72 F	KDM6A	49 WT	8	20872	21355	2757	75971
135743	5	642688 CRA_00414	72 F	KDM6A	49 WT	9	20825	21412	3774	75971
135743	5	642688 CRA_00414	72 F	KDM6A	49 WT	10	21014	21219	2539	75971
124378	5	642712 CRA_00363	72 M	KDM6A	18 mut	1	10207	16195	13586	122484
124378	5	642712 CRA_00363	72 M	KDM6A	18 mut	2	10054	16195	5846	122484
124378	5	642712 CRA_00363	72 M	KDM6A	18 mut	3	10090	16281	6626	122484
124378	5	642712 CRA_00363	72 M	KDM6A	18 mut	4	9979	16149	4883	122484
124378	5	642712 CRA_00363	72 M	KDM6A	18 mut	5	9914	16207	4807	122484

124378	5	642712 CRA_00363	72 M	KDM6A	18 mut	6	9979	16283	5228	122484
124378	5	642712 CRA_00363	72 M	KDM6A	18 mut	7	9877	16285	4690	122484
124378	5	642712 CRA_00363	72 M	KDM6A	18 mut	8	9816	16378	7669	122484
124378	5	642712 CRA_00363	72 M	KDM6A	18 mut	9	10079	16360	6728	122484
124378	5	642712 CRA_00363	72 M	KDM6A	18 mut	10	9996	16411	6860	122484
124378	5	642712 CRA_00363	72 M	KDM6A	19 WT	1	10100	16098	5098	114340
124378	5	642712 CRA_00363	72 M	KDM6A	19 WT	2	10026	16026	4778	114340
124378	5	642712 CRA_00363	72 M	KDM6A	19 WT	3	9952	16064	4109	114340
124378	5	642712 CRA_00363	72 M	KDM6A	19 WT	4	9863	16116	5723	114340
124378	5	642712 CRA_00363	72 M	KDM6A	19 WT	5	9957	15963	3675	114340
124378	5	642712 CRA_00363	72 M	KDM6A	19 WT	6	9854	15996	6210	114340
124378	5	642712 CRA_00363	72 M	KDM6A	19 WT	7	9767	16042	6287	114340
124378	5	642712 CRA_00363	72 M	KDM6A	19 WT	8	9795	16207	4602	114340
124378	5	642712 CRA_00363	72 M	KDM6A	19 WT	9	9698	16126	7838	114340
124378	5	642712 CRA_00363	72 M	KDM6A	19 WT	10	9846	15904	3442	114340
124378	5	642712 CRA_00363	72 M	KDM6A	20 WT	1	9746	15864	3906	105659
124378	5	642712 CRA_00363	72 M	KDM6A	20 WT	2	9711	15932	4475	105659
124378	5	642712 CRA_00363	72 M	KDM6A	20 WT	3	9636	15977	5921	105659
124378	5	642712 CRA_00363	72 M	KDM6A	20 WT	4	9560	16033	5102	105659
124378	5	642712 CRA_00363	72 M	KDM6A	20 WT	5	9789	15810	4191	105659
124378	5	642712 CRA_00363	72 M	KDM6A	20 WT	6	9633	15821	4800	105659
124378	5	642712 CRA_00363	72 M	KDM6A	20 WT	7	9576	15859	4165	105659
124378	5	642712 CRA_00363	72 M	KDM6A	20 WT	8	9513	15912	4223	105659
124378	5	642712 CRA_00363	72 M	KDM6A	20 WT	9	9428	15982	5119	105659
124378	5	642712 CRA_00363	72 M	KDM6A	20 WT	10	9529	15770	4483	105659
124378	5	642712 CRA_00363	72 M	KDM6A	21 WT	1	9468	15818	3574	118338
124378	5	642712 CRA_00363	72 M	KDM6A	21 WT	2	9386	15876	5145	118338
124378	5	642712 CRA_00363	72 M	KDM6A	21 WT	3	9317	15938	3561	118338
124378	5	642712 CRA_00363	72 M	KDM6A	21 WT	4	9274	16024	4626	118338
124378	5	642712 CRA_00363	72 M	KDM6A	21 WT	5	9325	15796	4996	118338
124378	5	642712 CRA_00363	72 M	KDM6A	21 WT	6	9233	15848	5718	118338
124378	5	642712 CRA_00363	72 M	KDM6A	21 WT	7	9175	15950	5823	118338
124378	5	642712 CRA_00363	72 M	KDM6A	21 WT	8	9223	15719	3621	118338
124378	5	642712 CRA_00363	72 M	KDM6A	21 WT	9	9146	15782	5329	118338
124378	5	642712 CRA_00363	72 M	KDM6A	21 WT	10	9369	15718	6481	118338
124378	5	642712 CRA_00363	72 M	KDM6A	105 mut3_WT7	1	10090	16281	6626	143289
124378	5	642712 CRA_00363	72 M	KDM6A	105 mut3_WT7	2	10054	16195	5846	143289
124378	5	642712 CRA_00363	72 M	KDM6A	105 mut3_WT7	3	10207	16195	13586	143289
124378	5	642712 CRA_00363	72 M	KDM6A	105 mut3_WT7	4	10100	16098	5098	143289
124378	5	642712 CRA_00363	72 M	KDM6A	105 mut3_WT7	5	10232	16356	11102	143289
124378	5	642712 CRA_00363	72 M	KDM6A	105 mut3_WT7	6	10325	16276	6671	143289

124378	5	642712 CRA_00363	72 M	KDM6A	105 mut3_WT7	7	10425	16219	4100	143289
124378	5	642712 CRA_00363	72 M	KDM6A	105 mut3_WT7	8	10327	16144	7125	143289
124378	5	642712 CRA_00363	72 M	KDM6A	105 mut3_WT7	9	10273	16045	7158	143289
124378	5	642712 CRA_00363	72 M	KDM6A	105 mut3_WT7	10	10424	16087	5794	143289
124378	5	642712 CRA_00363	72 M	KDM6A	106 mut3_WT7	1	9877	16285	4690	114032
124378	5	642712 CRA_00363	72 M	KDM6A	106 mut3_WT7	2	9914	16207	4807	114032
124378	5	642712 CRA_00363	72 M	KDM6A	106 mut3_WT7	3	9979	16149	4883	114032
124378	5	642712 CRA_00363	72 M	KDM6A	106 mut3_WT7	4	9795	16207	4602	114032
124378	5	642712 CRA_00363	72 M	KDM6A	106 mut3_WT7	5	9863	16116	5723	114032
124378	5	642712 CRA_00363	72 M	KDM6A	106 mut3_WT7	6	9952	16064	4109	114032
124378	5	642712 CRA_00363	72 M	KDM6A	106 mut3_WT7	7	10026	16026	4778	114032
124378	5	642712 CRA_00363	72 M	KDM6A	106 mut3_WT7	8	9698	16126	7838	114032
124378	5	642712 CRA_00363	72 M	KDM6A	106 mut3_WT7	9	9767	16042	6287	114032
124378	5	642712 CRA_00363	72 M	KDM6A	106 mut3_WT7	10	9854	15996	6210	114032
124378	5	642712 CRA_00363	72 M	KDM6A	107 mut2_WT8	1	10090	16281	6626	137588
124378	5	642712 CRA_00363	72 M	KDM6A	107 mut2_WT8	2	10207	16195	13586	137588
124378	5	642712 CRA_00363	72 M	KDM6A	107 mut2_WT8	3	10232	16356	11102	137588
124378	5	642712 CRA_00363	72 M	KDM6A	107 mut2_WT8	4	10325	16276	6671	137588
124378	5	642712 CRA_00363	72 M	KDM6A	107 mut2_WT8	5	10425	16219	4100	137588
124378	5	642712 CRA_00363	72 M	KDM6A	107 mut2_WT8	6	10327	16144	7125	137588
124378	5	642712 CRA_00363	72 M	KDM6A	107 mut2_WT8	7	10424	16087	5794	137588
124378	5	642712 CRA_00363	72 M	KDM6A	107 mut2_WT8	8	10423	16291	2300	137588
124378	5	642712 CRA_00363	72 M	KDM6A	107 mut2_WT8	9	10516	16280	6346	137588
124378	5	642712 CRA_00363	72 M	KDM6A	107 mut2_WT8	10	10580	16213	2833	137588
124378	5	642712 CRA_00363	72 M	KDM6A	108 mut2_WT8	1	9914	16207	4807	99172
124378	5	642712 CRA_00363	72 M	KDM6A	108 mut2_WT8	2	9979	16149	4883	99172
124378	5	642712 CRA_00363	72 M	KDM6A	108 mut2_WT8	3	9863	16116	5723	99172
124378	5	642712 CRA_00363	72 M	KDM6A	108 mut2_WT8	4	9952	16064	4109	99172
124378	5	642712 CRA_00363	72 M	KDM6A	108 mut2_WT8	5	10026	16026	4778	99172
124378	5	642712 CRA_00363	72 M	KDM6A	108 mut2_WT8	6	9854	15996	6210	99172
124378	5	642712 CRA_00363	72 M	KDM6A	108 mut2_WT8	7	9767	16042	6287	99172
124378	5	642712 CRA_00363	72 M	KDM6A	108 mut2_WT8	8	9957	15963	3675	99172
124378	5	642712 CRA_00363	72 M	KDM6A	108 mut2_WT8	9	9846	15904	3442	99172
124378	5	642712 CRA_00363	72 M	KDM6A	108 mut2_WT8	10	10039	15918	3811	99172
124378	5	642712 CRA_00363	72 M	KDM6A	109 mut1_WT9	1	9914	16207	4807	114828
124378	5	642712 CRA_00363	72 M	KDM6A	109 mut1_WT9	2	9795	16207	4602	114828
124378	5	642712 CRA_00363	72 M	KDM6A	109 mut1_WT9	3	9698	16126	7838	114828
124378	5	642712 CRA_00363	72 M	KDM6A	109 mut1_WT9	4	9863	16116	5723	114828
124378	5	642712 CRA_00363	72 M	KDM6A	109 mut1_WT9	5	9952	16064	4109	114828
124378	5	642712 CRA_00363	72 M	KDM6A	109 mut1_WT9	6	9767	16042	6287	114828
124378	5	642712 CRA_00363	72 M	KDM6A	109 mut1_WT9	7	9854	15996	6210	114828

124378	5	642712 CRA_00363	72 M	KDM6A	109 mut1_WT9	8	9846	15904	3442	114828
124378	5	642712 CRA_00363	72 M	KDM6A	109 mut1_WT9	9	9711	15932	4475	114828
124378	5	642712 CRA_00363	72 M	KDM6A	109 mut1_WT9	10	9636	15977	5921	114828
124378	5	642712 CRA_00363	72 M	KDM6A	110 mut1_WT9	1	10207	16195	13586	131958
124378	5	642712 CRA_00363	72 M	KDM6A	110 mut1_WT9	2	10325	16276	6671	131958
124378	5	642712 CRA_00363	72 M	KDM6A	110 mut1_WT9	3	10425	16219	4100	131958
124378	5	642712 CRA_00363	72 M	KDM6A	110 mut1_WT9	4	10327	16144	7125	131958
124378	5	642712 CRA_00363	72 M	KDM6A	110 mut1_WT9	5	10424	16087	5794	131958
124378	5	642712 CRA_00363	72 M	KDM6A	110 mut1_WT9	6	10273	16045	7158	131958
124378	5	642712 CRA_00363	72 M	KDM6A	110 mut1_WT9	7	10351	15971	6177	131958
124378	5	642712 CRA_00363	72 M	KDM6A	110 mut1_WT9	8	10477	16002	3531	131958
124378	5	642712 CRA_00363	72 M	KDM6A	110 mut1_WT9	9	10520	16140	4792	131958
124378	5	642712 CRA_00363	72 M	KDM6A	110 mut1_WT9	10	10575	16056	2146	131958
124378	5	642712 CRA_00363	72 M	KDM6A	111 WT	1	10273	16045	7158	124660
124378	5	642712 CRA_00363	72 M	KDM6A	111 WT	2	10424	16087	5794	124660
124378	5	642712 CRA_00363	72 M	KDM6A	111 WT	3	10520	16140	4792	124660
124378	5	642712 CRA_00363	72 M	KDM6A	111 WT	4	10575	16056	2146	124660
124378	5	642712 CRA_00363	72 M	KDM6A	111 WT	5	10477	16002	3531	124660
124378	5	642712 CRA_00363	72 M	KDM6A	111 WT	6	10351	15971	6177	124660
124378	5	642712 CRA_00363	72 M	KDM6A	111 WT	7	10379	15891	5636	124660
124378	5	642712 CRA_00363	72 M	KDM6A	111 WT	8	10477	15863	7201	124660
124378	5	642712 CRA_00363	72 M	KDM6A	111 WT	9	10563	15953	5348	124660
124378	5	642712 CRA_00363	72 M	KDM6A	111 WT	10	10669	15997	5411	124660
124378	5	642712 CRA_00363	72 M	KDM6A	112 WT	1	10580	16213	2833	132312
124378	5	642712 CRA_00363	72 M	KDM6A	112 WT	2	10516	16280	6346	132312
124378	5	642712 CRA_00363	72 M	KDM6A	112 WT	3	10650	16304	8840	132312
124378	5	642712 CRA_00363	72 M	KDM6A	112 WT	4	10561	16392	7733	132312
124378	5	642712 CRA_00363	72 M	KDM6A	112 WT	5	10403	16377	6263	132312
124378	5	642712 CRA_00363	72 M	KDM6A	112 WT	6	10481	16419	2694	132312
124378	5	642712 CRA_00363	72 M	KDM6A	112 WT	7	10345	16478	10505	132312
124378	5	642712 CRA_00363	72 M	KDM6A	112 WT	8	10466	16489	2990	132312
124378	5	642712 CRA_00363	72 M	KDM6A	112 WT	9	10564	16504	4462	132312
124378	5	642712 CRA_00363	72 M	KDM6A	112 WT	10	10675	16482	7376	132312
128365	5	657521 CRA_00409	77 F	KDM6A	38 mut	1	6745	20581	5586	119334
128365	5	657521 CRA_00409	77 F	KDM6A	38 mut	2	6821	20640	5736	119334
128365	5	657521 CRA_00409	77 F	KDM6A	38 mut	3	6869	20736	7091	119334
128365	5	657521 CRA_00409	77 F	KDM6A	38 mut	4	6744	20739	7513	119334
128365	5	657521 CRA_00409	77 F	KDM6A	38 mut	5	6661	20651	6585	119334
128365	5	657521 CRA_00409	77 F	KDM6A	38 mut	6	6823	20822	5091	119334
128365	5	657521 CRA_00409	77 F	KDM6A	38 mut	7	6979	20754	8067	119334
128365	5	657521 CRA_00409	77 F	KDM6A	38 mut	8	6622	20762	5091	119334

128365	5	657521 CRA_00409	77 F	KDM6A	38 mut	9	6684	20847	5444	119334
128365	5	657521 CRA_00409	77 F	KDM6A	38 mut	10	6826	20927	5228	119334
128365	5	657521 CRA_00409	77 F	KDM6A	39 WT	1	6596	20561	3483	69696
128365	5	657521 CRA_00409	77 F	KDM6A	39 WT	2	6672	20519	4730	69696
128365	5	657521 CRA_00409	77 F	KDM6A	39 WT	3	6520	20608	3360	69696
128365	5	657521 CRA_00409	77 F	KDM6A	39 WT	4	6622	20436	3438	69696
128365	5	657521 CRA_00409	77 F	KDM6A	39 WT	5	6553	20484	2645	69696
128365	5	657521 CRA_00409	77 F	KDM6A	39 WT	6	6485	20510	1903	69696
128365	5	657521 CRA_00409	77 F	KDM6A	39 WT	7	6432	20544	2270	69696
128365	5	657521 CRA_00409	77 F	KDM6A	39 WT	8	6454	20616	2411	69696
128365	5	657521 CRA_00409	77 F	KDM6A	39 WT	9	6371	20518	2909	69696
128365	5	657521 CRA_00409	77 F	KDM6A	39 WT	10	6366	20630	2354	69696
128365	5	657521 CRA_00409	77 F	KDM6A	40 WT	1	6783	20480	3921	82276
128365	5	657521 CRA_00409	77 F	KDM6A	40 WT	2	6717	20433	2777	82276
128365	5	657521 CRA_00409	77 F	KDM6A	40 WT	3	6685	20354	3224	82276
128365	5	657521 CRA_00409	77 F	KDM6A	40 WT	4	6780	20355	5197	82276
128365	5	657521 CRA_00409	77 F	KDM6A	40 WT	5	6858	20414	4735	82276
128365	5	657521 CRA_00409	77 F	KDM6A	40 WT	6	6856	20532	3439	82276
128365	5	657521 CRA_00409	77 F	KDM6A	40 WT	7	6916	20479	2823	82276
128365	5	657521 CRA_00409	77 F	KDM6A	40 WT	8	6892	20322	3830	82276
128365	5	657521 CRA_00409	77 F	KDM6A	40 WT	9	6833	20259	4251	82276
128365	5	657521 CRA_00409	77 F	KDM6A	40 WT	10	6738	20261	4010	82276
128365	5	657521 CRA_00409	77 F	KDM6A	41 WT	1	6654	20100	3420	65748
128365	5	657521 CRA_00409	77 F	KDM6A	41 WT	2	6570	20107	2307	65748
128365	5	657521 CRA_00409	77 F	KDM6A	41 WT	3	6621	20021	2587	65748
128365	5	657521 CRA_00409	77 F	KDM6A	41 WT	4	6617	20192	3393	65748
128365	5	657521 CRA_00409	77 F	KDM6A	41 WT	5	6549	20200	2253	65748
128365	5	657521 CRA_00409	77 F	KDM6A	41 WT	6	6718	20142	3457	65748
128365	5	657521 CRA_00409	77 F	KDM6A	41 WT	7	6518	20069	2321	65748
128365	5	657521 CRA_00409	77 F	KDM6A	41 WT	8	6561	19997	2283	65748
128365	5	657521 CRA_00409	77 F	KDM6A	41 WT	9	6495	20161	1924	65748
128365	5	657521 CRA_00409	77 F	KDM6A	41 WT	10	6454	20108	2959	65748
116307	7	674358 CRA_00303	57 F	KDM6A	10 mut	1	2258	5397	4901	80220
116307	7	674358 CRA_00303	57 F	KDM6A	10 mut	2	2192	5360	3827	80220
116307	7	674358 CRA_00303	57 F	KDM6A	10 mut	3	2097	5350	5809	80220
116307	7	674358 CRA_00303	57 F	KDM6A	10 mut	4	2104	5450	5319	80220
116307	7	674358 CRA_00303	57 F	KDM6A	10 mut	5	2007	5359	5985	80220
116307	7	674358 CRA_00303	57 F	KDM6A	10 mut	6	2031	5458	3096	80220
116307	7	674358 CRA_00303	57 F	KDM6A	10 mut	7	1953	5436	5941	80220
116307	7	674358 CRA_00303	57 F	KDM6A	10 mut	8	1969	5531	5826	80220
116307	7	674358 CRA_00303	57 F	KDM6A	10 mut	9	2057	5533	4889	80220

116307	7	674358 CRA_00303	57 F	KDM6A	10 mut	10	2159	5543	6535	80220
116307	7	674358 CRA_00303	57 F	KDM6A	11 WT	1	1875	5453	3755	68612
116307	7	674358 CRA_00303	57 F	KDM6A	11 WT	2	1883	5550	4230	68612
116307	7	674358 CRA_00303	57 F	KDM6A	11 WT	3	1814	5497	4630	68612
116307	7	674358 CRA_00303	57 F	KDM6A	11 WT	4	1812	5604	3837	68612
116307	7	674358 CRA_00303	57 F	KDM6A	11 WT	5	1887	5615	1968	68612
116307	7	674358 CRA_00303	57 F	KDM6A	11 WT	6	1972	5631	4786	68612
116307	7	674358 CRA_00303	57 F	KDM6A	11 WT	7	1917	5688	4731	68612
116307	7	674358 CRA_00303	57 F	KDM6A	11 WT	8	1837	5695	3567	68612
116307	7	674358 CRA_00303	57 F	KDM6A	11 WT	9	1746	5649	3484	68612
116307	7	674358 CRA_00303	57 F	KDM6A	11 WT	10	1742	5560	4110	68612
116307	7	674358 CRA_00303	57 F	KDM6A	12 WT	1	1838	5786	4429	66588
116307	7	674358 CRA_00303	57 F	KDM6A	12 WT	2	1914	5765	3800	66588
116307	7	674358 CRA_00303	57 F	KDM6A	12 WT	3	2007	5742	4329	66588
116307	7	674358 CRA_00303	57 F	KDM6A	12 WT	4	1961	5825	3837	66588
116307	7	674358 CRA_00303	57 F	KDM6A	12 WT	5	1870	5862	3523	66588
116307	7	674358 CRA_00303	57 F	KDM6A	12 WT	6	1937	5877	3802	66588
116307	7	674358 CRA_00303	57 F	KDM6A	12 WT	7	2048	5822	3988	66588
116307	7	674358 CRA_00303	57 F	KDM6A	12 WT	8	2029	5899	4995	66588
116307	7	674358 CRA_00303	57 F	KDM6A	12 WT	9	1954	5965	4498	66588
116307	7	674358 CRA_00303	57 F	KDM6A	12 WT	10	2046	5982	4231	66588
116307	7	674358 CRA_00303	57 F	KDM6A	13 WT	1	1813	7593	3340	73794
116307	7	674358 CRA_00303	57 F	KDM6A	13 WT	2	1911	7612	5219	73794
116307	7	674358 CRA_00303	57 F	KDM6A	13 WT	3	1874	7680	4286	73794
116307	7	674358 CRA_00303	57 F	KDM6A	13 WT	4	1787	7662	2867	73794
116307	7	674358 CRA_00303	57 F	KDM6A	13 WT	5	1787	7750	4720	73794
116307	7	674358 CRA_00303	57 F	KDM6A	13 WT	6	1866	7768	3680	73794
116307	7	674358 CRA_00303	57 F	KDM6A	13 WT	7	1949	7742	4118	73794
116307	7	674358 CRA_00303	57 F	KDM6A	13 WT	8	1938	7830	4295	73794
116307	7	674358 CRA_00303	57 F	KDM6A	13 WT	9	1858	7847	3722	73794
116307	7	674358 CRA_00303	57 F	KDM6A	13 WT	10	1765	7842	4712	73794
121505	6	676354 NRA_00346	49 F	KDM6A	22 mut	1	6577	13917	7759	149975
121505	6	676354 NRA_00346	49 F	KDM6A	22 mut	2	6669	14005	7321	149975
121505	6	676354 NRA_00346	49 F	KDM6A	22 mut	3	6567	14084	8259	149975
121505	6	676354 NRA_00346	49 F	KDM6A	22 mut	4	6457	13981	11331	149975
121505	6	676354 NRA_00346	49 F	KDM6A	22 mut	5	6281	13873	6884	149975
121505	6	676354 NRA_00346	49 F	KDM6A	22 mut	6	6177	13940	9820	149975
121505	6	676354 NRA_00346	49 F	KDM6A	22 mut	7	6245	14025	8468	149975
121505	6	676354 NRA_00346	49 F	KDM6A	22 mut	8	6320	14045	8392	149975
121505	6	676354 NRA_00346	49 F	KDM6A	22 mut	9	6412	14118	10213	149975
121505	6	676354 NRA_00346	49 F	KDM6A	22 mut	10	6497	14176	7592	149975

121505	6	676354 NRA_00346	49 F	KDM6A	23 WT	1	6391	13883	8615	147226
121505	6	676354 NRA_00346	49 F	KDM6A	23 WT	2	6485	13811	9704	147226
121505	6	676354 NRA_00346	49 F	KDM6A	23 WT	3	6322	13764	9583	147226
121505	6	676354 NRA_00346	49 F	KDM6A	23 WT	4	6510	13696	7906	147226
121505	6	676354 NRA_00346	49 F	KDM6A	23 WT	5	6400	13673	7628	147226
121505	6	676354 NRA_00346	49 F	KDM6A	23 WT	6	6252	13661	8190	147226
121505	6	676354 NRA_00346	49 F	KDM6A	23 WT	7	6181	13769	5329	147226
121505	6	676354 NRA_00346	49 F	KDM6A	23 WT	8	6486	13552	8427	147226
121505	6	676354 NRA_00346	49 F	KDM6A	23 WT	9	6371	13563	9230	147226
121505	6	676354 NRA_00346	49 F	KDM6A	23 WT	10	6210	13573	5690	147226
121505	6	676354 NRA_00346	49 F	KDM6A	24 WT	1	6240	14175	7583	141293
121505	6	676354 NRA_00346	49 F	KDM6A	24 WT	2	6315	14204	6348	141293
121505	6	676354 NRA_00346	49 F	KDM6A	24 WT	3	6254	14327	7322	141293
121505	6	676354 NRA_00346	49 F	KDM6A	24 WT	4	6139	14275	5481	141293
121505	6	676354 NRA_00346	49 F	KDM6A	24 WT	5	6031	14231	5308	141293
121505	6	676354 NRA_00346	49 F	KDM6A	24 WT	6	6148	14148	5075	141293
121505	6	676354 NRA_00346	49 F	KDM6A	24 WT	7	6049	14385	5857	141293
121505	6	676354 NRA_00346	49 F	KDM6A	24 WT	8	6166	14409	5457	141293
121505	6	676354 NRA_00346	49 F	KDM6A	24 WT	9	6341	14417	8561	141293
121505	6	676354 NRA_00346	49 F	KDM6A	24 WT	10	6013	14138	5736	141293
121505	6	676354 NRA_00346	49 F	KDM6A	25 WT	1	6110	13854	5338	130642
121505	6	676354 NRA_00346	49 F	KDM6A	25 WT	2	6037	13964	5280	130642
121505	6	676354 NRA_00346	49 F	KDM6A	25 WT	3	5988	13870	6004	130642
121505	6	676354 NRA_00346	49 F	KDM6A	25 WT	4	5957	14054	5813	130642
121505	6	676354 NRA_00346	49 F	KDM6A	25 WT	5	5892	13972	6319	130642
121505	6	676354 NRA_00346	49 F	KDM6A	25 WT	6	5837	13874	6191	130642
121505	6	676354 NRA_00346	49 F	KDM6A	25 WT	7	5940	13785	5396	130642
121505	6	676354 NRA_00346	49 F	KDM6A	25 WT	8	6102	14063	4548	130642
121505	6	676354 NRA_00346	49 F	KDM6A	25 WT	9	6073	13741	4824	130642
121505	6	676354 NRA_00346	49 F	KDM6A	25 WT	10	6007	13662	5756	130642
123488	6	676367 CRA_00359	69 M	KDM6A	26 mut	1	8021	9047	4223	110336
123488	6	676367 CRA_00359	69 M	KDM6A	26 mut	2	8147	9097	3451	110336
123488	6	676367 CRA_00359	69 M	KDM6A	26 mut	3	8043	9142	4213	110336
123488	6	676367 CRA_00359	69 M	KDM6A	26 mut	4	7964	9191	4872	110336
123488	6	676367 CRA_00359	69 M	KDM6A	26 mut	5	8202	9169	4169	110336
123488	6	676367 CRA_00359	69 M	KDM6A	26 mut	6	8111	9242	2721	110336
123488	6	676367 CRA_00359	69 M	KDM6A	26 mut	7	8260	9227	3102	110336
123488	6	676367 CRA_00359	69 M	KDM6A	26 mut	8	8114	9322	4163	110336
123488	6	676367 CRA_00359	69 M	KDM6A	26 mut	9	8360	9205	3948	110336
123488	6	676367 CRA_00359	69 M	KDM6A	26 mut	10	8218	9307	6197	110336
123488	6	676367 CRA_00359	69 M	KDM6A	27 WT	1	8333	9273	2599	75920

123488	6	676367 CRA_00359	69 M	KDM6A	27 WT	2	8294	9384	2807	75920
123488	6	676367 CRA_00359	69 M	KDM6A	27 WT	3	8391	9355	2678	75920
123488	6	676367 CRA_00359	69 M	KDM6A	27 WT	4	8206	9397	2939	75920
123488	6	676367 CRA_00359	69 M	KDM6A	27 WT	5	8464	9295	2922	75920
123488	6	676367 CRA_00359	69 M	KDM6A	27 WT	6	8486	9389	2892	75920
123488	6	676367 CRA_00359	69 M	KDM6A	27 WT	7	8368	9430	2909	75920
123488	6	676367 CRA_00359	69 M	KDM6A	27 WT	8	8304	9473	3297	75920
123488	6	676367 CRA_00359	69 M	KDM6A	27 WT	9	8388	9514	2760	75920
123488	6	676367 CRA_00359	69 M	KDM6A	27 WT	10	8479	9470	2509	75920
123488	6	676367 CRA_00359	69 M	KDM6A	28 WT	1	7916	9071	2071	80458
123488	6	676367 CRA_00359	69 M	KDM6A	28 WT	2	7817	9122	2633	80458
123488	6	676367 CRA_00359	69 M	KDM6A	28 WT	3	7871	9206	2680	80458
123488	6	676367 CRA_00359	69 M	KDM6A	28 WT	4	7776	9170	1705	80458
123488	6	676367 CRA_00359	69 M	KDM6A	28 WT	5	7866	9274	3334	80458
123488	6	676367 CRA_00359	69 M	KDM6A	28 WT	6	7754	9268	3140	80458
123488	6	676367 CRA_00359	69 M	KDM6A	28 WT	7	7724	9195	1825	80458
123488	6	676367 CRA_00359	69 M	KDM6A	28 WT	8	7698	9123	2361	80458
123488	6	676367 CRA_00359	69 M	KDM6A	28 WT	9	7761	9057	2185	80458
123488	6	676367 CRA_00359	69 M	KDM6A	28 WT	10	7672	9044	2732	80458
123488	6	676367 CRA_00359	69 M	KDM6A	29 WT	1	8025	9253	1778	72079
123488	6	676367 CRA_00359	69 M	KDM6A	29 WT	2	7976	9300	3424	72079
123488	6	676367 CRA_00359	69 M	KDM6A	29 WT	3	7954	9369	5457	72079
123488	6	676367 CRA_00359	69 M	KDM6A	29 WT	4	8058	9376	2608	72079
123488	6	676367 CRA_00359	69 M	KDM6A	29 WT	5	7979	9442	3056	72079
123488	6	676367 CRA_00359	69 M	KDM6A	29 WT	6	7884	9439	2405	72079
123488	6	676367 CRA_00359	69 M	KDM6A	29 WT	7	8085	9442	2954	72079
123488	6	676367 CRA_00359	69 M	KDM6A	29 WT	8	8036	9491	1991	72079
123488	6	676367 CRA_00359	69 M	KDM6A	29 WT	9	7924	9507	2716	72079
123488	6	676367 CRA_00359	69 M	KDM6A	29 WT	10	8129	9517	2754	72079
157463	5	679221 CRA_00478	83 M	KDM6A	50 mut	1	12016	9953	5071	78463
157463	5	679221 CRA_00478	83 M	KDM6A	50 mut	2	11982	9882	4301	78463
157463	5	679221 CRA_00478	83 M	KDM6A	50 mut	3	11881	9868	2147	78463
157463	5	679221 CRA_00478	83 M	KDM6A	50 mut	4	11896	9936	2642	78463
157463	5	679221 CRA_00478	83 M	KDM6A	50 mut	5	11917	10023	3654	78463
157463	5	679221 CRA_00478	83 M	KDM6A	50 mut	6	11808	9877	1810	78463
157463	5	679221 CRA_00478	83 M	KDM6A	50 mut	7	11816	9951	1852	78463
157463	5	679221 CRA_00478	83 M	KDM6A	50 mut	8	11848	10019	2983	78463
157463	5	679221 CRA_00478	83 M	KDM6A	50 mut	9	11728	9951	2961	78463
157463	5	679221 CRA_00478	83 M	KDM6A	50 mut	10	11738	10040	4918	78463
157463	5	679221 CRA_00478	83 M	KDM6A	51 WT	1	11748	9816	2274	73128
157463	5	679221 CRA_00478	83 M	KDM6A	51 WT	2	11703	9881	1902	73128

157463	5	679221 CRA_00478	83 M	KDM6A	51 WT	3	11626	9876	1870	73128
157463	5	679221 CRA_00478	83 M	KDM6A	51 WT	4	11630	9953	1810	73128
157463	5	679221 CRA_00478	83 M	KDM6A	51 WT	5	11757	9740	2817	73128
157463	5	679221 CRA_00478	83 M	KDM6A	51 WT	6	11656	9768	2186	73128
157463	5	679221 CRA_00478	83 M	KDM6A	51 WT	7	11591	9813	1745	73128
157463	5	679221 CRA_00478	83 M	KDM6A	51 WT	8	11552	9925	5305	73128
157463	5	679221 CRA_00478	83 M	KDM6A	51 WT	9	11508	9805	2963	73128
157463	5	679221 CRA_00478	83 M	KDM6A	51 WT	10	11847	9803	2273	73128
157463	5	679221 CRA_00478	83 M	KDM6A	52 WT	1	11650	10053	3948	89450
157463	5	679221 CRA_00478	83 M	KDM6A	52 WT	2	11577	10035	2646	89450
157463	5	679221 CRA_00478	83 M	KDM6A	52 WT	3	11513	10015	2344	89450
157463	5	679221 CRA_00478	83 M	KDM6A	52 WT	4	11425	10003	3508	89450
157463	5	679221 CRA_00478	83 M	KDM6A	52 WT	5	11452	10101	5080	89450
157463	5	679221 CRA_00478	83 M	KDM6A	52 WT	6	11568	10133	5594	89450
157463	5	679221 CRA_00478	83 M	KDM6A	52 WT	7	11660	10157	3445	89450
157463	5	679221 CRA_00478	83 M	KDM6A	52 WT	8	11465	10206	5269	89450
157463	5	679221 CRA_00478	83 M	KDM6A	52 WT	9	11572	10231	3109	89450
157463	5	679221 CRA_00478	83 M	KDM6A	52 WT	10	11666	10252	3493	89450
157463	5	679221 CRA_00478	83 M	KDM6A	53 WT	1	11394	10266	3817	86162
157463	5	679221 CRA_00478	83 M	KDM6A	53 WT	2	11500	10300	2770	86162
157463	5	679221 CRA_00478	83 M	KDM6A	53 WT	3	11586	10326	3289	86162
157463	5	679221 CRA_00478	83 M	KDM6A	53 WT	4	11456	10363	4387	86162
157463	5	679221 CRA_00478	83 M	KDM6A	53 WT	5	11365	10373	4735	86162
157463	5	679221 CRA_00478	83 M	KDM6A	53 WT	6	11526	10431	4233	86162
157463	5	679221 CRA_00478	83 M	KDM6A	53 WT	7	11611	10432	3879	86162
157463	5	679221 CRA_00478	83 M	KDM6A	53 WT	8	11462	10482	3621	86162
157463	5	679221 CRA_00478	83 M	KDM6A	53 WT	9	11380	10463	3371	86162
157463	5	679221 CRA_00478	83 M	KDM6A	53 WT	10	11558	10532	3166	86162
171027	12	685082 CRA_00489	79 F	KDM6A	70 mut	1	18431	12266	5641	149278
171027	12	685082 CRA_00489	79 F	KDM6A	70 mut	2	18314	12435	4811	149278
171027	12	685082 CRA_00489	79 F	KDM6A	70 mut	3	18203	13425	6062	149278
171027	12	685082 CRA_00489	79 F	KDM6A	70 mut	4	18104	12529	4136	149278
171027	12	685082 CRA_00489	79 F	KDM6A	70 mut	5	18245	12553	3671	149278
171027	12	685082 CRA_00489	79 F	KDM6A	70 mut	6	18370	12561	3837	149278
171027	12	685082 CRA_00489	79 F	KDM6A	70 mut	7	18168	12615	3073	149278
171027	12	685082 CRA_00489	79 F	KDM6A	70 mut	8	18077	12642	3066	149278
171027	12	685082 CRA_00489	79 F	KDM6A	70 mut	9	18120	12725	2526	149278
171027	12	685082 CRA_00489	79 F	KDM6A	70 mut	10	18272	12672	3552	149278
171027	12	685082 CRA_00489	79 F	KDM6A	71 WT	1	18707	12455	5624	148873
171027	12	685082 CRA_00489	79 F	KDM6A	71 WT	2	18609	12558	3654	148873
171027	12	685082 CRA_00489	79 F	KDM6A	71 WT	3	18460	12597	6450	148873

171027	12	685082 CRA_00489	79 F	KDM6A	71 WT	4	18565	12713	2251	148873
171027	12	685082 CRA_00489	79 F	KDM6A	71 WT	5	18472	12728	4060	148873
171027	12	685082 CRA_00489	79 F	KDM6A	71 WT	6	18365	12718	3540	148873
171027	12	685082 CRA_00489	79 F	KDM6A	71 WT	7	18361	12801	2341	148873
171027	12	685082 CRA_00489	79 F	KDM6A	71 WT	8	18479	12832	1956	148873
171027	12	685082 CRA_00489	79 F	KDM6A	71 WT	9	18679	12706	5319	148873
171027	12	685082 CRA_00489	79 F	KDM6A	71 WT	10	18570	12878	2826	148873
171027	12	685082 CRA_00489	79 F	KDM6A	72 WT	1	18143	11883	4487	130829
171027	12	685082 CRA_00489	79 F	KDM6A	72 WT	2	18065	12034	3036	130829
171027	12	685082 CRA_00489	79 F	KDM6A	72 WT	3	17978	11999	3391	130829
171027	12	685082 CRA_00489	79 F	KDM6A	72 WT	4	18074	12146	5311	130829
171027	12	685082 CRA_00489	79 F	KDM6A	72 WT	5	17955	12110	2947	130829
171027	12	685082 CRA_00489	79 F	KDM6A	72 WT	6	17918	12214	4608	130829
171027	12	685082 CRA_00489	79 F	KDM6A	72 WT	7	17816	12195	5173	130829
171027	12	685082 CRA_00489	79 F	KDM6A	72 WT	8	17863	12048	3309	130829
171027	12	685082 CRA_00489	79 F	KDM6A	72 WT	9	21182	11959	3470	130829
171027	12	685082 CRA_00489	79 F	KDM6A	72 WT	10	18189	12060	3627	130829
171027	12	685082 CRA_00489	79 F	KDM6A	73 WT	1	18023	11230	4269	151093
171027	12	685082 CRA_00489	79 F	KDM6A	73 WT	2	17887	11342	3264	151093
171027	12	685082 CRA_00489	79 F	KDM6A	73 WT	3	17776	11386	3879	151093
171027	12	685082 CRA_00489	79 F	KDM6A	73 WT	4	17873	11471	3407	151093
171027	12	685082 CRA_00489	79 F	KDM6A	73 WT	5	17789	11523	2974	151093
171027	12	685082 CRA_00489	79 F	KDM6A	73 WT	6	17665	11482	4409	151093
171027	12	685082 CRA_00489	79 F	KDM6A	73 WT	7	17677	11598	3622	151093
171027	12	685082 CRA_00489	79 F	KDM6A	73 WT	8	17828	11616	2922	151093
171027	12	685082 CRA_00489	79 F	KDM6A	73 WT	9	17734	11705	6124	151093
171027	12	685082 CRA_00489	79 F	KDM6A	73 WT	10	17989	11379	3535	151093
171018	12	685100 CRA_00485	80 M	KDM6A	54 mut	1	17984	11157	7982	110312
171018	12	685100 CRA_00485	80 M	KDM6A	54 mut	2	18056	11071	4525	110312
171018	12	685100 CRA_00485	80 M	KDM6A	54 mut	3	18134	11010	4915	110312
171018	12	685100 CRA_00485	80 M	KDM6A	54 mut	4	18152	11105	4629	110312
171018	12	685100 CRA_00485	80 M	KDM6A	54 mut	5	18164	11186	4661	110312
171018	12	685100 CRA_00485	80 M	KDM6A	54 mut	6	18068	11206	3567	110312
171018	12	685100 CRA_00485	80 M	KDM6A	54 mut	7	18091	11288	3774	110312
171018	12	685100 CRA_00485	80 M	KDM6A	54 mut	8	18005	11369	6035	110312
171018	12	685100 CRA_00485	80 M	KDM6A	54 mut	9	17971	11285	5374	110312
171018	12	685100 CRA_00485	80 M	KDM6A	54 mut	10	17873	11237	6657	110312
171018	12	685100 CRA_00485	80 M	KDM6A	55 WT	1	18207	11275	5583	102662
171018	12	685100 CRA_00485	80 M	KDM6A	55 WT	2	18308	11271	5173	102662
171018	12	685100 CRA_00485	80 M	KDM6A	55 WT	3	18242	11370	3897	102662
171018	12	685100 CRA_00485	80 M	KDM6A	55 WT	4	18118	11366	4937	102662

171018	12	685100 CRA_00485	80 M	KDM6A	55 WT	5	18171	11445	4088	102662
171018	12	685100 CRA_00485	80 M	KDM6A	55 WT	6	18364	11369	4029	102662
171018	12	685100 CRA_00485	80 M	KDM6A	55 WT	7	18315	11452	3869	102662
171018	12	685100 CRA_00485	80 M	KDM6A	55 WT	8	18223	11517	5019	102662
171018	12	685100 CRA_00485	80 M	KDM6A	55 WT	9	18397	11289	3013	102662
171018	12	685100 CRA_00485	80 M	KDM6A	55 WT	10	18472	11368	5124	102662
171018	12	685100 CRA_00485	80 M	KDM6A	56 WT	1	18432	10984	4241	104342
171018	12	685100 CRA_00485	80 M	KDM6A	56 WT	2	18329	11052	6113	104342
171018	12	685100 CRA_00485	80 M	KDM6A	56 WT	3	18430	11086	4033	104342
171018	12	685100 CRA_00485	80 M	KDM6A	56 WT	4	18375	11181	5065	104342
171018	12	685100 CRA_00485	80 M	KDM6A	56 WT	5	18256	11144	5610	104342
171018	12	685100 CRA_00485	80 M	KDM6A	56 WT	6	18507	11143	4862	104342
171018	12	685100 CRA_00485	80 M	KDM6A	56 WT	7	18529	11037	3184	104342
171018	12	685100 CRA_00485	80 M	KDM6A	56 WT	8	18600	11116	4052	104342
171018	12	685100 CRA_00485	80 M	KDM6A	56 WT	9	18536	10939	3648	104342
171018	12	685100 CRA_00485	80 M	KDM6A	56 WT	10	18613	10995	4357	104342
171018	12	685100 CRA_00485	80 M	KDM6A	57 WT	1	18073	11447	3968	80778
171018	12	685100 CRA_00485	80 M	KDM6A	57 WT	2	18083	11528	3723	80778
171018	12	685100 CRA_00485	80 M	KDM6A	57 WT	3	17970	11458	4192	80778
171018	12	685100 CRA_00485	80 M	KDM6A	57 WT	4	19993	11547	5628	80778
171018	12	685100 CRA_00485	80 M	KDM6A	57 WT	5	17896	11531	4653	80778
171018	12	685100 CRA_00485	80 M	KDM6A	57 WT	6	17983	11623	3053	80778
171018	12	685100 CRA_00485	80 M	KDM6A	57 WT	7	18048	11644	3551	80778
171018	12	685100 CRA_00485	80 M	KDM6A	57 WT	8	18122	11607	5000	80778
171018	12	685100 CRA_00485	80 M	KDM6A	57 WT	9	18164	11679	3368	80778
171018	12	685100 CRA_00485	80 M	KDM6A	57 WT	10	17883	11613	3949	80778
126462	6	685252 CRA_00373	73 F	KDM6A	34 mut	1	10877	13994	4460	147745
126462	6	685252 CRA_00373	73 F	KDM6A	34 mut	2	10828	14079	3447	147745
126462	6	685252 CRA_00373	73 F	KDM6A	34 mut	3	10883	14176	5997	147745
126462	6	685252 CRA_00373	73 F	KDM6A	34 mut	4	10960	14127	4482	147745
126462	6	685252 CRA_00373	73 F	KDM6A	34 mut	5	10987	14050	4833	147745
126462	6	685252 CRA_00373	73 F	KDM6A	34 mut	6	11084	14099	5420	147745
126462	6	685252 CRA_00373	73 F	KDM6A	34 mut	7	11109	14186	4733	147745
126462	6	685252 CRA_00373	73 F	KDM6A	34 mut	8	11019	14215	6324	147745
126462	6	685252 CRA_00373	73 F	KDM6A	34 mut	9	10979	14328	11265	147745
126462	6	685252 CRA_00373	73 F	KDM6A	34 mut	10	11192	14306	12179	147745
126462	6	685252 CRA_00373	73 F	KDM6A	35 WT	1	10627	14135	12217	146045
126462	6	685252 CRA_00373	73 F	KDM6A	35 WT	2	10592	13995	4854	146045
126462	6	685252 CRA_00373	73 F	KDM6A	35 WT	3	10723	14054	6463	146045
126462	6	685252 CRA_00373	73 F	KDM6A	35 WT	4	10689	13952	3942	146045
126462	6	685252 CRA_00373	73 F	KDM6A	35 WT	5	10497	14053	10408	146045

126462	6	685252 CRA_00373	73 F	KDM6A	35 WT	6	10778	13924	6498	146045
126462	6	685252 CRA_00373	73 F	KDM6A	35 WT	7	10700	13837	6400	146045
126462	6	685252 CRA_00373	73 F	KDM6A	35 WT	8	10550	13890	2640	146045
126462	6	685252 CRA_00373	73 F	KDM6A	35 WT	9	10605	13819	3956	146045
126462	6	685252 CRA_00373	73 F	KDM6A	35 WT	10	10879	13844	8450	146045
126462	6	685252 CRA_00373	73 F	KDM6A	36 WT	1	12055	14089	11517	176458
126462	6	685252 CRA_00373	73 F	KDM6A	36 WT	2	12192	14052	10628	176458
126462	6	685252 CRA_00373	73 F	KDM6A	36 WT	3	12102	13949	9413	176458
126462	6	685252 CRA_00373	73 F	KDM6A	36 WT	4	12325	14095	7009	176458
126462	6	685252 CRA_00373	73 F	KDM6A	36 WT	5	11918	13973	7340	176458
126462	6	685252 CRA_00373	73 F	KDM6A	36 WT	6	11926	14065	4853	176458
126462	6	685252 CRA_00373	73 F	KDM6A	36 WT	7	11913	14179	5510	176458
126462	6	685252 CRA_00373	73 F	KDM6A	36 WT	8	11820	14073	7025	176458
126462	6	685252 CRA_00373	73 F	KDM6A	36 WT	9	12075	14223	4167	176458
126462	6	685252 CRA_00373	73 F	KDM6A	36 WT	10	12200	14191	9068	176458
126462	6	685252 CRA_00373	73 F	KDM6A	37 WT	1	10228	13074	8202	136948
126462	6	685252 CRA_00373	73 F	KDM6A	37 WT	2	10169	12988	6773	136948
126462	6	685252 CRA_00373	73 F	KDM6A	37 WT	3	10075	13057	9143	136948
126462	6	685252 CRA_00373	73 F	KDM6A	37 WT	4	10281	13177	8462	136948
126462	6	685252 CRA_00373	73 F	KDM6A	37 WT	5	10138	13175	7005	136948
126462	6	685252 CRA_00373	73 F	KDM6A	37 WT	6	10031	13136	6376	136948
126462	6	685252 CRA_00373	73 F	KDM6A	37 WT	7	10380	13101	6620	136948
126462	6	685252 CRA_00373	73 F	KDM6A	37 WT	8	10287	12964	8367	136948
126462	6	685252 CRA_00373	73 F	KDM6A	37 WT	9	10386	13011	8156	136948
126462	6	685252 CRA_00373	73 F	KDM6A	37 WT	10	10046	13243	6832	136948

DW.Patient.n	NCrypts	NMutantCryp	Age	Sex	WT_Fufi	Mut_Fufi	Mut_Fufi_fra	WT_Fufi_frac	Total_Fufi_fr	mark
CDA_00016	2483	2	66	F	7	0	0	0.00282144	0.00281917	KDM6A
CDA_00076	2239	6	81	M	6	1	0.16666667	0.00268697	0.0031264	KDM6A
CDA_00080	4443	1	64	M	12	0	0	0.00270149	0.00270088	KDM6A
CDA_00087	4488	23	79	F	28	0	0	0.006271	0.00623886	KDM6A
CDA_00088	4876	4	41	F	1	0	0	2.05E-04	2.05E-04	KDM6A
CDA_00089	2673	15	82	F	0	0	0	0	0	KDM6A
CDA_00097	3936	30	77	F	4	0	0	0.00102407	0.00101626	KDM6A
CRA_00117	13969	21	73	M	34	1	0.04761905	0.00243763	0.00250555	KDM6A
CRA_00125	10479	49	75	M	13	0	0	0.0012464	0.00124058	KDM6A
CRA_00126	5728	2	70	M	5	0	0	8.73E-04	8.73E-04	KDM6A
CRA_00127	14337	25	85	M	12	0	0	8.38E-04	8.37E-04	KDM6A
CRA_00128	14655	31	70	F	3	0	0	2.05E-04	2.05E-04	KDM6A
CRA_00129	68371	512	93	M	89	0	0	0.00131154	0.00130172	KDM6A
CRA_00130	106674	54	55	F	139	1	0.01851852	0.0013037	0.00131241	KDM6A
CRA_00131	28222	79	62	M	25	0	0	8.88E-04	8.86E-04	KDM6A
CRA_00134	49684	34	64	F	134	0	0	0.00269889	0.00269705	KDM6A
CRA_00294	3020	4	89	M	35	0	0	0.01160477	0.0115894	KDM6A
CRA_00295	9718	4	85	F	12	0	0	0.00123533	0.00123482	KDM6A
CRA_00297	25757	112	50	M	275	8	0.07142857	0.01072334	0.0109873	KDM6A
CRA_00298	17175	1	76	F	20	0	0	0.00116455	0.00116448	KDM6A
CRA_00299	506	21	37	F	1	2	0.0952381	0.00206186	0.00592885	KDM6A
CRA_00300	20583	10	60	F	1	0	0	4.86E-05	4.86E-05	KDM6A
CRA_00301	50018	248	69	M	18	1	0.00403226	3.62E-04	3.80E-04	KDM6A
CRA_00302	56770	33	83	M	167	0	0	0.00294341	0.00294169	KDM6A
CRA_00303	141360	335	57	F	51	0	0	3.62E-04	3.61E-04	KDM6A
CRA_00304	68797	68	60	M	105	0	0	0.00152774	0.00152623	KDM6A
CRA_00305	13187	32	51	M	58	1	0.03125	0.00440897	0.0044741	KDM6A
CRA_00306	4620	29	76	F	19	1	0.03448276	0.00413853	0.004329	KDM6A
CRA_00307	33595	112	62	F	9	1	0.00892857	2.69E-04	2.98E-04	KDM6A
CRA_00308	14036	60	73	F	0	0	0	0	0	KDM6A

CRA_00309	12864	10	80 F	137	0	0	0.01065816	0.01064988	KDM6A
CRA_00311	4477	6	62 M	83	0	0	0.01856408	0.0185392	KDM6A
CRA_00312	32449	10	67 M	102	1	0.1	0.00314436	0.00317421	KDM6A
CRA_00313	1425	3	57 M	1	0	0	7.03E-04	7.02E-04	KDM6A
CRA_00314	7043	13	89 M	4	0	0	5.69E-04	5.68E-04	KDM6A
CRA_00315	9209	52	60 F	60	0	0	0.00655236	0.00651537	KDM6A
CRA_00316	20166	242	85 M	92	1	0.00413223	0.00461755	0.00461172	KDM6A
CRA_00317	26112	204	69 M	12	1	0.00490196	4.63E-04	4.98E-04	KDM6A
CRA_00318	8123	16	48 M	3	0	0	3.70E-04	3.69E-04	KDM6A
CRA_00348	7851	12	56 F	0	1	0.08333333	0	1.27E-04	KDM6A
CRA_00349	30220	353	37 M	17	1	0.00283286	5.69E-04	5.96E-04	KDM6A
CRA_00350	21396	50	70 M	11	0	0	5.15E-04	5.14E-04	KDM6A
CRA_00351	27495	15	68 F	14	0	0	5.09E-04	5.09E-04	KDM6A
CRA_00357	31766	21	79 M	435	0	0	0.01370295	0.01369389	KDM6A
CRA_00360	29773	377	65 F	1	1	0.00265252	3.40E-05	6.72E-05	KDM6A
CRA_00361	20941	6	65 F	30	0	0	0.00143301	0.0014326	KDM6A
CRA_00363	28745	80	72 M	28	1	0.0125	9.77E-04	0.00100887	KDM6A
CRA_00364	34141	169	74 M	105	5	0.0295858	0.00309078	0.00322193	KDM6A
CRA_00365	32482	38	74 F	32	0	0	9.86E-04	9.85E-04	KDM6A
CRA_00366	49654	53	77 F	118	0	0	0.00237898	0.00237644	KDM6A
CRA_00374	12091	12	84 M	64	0	0	0.00529845	0.00529319	KDM6A
CRA_00409	26611	116	77 F	6	0	0	2.26E-04	2.25E-04	KDM6A
CRA_00412	29293	392	68 F	106	3	0.00765306	0.00366769	0.00372103	KDM6A
CRA_00413	107432	224	65 F	547	12	0.05357143	0.00510223	0.00520329	KDM6A
CRA_00414	135100	408	72 F	40	0	0	2.97E-04	2.96E-04	KDM6A
CRA_00415	15665	36	85 M	230	2	0.05555556	0.01471623	0.01481009	KDM6A
CRA_00419	13131	37	46 F	834	5	0.13513514	0.06369329	0.0638946	KDM6A
CRA_00427	4159	19	67 F	185	1	0.05263158	0.04468599	0.04472229	KDM6A
CRA_00428	17802	56	73 F	82	0	0	0.00462076	0.00460622	KDM6A
CRA_00429	31372	48	63 M	32	1	0.02083333	0.00102158	0.00105189	KDM6A
CRA_00430	14944	10	69 M	2	0	0	1.34E-04	1.34E-04	KDM6A

CRA_00431	32878	108	75 F	170	0	0	0.00518767	0.00517063	KDM6A
CRA_00469	10551	51	66 M	94	4	0.07843137	0.00895238	0.00928822	KDM6A
CRA_00473	4683	12	85 F	9	1	0.08333333	0.00192678	0.00213538	KDM6A
CRA_00479	7614	19	61 F	1	1	0.05263158	1.32E-04	2.63E-04	KDM6A
NDX_00247	5155	5	85 F	1	0	0	1.94E-04	1.94E-04	KDM6A
NDX_00252	2340	2	45 F	0	0	0	0	0	KDM6A
NDX_00253	17704	9	56 F	55	0	0	0.00310822	0.00310664	KDM6A
NDX_00254	5252	1	82 F	28	0	0	0.00533232	0.0053313	KDM6A
NDX_00258	1312	0	49 F	0	0	0	0	0	KDM6A
NDX_00260	2258	1	53 M	39	0	0	0.01727957	0.01727192	KDM6A
NDX_00261	3060	2	71 F	1	0	0	3.27E-04	3.27E-04	KDM6A
NDX_00263	1461	0	66 F	1	0	0	6.84E-04	6.84E-04	KDM6A
NDX_00264	1413	0	82 M	8	0	0	0.00566171	0.00566171	KDM6A
NDX_00265	441	8	58 F	1	0	0	0.00230947	0.00226757	KDM6A
NDX_00266	717	0	13 M	0	0	0	0	0	KDM6A
NDX_00324	2692	1	33 F	5	0	0	0.00185805	0.00185736	KDM6A
NDX_00327	5121	0	69 M	3	0	0	5.86E-04	5.86E-04	KDM6A
NDX_00369	2375	7	68 F	9	0	0	0.00380068	0.00378947	KDM6A
NDX_00391	6249	1	0 F	6	1	1	9.60E-04	0.00112018	KDM6A
NDX_00393	4460	1	78 M	56	0	0	0.01255887	0.01255605	KDM6A
NDX_00394	3248	6	73 F	21	0	0	0.00647748	0.00646552	KDM6A
NDX_00398	5210	1	59 M	5	0	0	9.60E-04	9.60E-04	KDM6A
NDX_00403	3008	10	64 M	3	0	0	0.00100067	9.97E-04	KDM6A
NDX_00405	3836	7	59 M	4	0	0	0.00104466	0.00104275	KDM6A
NDX_00406	2362	0	74 M	4	0	0	0.00169348	0.00169348	KDM6A
NDX_00407	928	2	71 M	0	0	0	0	0	KDM6A
NRA_00346	6657	9	49 F	25	1	0.11111111	0.00376053	0.00390566	KDM6A
NRA_00368	14173	10	79 F	455	2	0.2	0.03212596	0.03224441	KDM6A
NRA_00369	6809	24	72 F	23	0	0	0.00338983	0.00337788	KDM6A
NRA_00416	18371	11	77 F	505	0	0	0.02750545	0.02748898	KDM6A
CRA_00118	1826	7	74 M	6	0	0	0.00329852	0.00328587	STAG2

CRA_00121	4430	8	60 M	27	0	0	0.00610583	0.00609481	STAG2
CRA_00125	27820	101	75 M	71	0	0	0.00256142	0.00255212	STAG2
CRA_00126	41925	21	70 M	286	0	0	0.00682512	0.00682171	STAG2
CRA_00127	20731	72	85 M	12	1	0.01388889	5.81E-04	6.27E-04	STAG2
CRA_00128	62251	542	70 F	229	4	0.00738007	0.00371097	0.00374291	STAG2
CRA_00129	134491	647	93 M	350	1	0.0015456	0.00261498	0.00260984	STAG2
CRA_00130	86970	150	55 F	251	2	0.01333333	0.00289104	0.00290905	STAG2
CRA_00131	106938	139	62 M	178	0	0	0.00166668	0.00166452	STAG2
CRA_00132	28191	170	74 M	122	1	0.00588235	0.00435388	0.00436309	STAG2
CRA_00133	40703	271	68 F	44	3	0.01107011	0.00108825	0.00115471	STAG2
CRA_00134	61278	58	64 F	273	1	0.01724138	0.00445933	0.00447143	STAG2
CRA_00183	18412	3	69 M	25	0	0	0.00135803	0.00135781	STAG2
CRA_00184	94914	450	64 F	212	0	0	0.00224424	0.0022336	STAG2
CRA_00294	44394	82	89 M	659	3	0.03658537	0.01487182	0.01491193	STAG2
CRA_00295	54981	185	85 F	206	1	0.00540541	0.0037594	0.00376494	STAG2
CRA_00302	96834	205	83 M	189	0	0	0.00195593	0.00195179	STAG2
CRA_00303	113511	312	57 F	73	0	0	6.45E-04	6.43E-04	STAG2
CRA_00304	75238	90	60 M	208	0	0	0.00276787	0.00276456	STAG2
CRA_00305	80722	199	51 M	490	4	0.0201005	0.00608522	0.00611977	STAG2
CRA_00307	60587	564	62 F	17	0	0	2.83E-04	2.81E-04	STAG2
CRA_00308	92564	375	73 F	33	1	0.00266667	3.58E-04	3.67E-04	STAG2
CRA_00309	93690	1165	80 F	633	23	0.01974249	0.00684139	0.00700181	STAG2
CRA_00310	72304	475	78 F	48	2	0.00421053	6.68E-04	6.92E-04	STAG2
CRA_00311	21234	177	62 M	86	0	0	0.00408415	0.00405011	STAG2
CRA_00312	96870	265	67 M	377	1	0.00377358	0.00390249	0.00390214	STAG2
CRA_00313	5442	44	57 M	7	1	0.02272727	0.00129678	0.00147005	STAG2
CRA_00314	8285	11	89 M	17	0	0	0.00205463	0.0020519	STAG2
CRA_00315	130326	970	60 F	2553	21	0.02164948	0.01973623	0.01975047	STAG2
CRA_00316	96543	187	85 M	134	1	0.00534759	0.00139068	0.00139834	STAG2
CRA_00317	87989	115	69 M	125	1	0.00869565	0.00142249	0.001432	STAG2
CRA_00318	73090	315	48 M	35	0	0	4.81E-04	4.79E-04	STAG2

CRA_00347	15096	21	68 M	8	0	0	5.31E-04	5.30E-04	STAG2
CRA_00349	74441	90	37 M	144	0	0	0.00193676	0.00193442	STAG2
CRA_00350	103506	149	70 M	111	1	0.00671141	0.00107395	0.00108206	STAG2
CRA_00351	96731	380	68 F	152	1	0.00263158	0.00157757	0.00158171	STAG2
CRA_00353	171436	1244	83 F	889	8	0.00643087	0.00522351	0.00523227	STAG2
CRA_00354	126171	915	83 F	1544	11	0.01202186	0.01232675	0.01232454	STAG2
CRA_00355	134996	640	65 F	112	0	0	8.34E-04	8.30E-04	STAG2
CRA_00357	117291	142	79 M	2302	3	0.02112676	0.01965019	0.01965198	STAG2
CRA_00362	61537	221	85 F	51	0	0	8.32E-04	8.29E-04	STAG2
CRA_00366	116012	1751	77 F	175	15	0.00856653	0.00153158	0.00163776	STAG2
CRA_00367	129267	1096	82 M	473	16	0.01459854	0.00369038	0.00378287	STAG2
CRA_00371	83682	79	60 F	1337	1	0.01265823	0.01599225	0.0159891	STAG2
CRA_00372	82650	282	81 M	2861	22	0.07801418	0.03473436	0.03488203	STAG2
CRA_00373	57549	780	73 F	295	3	0.00384615	0.0051965	0.0051782	STAG2
CRA_00374	111586	281	84 M	716	3	0.01067616	0.00643277	0.00644346	STAG2
CRA_00409	122761	1174	77 F	46	2	0.00170358	3.78E-04	3.91E-04	STAG2
CRA_00410	87852	428	55 F	4259	9	0.02102804	0.0487166	0.04858171	STAG2
CRA_00411	166506	838	90 M	64	0	0	3.86E-04	3.84E-04	STAG2
NDA_00123	889	5	42 M	1	0	0	0.00113122	0.00112486	STAG2
NDA_00124	840	13	60 M	1	0	0	0.00120919	0.00119048	STAG2
NDX_00245	2573	20	81 M	4	0	0	0.00156678	0.00155461	STAG2
NDX_00252	2238	4	45 F	3	0	0	0.00134288	0.00134048	STAG2
CDA_00031	3331	2	79 M	2	0	0	6.01E-04	6.00E-04	mPAS
CDA_00035	4703	1	69 M	43	0	0	0.00914504	0.0091431	mPAS
CDA_00039	2113	1	84 M	15	0	0	0.00710227	0.00709891	mPAS
CDA_00048	4240	1	77 M	11	0	0	0.00259495	0.00259434	mPAS
CDA_00050	715	2	73 M	3	0	0	0.00420757	0.0041958	mPAS
CDA_00052	4654	2	85 M	25	0	0	0.00537403	0.00537172	mPAS
CDA_00061	2732	2	73 M	8	0	0	0.0029304	0.00292826	mPAS
CDA_00064	3283	2	52 F	7	0	0	0.0021335	0.0021322	mPAS
CDA_00066	2289	2	84 F	69	0	0	0.03017053	0.03014417	mPAS

CDA_00067	2530	1	88 F	15	0	0	0.0059312	0.00592885	mPAS
CDA_00068	1708	0	81 F	0	0	0	0	0	mPAS
CDA_00071	2669	1	62 F	26	0	0	0.00974513	0.00974148	mPAS
CDA_00078	1233	1	43 M	0	0	0	0	0	mPAS
CDA_00082	4819	0	76 F	34	0	0	0.00705541	0.00705541	mPAS
CDA_00083	553	1	61 M	0	0	0	0	0	mPAS
CDA_00084	2029	1	45 F	3	0	0	0.00147929	0.00147856	mPAS
CDA_00089	2722	3	82 F	8	0	0	0.00294226	0.00293902	mPAS
CDA_00090	2562	3	72 M	6	0	0	0.00234467	0.00234192	mPAS
CDA_00095	1449	2	81 F	28	1	0.5	0.01935038	0.0200138	mPAS
CDA_00096	3022	1	80 F	18	0	0	0.00595829	0.00595632	mPAS
CDA_00097	5569	4	77 F	19	0	0	0.0034142	0.00341174	mPAS
CDA_00100	2608	2	66 M	0	0	0	0	0	mPAS
CDA_00107	1880	6	84 F	4	0	0	0.00213447	0.00212766	mPAS
CDA_00112	2071	0	33 M	8	0	0	0.00386287	0.00386287	mPAS
CDA_00115	3212	11	53 M	33	0	0	0.01030928	0.01027397	mPAS
CRA_00296	27094	13	50 M	63	0	0	0.00232635	0.00232524	mPAS
CRA_00297	26941	69	50 M	295	1	0.01449275	0.01097797	0.01098697	mPAS
CRA_00298	33453	2	76 F	124	1	0.5	0.00370691	0.00373659	mPAS
CRA_00302	97154	87	83 M	174	0	0	0.00179258	0.00179097	mPAS
CRA_00305	63642	40	51 M	369	1	0.025	0.0058017	0.00581377	mPAS
CRA_00307	58392	41	62 F	16	0	0	2.74E-04	2.74E-04	mPAS
CRA_00308	92500	53	73 F	46	1	0.01886792	4.98E-04	5.08E-04	mPAS
CRA_00314	16390	6	89 M	23	0	0	0.00140381	0.00140329	mPAS
CRA_00316	71828	201	85 M	144	1	0.00497512	0.00201042	0.00201871	mPAS
CRA_00317	16750	0	69 M	64	0	0	0.0038209	0.0038209	mPAS
CRA_00351	103333	180	68 F	203	1	0.00555556	0.00196795	0.0019742	mPAS
CRA_00354	127503	66	83 F	1553	0	0	0.01218641	0.01218011	mPAS
CRA_00355	96090	106	65 F	88	1	0.00943396	9.17E-04	9.26E-04	mPAS
CRA_00357	92598	66	79 M	2034	4	0.06060606	0.02198158	0.02200911	mPAS
CRA_00359	62638	34	69 M	78	0	0	0.00124593	0.00124525	mPAS

CRA_00364	14861	0	74 M	145	0	0	0.00975708	0.00975708	mPAS
CRA_00365	8251	9	74 F	3	0	0	3.64E-04	3.64E-04	mPAS
CRA_00366	116757	86	77 F	204	1	0.01162791	0.00174851	0.00175578	mPAS
CRA_00367	156630	138	82 M	726	0	0	0.00463921	0.00463513	mPAS
CRA_00410	117499	53	55 F	4692	3	0.05660377	0.03995028	0.03995779	mPAS
CRA_00419	35436	23	46 F	1693	1	0.04347826	0.0478073	0.04780449	mPAS
CRA_00420	43180	19	67 M	39	0	0	9.04E-04	9.03E-04	mPAS
CRA_00421	9137	10	77 M	205	1	0.1	0.02246083	0.02254569	mPAS
CRA_00429	28961	18	63 M	20	0	0	6.91E-04	6.91E-04	mPAS
CRA_00430	33014	18	69 M	18	1	0.05555556	5.46E-04	5.76E-04	mPAS
CRA_00433	3567	3	80 F	10	0	0	0.00280584	0.00280348	mPAS
CRA_00435	84435	59	72 M	34	0	0	4.03E-04	4.03E-04	mPAS
CRA_00437	21697	13	55 M	191	0	0	0.00880834	0.00880306	mPAS
CRA_00438	8531	7	76 F	13	0	0	0.00152511	0.00152385	mPAS
CRA_00439	9908	6	71 M	7	0	0	7.07E-04	7.06E-04	mPAS
CRA_00441	69911	104	69 M	337	6	0.05769231	0.0048276	0.00490624	mPAS
CRA_00446	27907	21	44 M	258	0	0	0.00925195	0.00924499	mPAS
CRA_00450	7991	0	40 M	117	0	0	0.01464147	0.01464147	mPAS
CRA_00451	15244	27	84 M	88	2	0.07407407	0.00578301	0.00590396	mPAS
CRA_00469	17127	11	66 M	111	4	0.36363636	0.00648516	0.00671454	mPAS
CRA_00480	15007	20	57 M	17	0	0	0.00113432	0.0011328	mPAS
NDX_00326	2880	3	64 F	17	0	0	0.00590893	0.00590278	mPAS
NDX_00327	2818	4	69 M	3	0	0	0.0010661	0.00106458	mPAS
NDX_00335	1733	1	75 F	4	0	0	0.00230947	0.00230814	mPAS
NDX_00338	4711	16	65 F/M	5	0	0	0.00106496	0.00106135	mPAS
NDX_00339	1541	3	74 F	10	0	0	0.00650195	0.00648929	mPAS
NDX_00344	4296	4	64 M	6	0	0	0.00139795	0.00139665	mPAS
NDX_00369	16757	21	68 F	165	0	0	0.00985899	0.00984663	mPAS
NDX_00370	7595	8	68 M	20	0	0	0.00263609	0.00263331	mPAS
NDX_00373	2870	1	58 F	7	0	0	0.00243987	0.00243902	mPAS
NDX_00378	2406	3	62 M	0	1	0.33333333	0	4.16E-04	mPAS

NDX_00379	10262	11	62 M	18	0	0	0.00175593	0.00175404	mPAS
NDX_00383	7262	13	71 F	10	0	0	0.0013795	0.00137703	mPAS
NDX_00389	4627	5	63 F	0	0	0	0	0	mPAS
NDX_00390	1541	1	79 F	3	1	1	0.00194805	0.00259572	mPAS
NDX_00396	4956	4	80 F	17	0	0	0.00343296	0.00343019	mPAS
NDX_00403	1950	4	64 M	2	0	0	0.00102775	0.00102564	mPAS
NDX_00407	917	1	71 M	1	0	0	0.0010917	0.00109051	mPAS
NRA_00346	54866	26	49 F	495	0	0	0.00902626	0.00902198	mPAS
NRA_00368	21169	0	79 F	1883	0	0	0.08895082	0.08895082	mPAS
NRA_00416	7546	0	77 F	386	0	0	0.05115293	0.05115293	mPAS

mark	event_type	mut_nbrs	wt_nbrs
mPAS	M/M	1	4
mPAS	M/M	1	4
mPAS	M/M	2	4
mPAS	M/M	1	5
mPAS	M/M	0	6
mPAS	M/M	0	6
mPAS	M/M	0	6
mPAS	M/M	0	6
mPAS	M/M	0	6
mPAS	M/M	0	6
mPAS	M/M	0	6
mPAS	M/M	0	6
mPAS	M/M	0	6
mPAS	M/M	0	6
mPAS	M/M	0	6
mPAS	M/M	0	6
mPAS	M/M	0	6
mPAS	M/W	0	6
mPAS	M/W	0	6
mPAS	M/W	0	6
mPAS	M/W	0	6
mPAS	M/W	0	6
mPAS	M/W	0	6
mPAS	M/W	0	6
mPAS	M/W	0	6
mPAS	M/W	0	6
mPAS	M/W	0	6
mPAS	M/W	0	6
mPAS	M/W	0	6
mPAS	M/W	0	6
mPAS	M/W	0	6
STAG2	M/M	1	5
STAG2	M/M	1	5
STAG2	M/M	1	5
STAG2	M/M	2	4
STAG2	M/M	1	4
STAG2	M/M	1	4
STAG2	M/M	1	5
STAG2	M/M	2	4
STAG2	M/M	3	2
STAG2	M/M	1	6
STAG2	M/M	5	1
STAG2	M/M	1	4
STAG2	M/M	2	5

STAG2	M/M	3	3
STAG2	M/M	2	4
STAG2	M/M	1	5
STAG2	M/M	4	4
STAG2	M/M	3	4
STAG2	M/M	1	4
STAG2	M/M	2	4
STAG2	M/M	5	1
STAG2	M/M	5	1
STAG2	M/M	3	3
STAG2	M/M	1	5
STAG2	M/M	3	3
STAG2	M/M	3	3
STAG2	M/M	2	3
STAG2	M/M	5	1
STAG2	M/M	4	3
STAG2	M/M	6	1
STAG2	M/M	1	5
STAG2	M/M	1	4
STAG2	M/M	3	3
STAG2	M/M	3	5
STAG2	M/M	1	4
STAG2	M/M	2	3
STAG2	M/M	4	2
STAG2	M/M	3	3
STAG2	M/M	2	3
STAG2	M/M	1	4
STAG2	M/M	1	5
STAG2	M/M	1	6
STAG2	M/M	4	2
STAG2	M/M	1	5
STAG2	M/M	3	3
STAG2	M/M	4	2
STAG2	M/M	1	5
STAG2	M/M	3	3
STAG2	M/M	1	5
STAG2	M/M	1	5
STAG2	M/M	2	3
STAG2	M/M	2	4
STAG2	M/M	1	5
STAG2	M/M	1	5
STAG2	M/M	1	5
STAG2	M/M	2	3
STAG2	M/M	1	5
STAG2	M/M	1	4
STAG2	M/M	2	4

STAG2	M/M	1	4
STAG2	M/M	3	2
STAG2	M/M	3	2
STAG2	M/M	4	2
STAG2	M/M	3	2
STAG2	M/M	3	3
STAG2	M/M	2	4
STAG2	M/M	3	3
STAG2	M/M	1	4
STAG2	M/M	1	3
STAG2	M/M	2	4
STAG2	M/M	1	5
STAG2	M/M	1	3
STAG2	M/M	1	4
STAG2	M/M	2	4
STAG2	M/M	1	5
STAG2	M/M	3	2
STAG2	M/M	5	2
STAG2	M/M	2	3
STAG2	M/M	1	4
STAG2	M/M	2	3
STAG2	M/M	2	3
STAG2	M/M	2	3
STAG2	M/M	1	4
STAG2	M/M	2	4
STAG2	M/M	3	2
STAG2	M/M	2	3
STAG2	M/M	6	2
STAG2	M/M	4	3
STAG2	M/M	2	4
STAG2	M/M	2	2
STAG2	M/M	1	5
STAG2	M/M	2	3
STAG2	M/M	2	4
STAG2	M/M	2	4
STAG2	M/M	2	3
STAG2	M/M	3	4
STAG2	M/M	1	6
STAG2	M/M	4	2
STAG2	M/M	1	4
STAG2	M/M	1	5
STAG2	M/M	0	6
STAG2	M/M	0	6
STAG2	M/M	0	6
STAG2	M/M	0	6
STAG2	M/M	0	6

STAG2	M/M	0	6
STAG2	M/M	0	6
STAG2	M/M	0	6
STAG2	M/M	0	6
STAG2	M/M	0	6
STAG2	M/M	0	6
STAG2	M/M	0	6
STAG2	M/M	0	6
STAG2	M/M	0	6
STAG2	M/M	0	6
STAG2	M/M	0	6
STAG2	M/M	0	6
STAG2	M/M	0	6
STAG2	M/M	0	6
STAG2	M/M	0	6
STAG2	M/M	0	6
STAG2	M/M	0	6
STAG2	M/M	0	6
STAG2	M/M	0	6
STAG2	M/M	0	6
STAG2	M/M	0	6
STAG2	M/M	0	6
STAG2	M/M	0	6
STAG2	M/M	0	6
STAG2	M/M	0	6
STAG2	M/M	0	6
STAG2	M/M	0	6
STAG2	M/M	0	6
STAG2	M/M	0	6
STAG2	M/M	0	6
STAG2	M/M	0	6
STAG2	M/W	4	3
STAG2	M/W	1	5
STAG2	M/W	1	6
STAG2	M/W	1	6
STAG2	M/W	2	4
STAG2	M/W	1	5
STAG2	M/W	1	6
STAG2	M/W	2	6
STAG2	M/W	4	3
STAG2	M/W	4	2
STAG2	M/W	1	6
STAG2	M/W	1	6
STAG2	M/W	3	4
STAG2	M/W	1	5
STAG2	M/W	2	4
STAG2	M/W	1	6
STAG2	M/W	2	4

STAG2	M/W	5	3
STAG2	M/W	2	5
STAG2	M/W	3	3
STAG2	M/W	1	5
STAG2	M/W	0	6
STAG2	M/W	0	6
STAG2	M/W	0	6
STAG2	M/W	0	6
STAG2	M/W	0	6
STAG2	M/W	0	6
STAG2	M/W	0	6
STAG2	M/W	0	6
STAG2	M/W	0	6
STAG2	M/W	0	6
STAG2	M/W	0	6
STAG2	M/W	0	6
STAG2	M/W	0	6
STAG2	M/W	0	6
STAG2	M/W	0	6
STAG2	M/W	0	6
STAG2	M/W	0	6
STAG2	M/W	0	6
STAG2	M/W	0	6
KDM6A	M/M	0	6
KDM6A	M/M	0	5
KDM6A	M/M	0	6
KDM6A	M/M	0	5
KDM6A	M/M	0	4
KDM6A	M/M	0	4
KDM6A	M/M	0	6
KDM6A	M/M	0	5
KDM6A	M/M	0	6
KDM6A	M/M	0	3
KDM6A	M/M	3	3
KDM6A	M/M	3	4
KDM6A	M/M	1	4
KDM6A	M/M	6	1
KDM6A	M/M	2	3
KDM6A	M/M	3	2
KDM6A	M/M	4	2
KDM6A	M/M	3	3
KDM6A	M/M	1	4
KDM6A	M/M	2	4
KDM6A	M/M	3	2
KDM6A	M/M	3	3
KDM6A	M/M	2	3
KDM6A	M/M	2	4
KDM6A	M/M	1	4
KDM6A	M/M	5	1

KDM6A	M/M	1	5
KDM6A	M/M	2	2
KDM6A	M/M	2	4
KDM6A	M/M	3	2
KDM6A	M/M	4	4
KDM6A	M/M	3	2
KDM6A	M/M	3	1
KDM6A	M/M	2	1
KDM6A	M/M	3	2
KDM6A	M/M	1	4
KDM6A	M/M	1	4
KDM6A	M/M	1	6
KDM6A	M/M	2	4
KDM6A	M/M	2	4
KDM6A	M/M	2	2
KDM6A	M/M	1	5
KDM6A	M/M	3	3
KDM6A	M/M	2	4
KDM6A	M/M	5	1
KDM6A	M/M	2	4
KDM6A	M/M	3	3
KDM6A	M/M	3	1
KDM6A	M/M	5	5
KDM6A	M/M	2	3
KDM6A	M/M	4	1
KDM6A	M/M	4	1
KDM6A	M/M	1	5
KDM6A	M/M	2	4
KDM6A	M/M	4	1
KDM6A	M/W	0	7
KDM6A	M/W	0	5
KDM6A	M/W	0	6
KDM6A	M/W	0	5
KDM6A	M/W	0	7
KDM6A	M/W	3	3
KDM6A	M/W	1	7
KDM6A	M/W	2	4
KDM6A	M/W	2	4
KDM6A	M/W	5	1
KDM6A	M/W	2	7

What you need to know

BACKGROUND AND CONTEXT

As colorectal cancer is thought to arise from outgrowth of crypts harbouring excess genomic alterations, quantification of mutation accumulation and spread within this tissue is key to understanding disease initiation.

NEW FINDINGS

Exploiting loss of the cancer driver KDM6A we demonstrate that newly generated crypts resulting from increased crypt fission, are accommodated by mass movement of surrounding crypts in a diffusion-type process.

LIMITATIONS

Only two cancer driver genes, KDM6A and KRAS, are modelled here, which does not preclude the existence of alternative expansion mechanisms.

IMPACT

The threshold fission rate beyond which diffusion cannot accommodate newly generated crypts is calculable defining when identifiable pathologies may form.

Short summary

In human colon, mutations in KDM6A accelerate gland division. Modelling their dispersal as a diffusion process enabled calculation of the threshold fission rate beyond which polyp growth may occur.

Supplementary Information for

A diffusion-like process accommodates new crypts during clonal expansion in human colonic epithelium

Cora Olpe, Doran Khamis, Maria Chukanova, Nefeli Skoufou-Papoutsaki, Richard Kemp, Kate Marks, Cerys Tatton, Cecilia Lindskog, Anna Nicholson, Roxanne Brunton-Sim, Shalini Malhotra, Rogier ten Hoopen, Rachael Stanley, Edward Morrissey, Doug Winton,

* Corresponding author:

Doug Winton

Email: doug.winton@cruk.cam.ac.uk

This file includes:

Figures S1 to S13

Tables S1 to S8

Mathematical background

Journal Pre-proof

Supplemental Figures

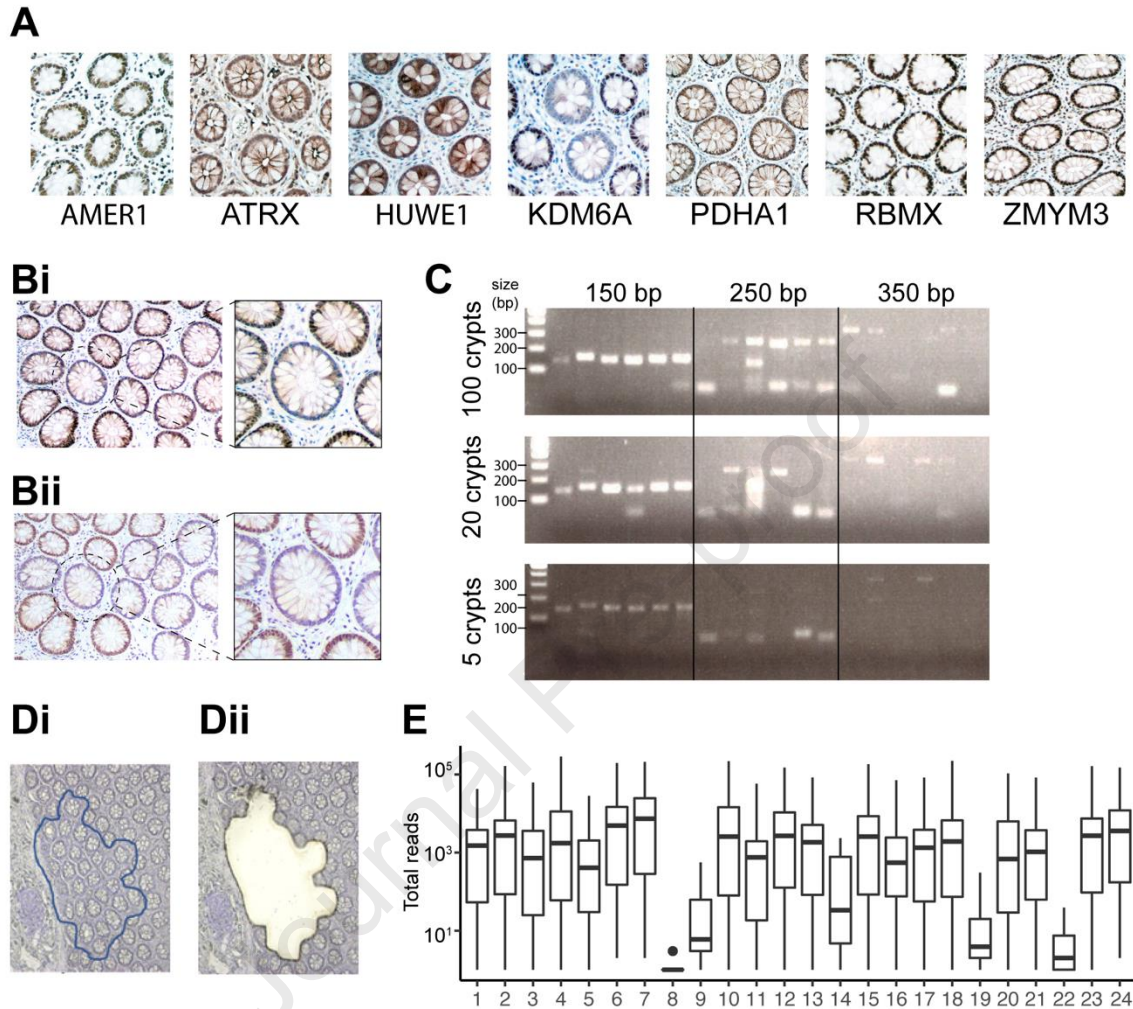


Fig. S1. Detection and laser capture of KDM6A-negative clones

(A) Representative images of IHC for cancer-associated X-linked genes on human colonic sections. Out of the 7 assessed genes, a staining pattern indicative of loss-of-function mutation was only found for KDM6A (middle panel). (B) Serial human colonic sections stained with two independent antibodies against KDM6A: (i) human protein atlas, (ii) Cell Signaling Technology. KDM6A⁺ crypts are circled and enlarged. (C) For assessment of optimal amplicon size, DNA extracted from FFPE sections was diluted to equivalents of 5, 20 and 100 crypts and used for PCR reactions (primers in table S2). Image of gel electrophoresis of PCR products on FFPE DNA diluted to equivalents of varying amounts of crypts. This revealed that an amplicon size of 150 bp ensures reliable amplification. (D) Image of IHC for KDM6A on laser capture slide (i) before and (ii) after laser capture microdissection. (E) Box plot showing reads obtained for each of the 24 amplicons used for sequencing of KDM6A-negative and control patches. Amplicon libraries from four patches failed QC. Of the remaining seven patches mutations were identified in four at mutant allele frequencies consistent with patient sex and estimated stromal fraction within the captured material (Table S4). These results both confirm antibody specificity for KDM6A and the clonality of multicrypt patches that share only a single mutation

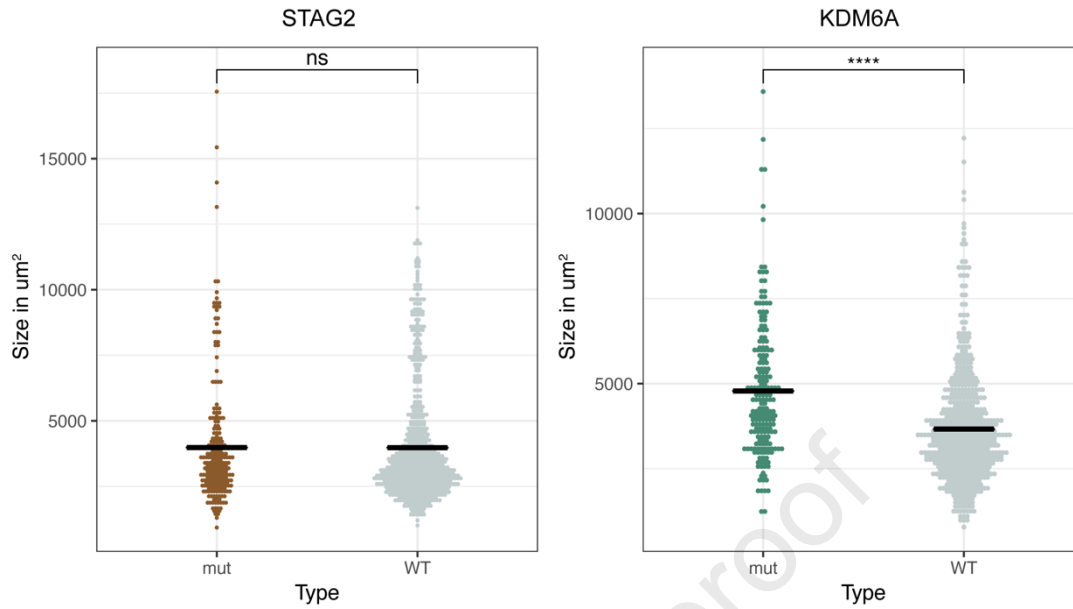


Fig. S2. Size measurement of STAG2⁻ and KDM6A⁻ crypts

Crypt areas in multicrypt clones containing 10 crypts that are STAG2⁻ or KDM6A⁻ negative (24 and 20, respectively). The area of individual crypts was determined using QuPath software. As controls, adjacent or nearby wild type groups of 10 crypts were analysed in the same way. Jitter plots show areas of crypts. Black line = median, **** = p-value = < 0.001.

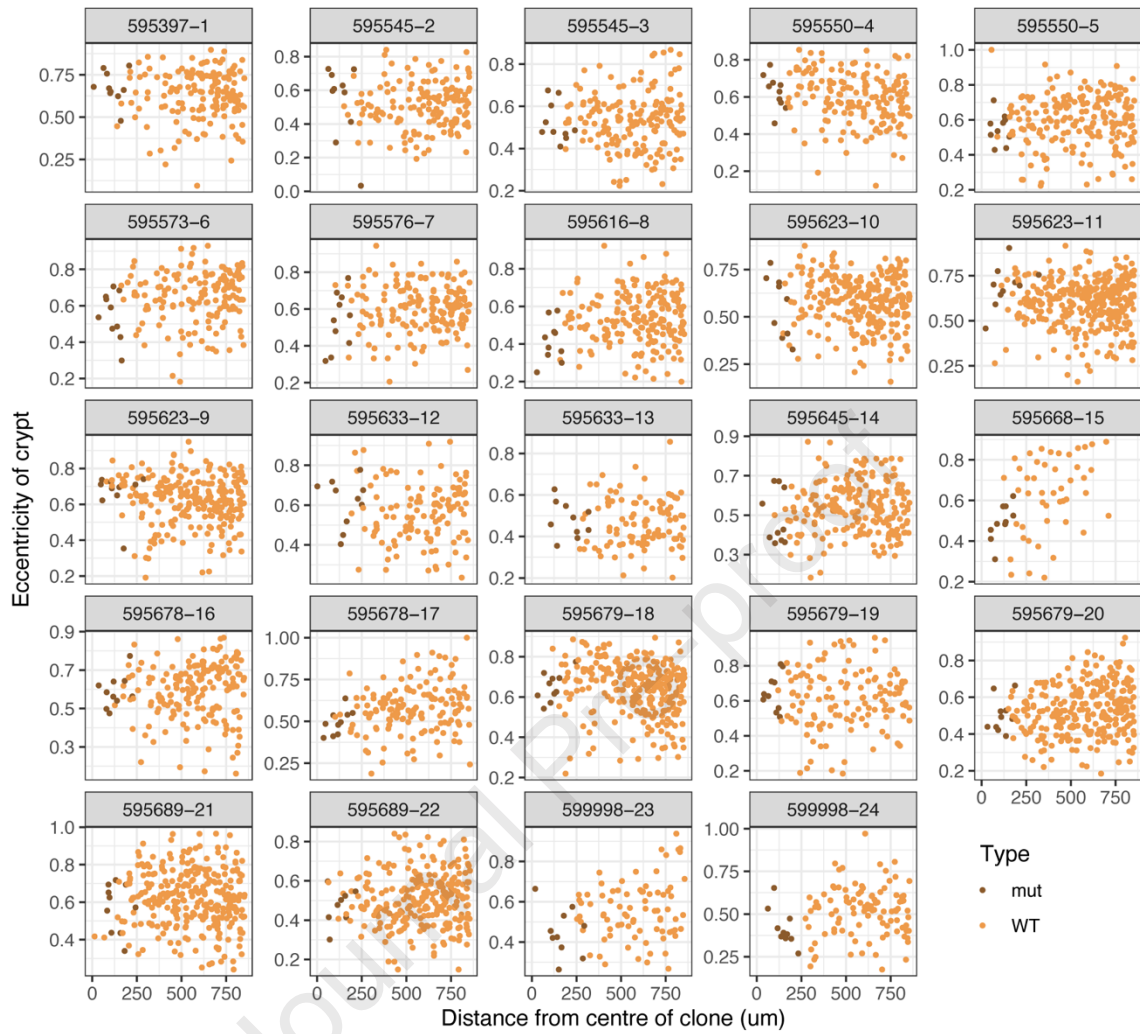


Fig. S3. Eccentricities of crypts around $STAG2^{-}$ clones of size 10 as a function of radial distance from crypt centroid.

Crypt squashing due to clone growth would impact WT (orange) crypts closest to the expanding patch, predicting a right to left decline in the crypt eccentricities in the plots above with distance from mutant (brown) crypts. This pattern is not observed.

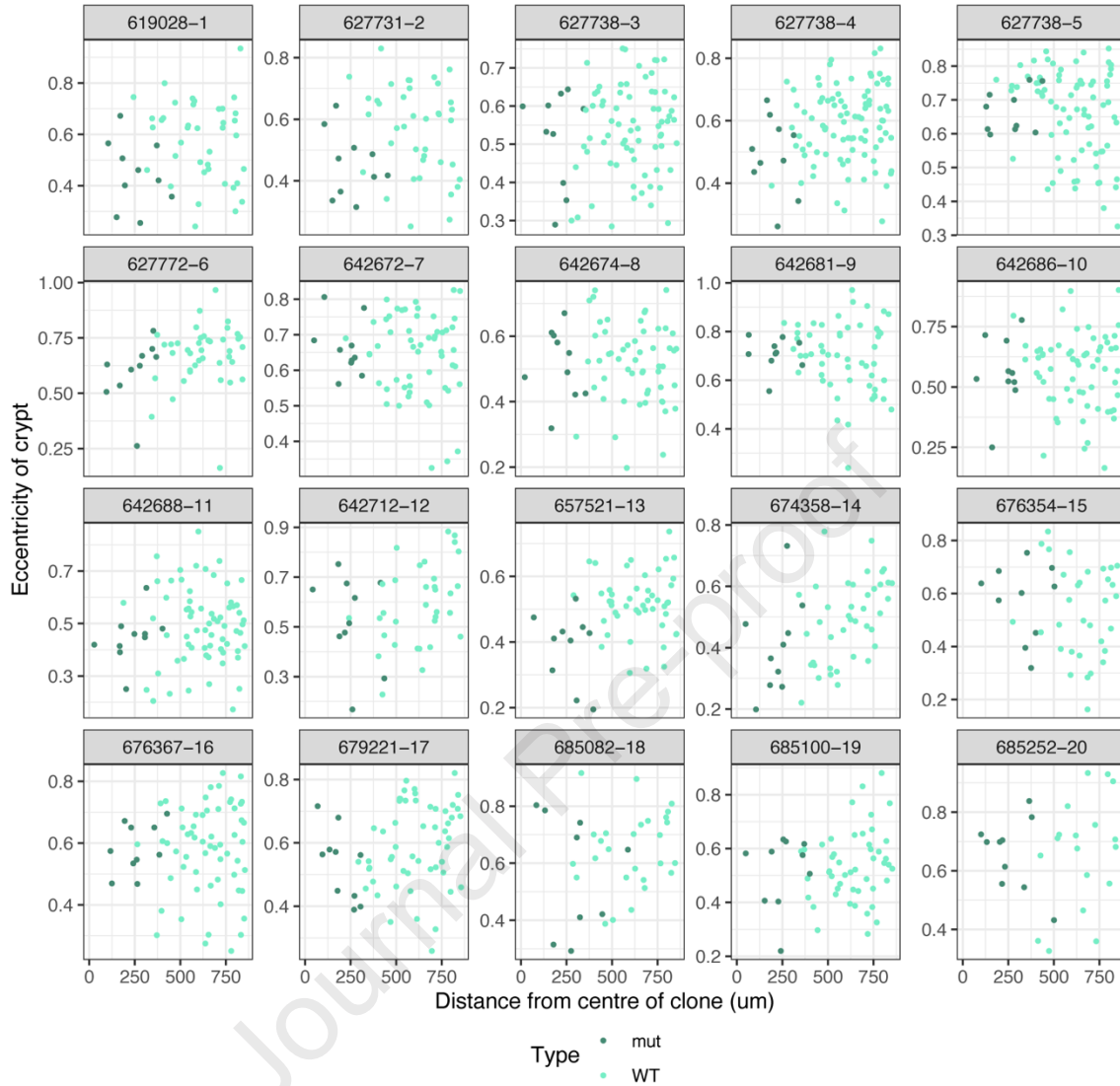


Fig. S4. Eccentricities of crypts around $KDM6A^{-}$ clones of size 10 as a function of radial distance from crypt centroid.

Crypt squashing due to clone growth would impact WT (light turquoise) crypts closest to the expanding patch, predicting a right to left decline in the crypt eccentricities in the plots above with distance from mutant (teal) crypts. This pattern is not observed.

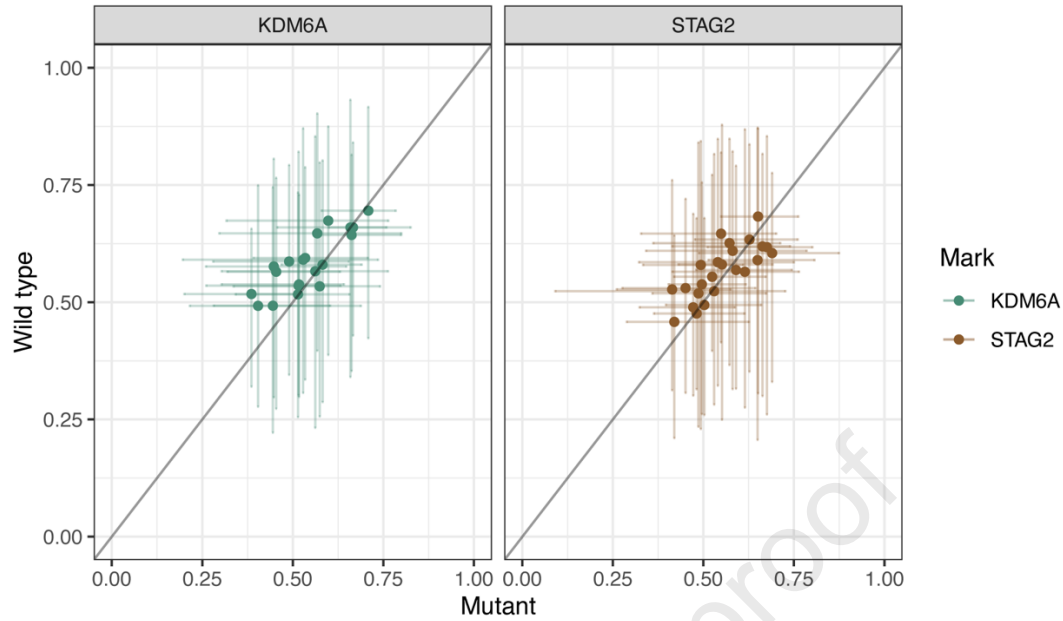


Fig. S5. Comparison of mean eccentricities of mutant and adjacent WT crypts in clones
For each assessed patch of 10 KDM6A⁻ or STAG2⁻ crypts, the mean eccentricity of the mutant crypts is plotted on the x-axis (0 = perfect circle) against the mean eccentricity of the surrounding wild type crypts on the y-axis. The diagonal line represents $x=y$, where the mean eccentricities of mutant and surrounding WT crypts correspond. Error bars = 95% confidence interval around the mean.

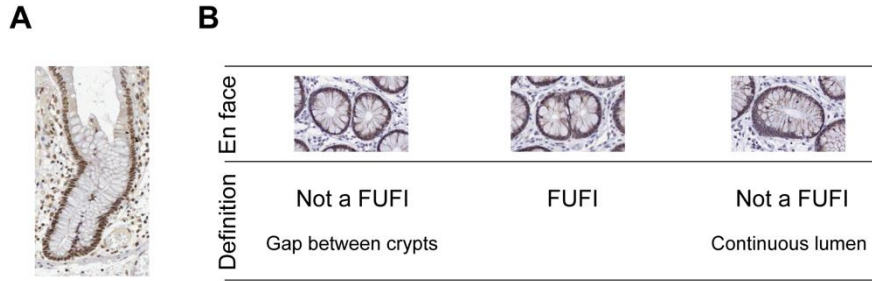


Fig. S6. Defining the FUPI

(A) Representative image of KDM6A-positive bifurcating crypts sectioned longitudinally. (B) A FUPI is defined as two adjoining crypts viewed in a transverse section with two clearly discernible lumina lacking any separating gap.

Journal Pre-proof

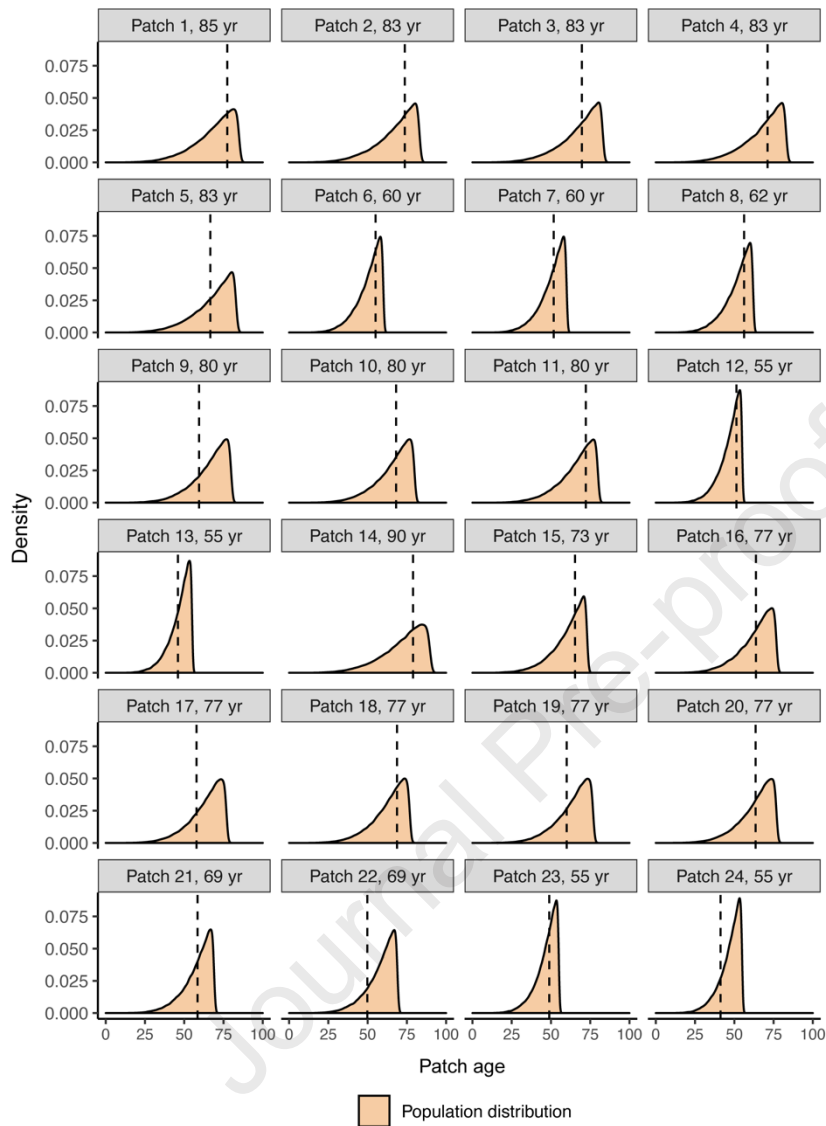


Fig. S7. Inferred ages of STAG2⁻ clones

Theoretical distributions for the age of STAG2⁻ clones in years covering the period from single crypt to a clone comprising 10 crypts. The theoretical density of patch age is calculated using the mutation rate, the monoclonal accumulation rate and the fission rate (modelling fission as a stochastic birth process). Dashed lines show the most likely patch age for each clone derived from the average of the 25 most likely trajectories.

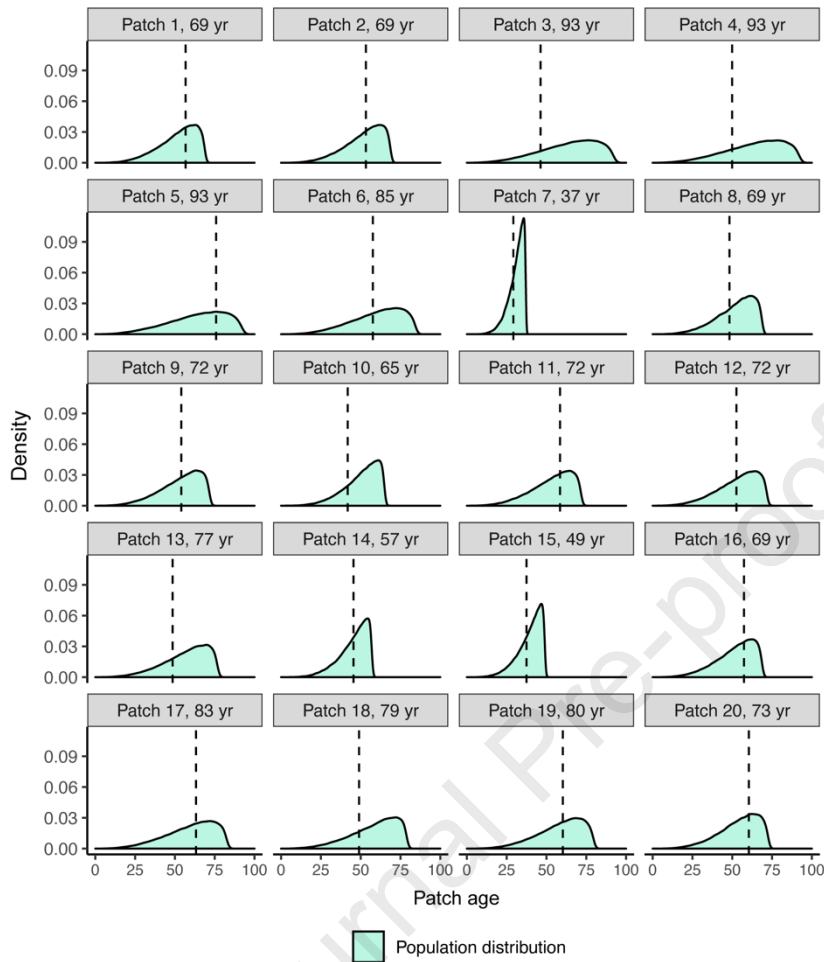


Fig. S8. Inferred ages of KDM6A⁺ clones

Theoretical distributions for the age of KDM6A⁺ clones in years covering the period from single crypt to a clone comprising 10 crypts. The theoretical density of patch age is calculated using the mutation rate, the monoclonal accumulation rate and the fission rate (modelling fission as a stochastic birth process). Dashed lines show the most likely patch age for each clone derived from the average of the 25 most likely trajectories.

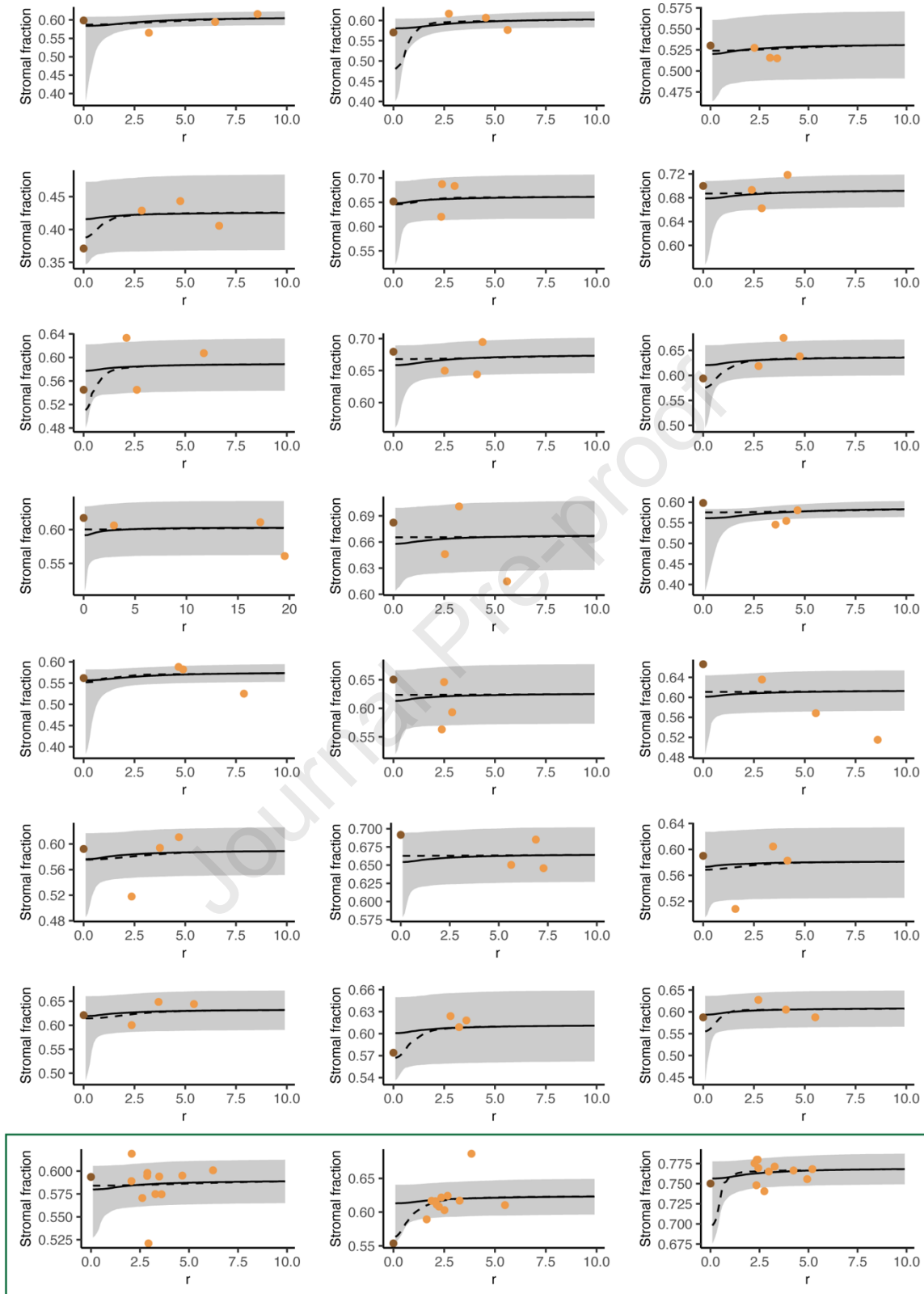


Fig. S9. Diffusion model prediction of stromal fraction changes for STAG2⁻ clones
 Plots show the stromal fraction measured for STAG2⁻ as well as surrounding wild type patches of 10 crypts. The radial distance r (in crypt domains) is measured from adjacent patch centroid to

mutant patch centroid. The black line and grey ribbon is the median and 95% CI theoretical stromal fraction as fitted from the diffusion model. Dashed line shows the solution from averaging the 25 most likely trajectories from initial mutation to clone of size 10, assuming population average diffusion and neighbourhood ambient stromal fraction. Green box: patches for which a “rolling window” was applied. For each mutant patch, surrounding measurements included two areas comprising 3 mutant and 7 WT, 2 mutant and 8 WT and 1 mutant and 9 WT crypts as well as five surrounding WT patches at varying distances (combined: 1 data point for the mutant patch and 11 for surrounding patches).

Journal Pre-proof

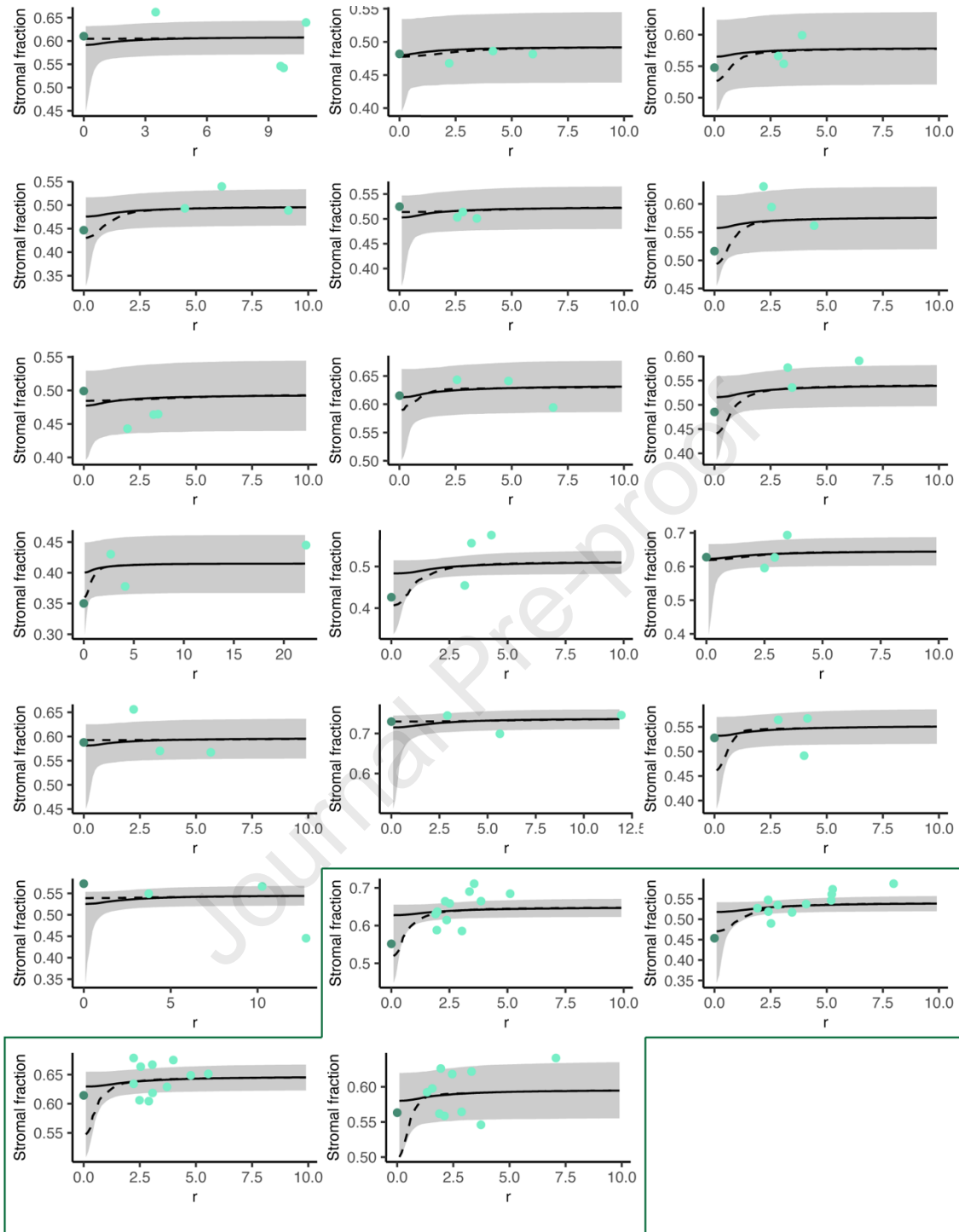


Fig. S10. Diffusion model prediction of stromal fraction changes for KDM6A⁻ clones
 Plots show the stromal fraction measured for KDM6A⁻ as well as surrounding wild type patches of 10 crypts. The radial distance r (in crypt domains) is measured from adjacent patch centroid to mutant patch centroid. The black line and grey ribbon is the median and 95% CI theoretical stromal fraction as fitted from the diffusion model. Dashed line shows the solution from averaging the 25 most likely trajectories from initial mutation to clone of size 10, assuming population average diffusion and neighbourhood ambient stromal fraction. Green box: patches for which a “rolling window” was applied. For each mutant patch, surrounding measurements included two areas comprising 3 mutant and 7 WT, 2 mutant and 8 WT and 1 mutant and 9 WT

crypts as well as five surrounding WT patches at varying distances (combined: 1 data point for the mutant patch and 11 for surrounding patches).

Journal Pre-proof

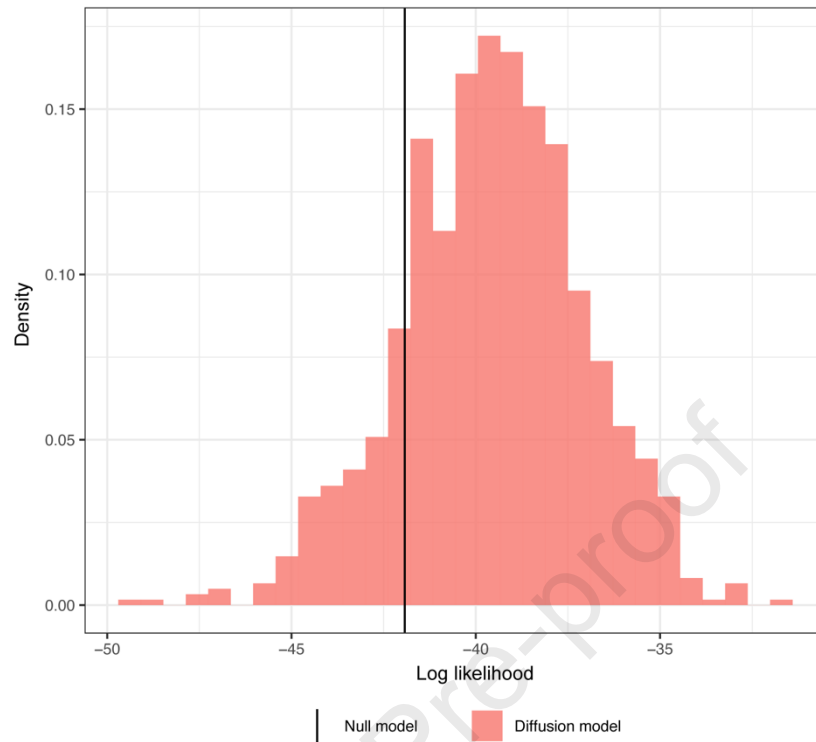


Fig. S11. Comparison of diffusion model to null model

Results for model fit comparison where the log likelihood of the data under a null model with constant per-clone stromal fraction is compared to the log likelihood of the data under the diffusion model for 1000 potential trajectories (from WT to 10-crypt mutant clone) per clone. The black line lies to the left of the density mass, meaning there is evidence for a diffusion-like radial dependence in the crypt packing data.

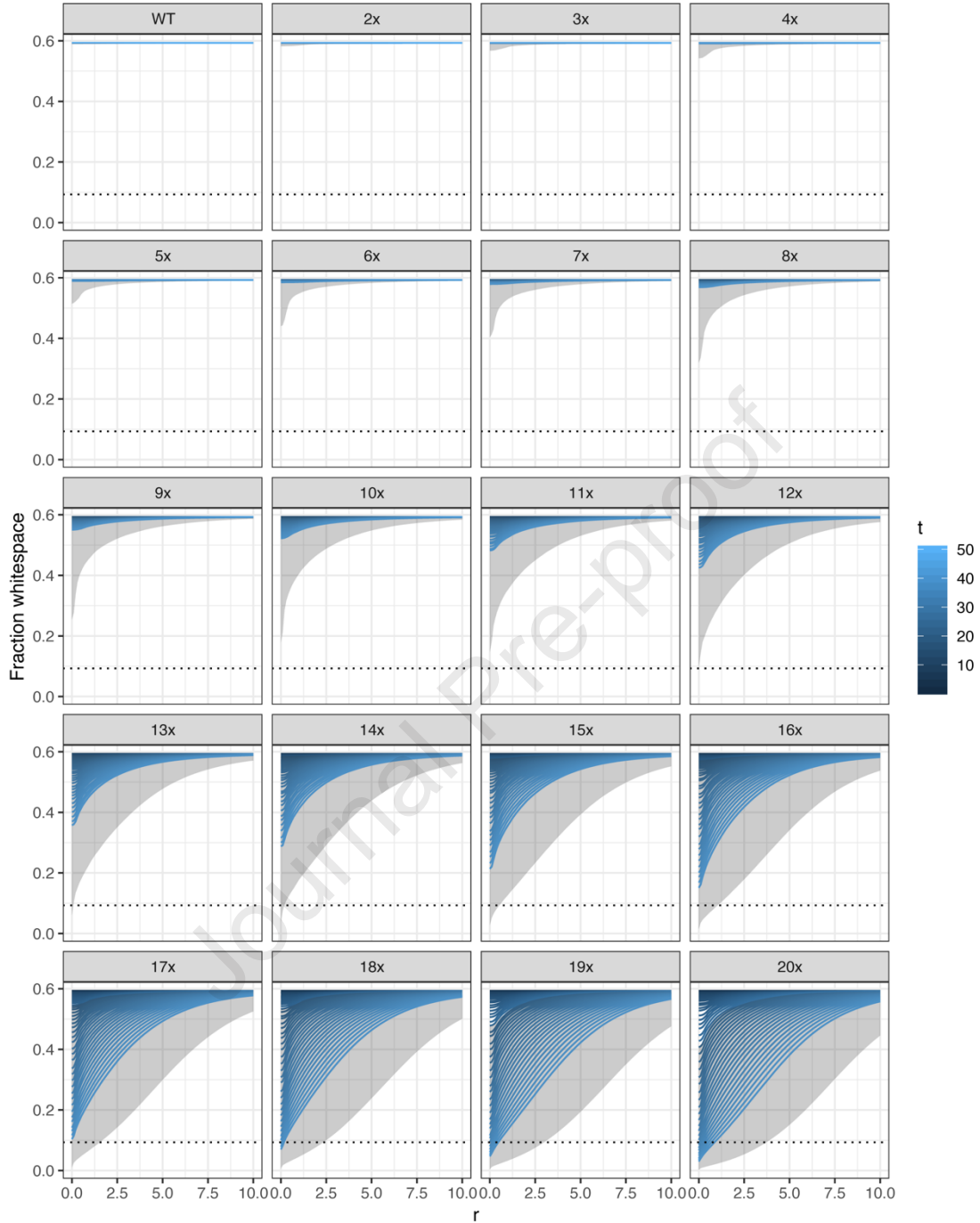


Fig. S12. Simulating the 'breaking point'

Simulations were performed to find the fission rate at which clones may generate new crypts more quickly than can be accommodated by crypt diffusion. Line graphs show the stromal fraction resulting from crypt diffusion and different crypt fission rates in multiples of the homeostatic (wild type) rate (0.7% per year). Dotted line = stromal fraction calculated from optimal hexagonal packing of circles. r = distance from centroid of patch in crypt domains. Grey area = 95% CI.

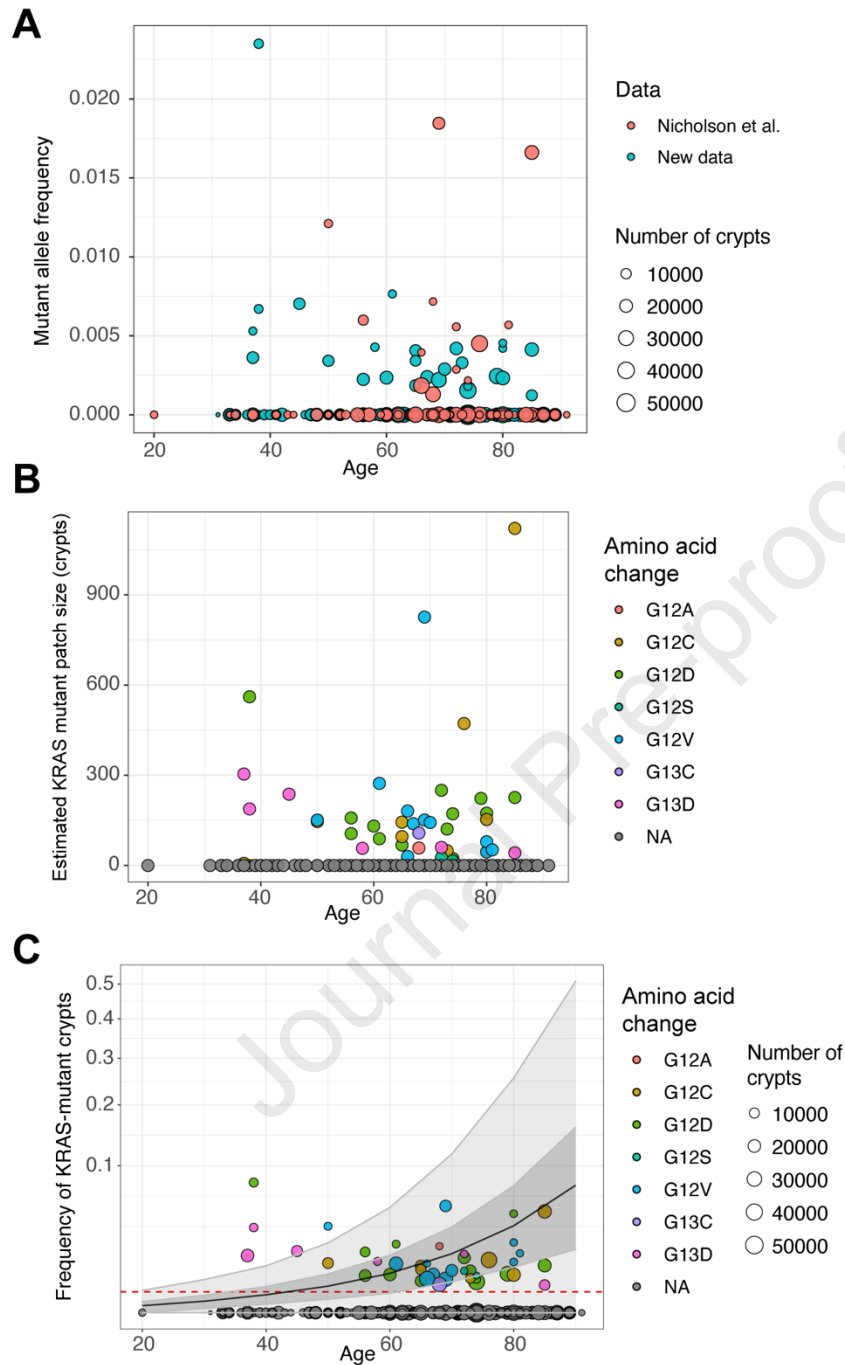


Fig. S13. Evidence for expansion of *KRAS*-mutant clones in human colon

Targeted amplicon sequencing focusing on *KRAS* codons 12 and 13 was performed on DNA from FFPE tissue sections from 256 patients of the age range 20-91 years. In total, 35 individuals displayed detectable mutations. (A) Mutant allele frequency data of *KRAS* codons 12 and 13 mutations plotted against age. Data previously published separated from new data obtained as part of this study. (B) *KRAS*-mutant patch sizes inferred from the mutant allele frequencies and known crypt numbers for 256 individuals plotted against age. (C) Frequency of *KRAS* mutant crypts for 256 individuals plotted against age. The mean accumulation of mutant clones using the model is plotted in black as well as the 95%CI in grey. Red dotted line shows detection threshold.

Supplemental Tables**Table S1.** Primary antibodies used for immunohistochemistry.

Antigen	Antibody	Supplier	Titre
KDM6A	HPA002111	HPA	1:100
KDM6A	#33510	CST	1:200
MAOA	SC-271123	Santa Cruz	1:200
STAG2	LS-B11284	LSBio	1:1000

Journal Pre-proof

Table S2. Primers used for amplification of FFPE to assess amplifiability.

Primer	Sequence (5' -> 3')
MAOA_150_F1	ACCCATCAGTTACTCCTTCCC
MAOA_150_R1	GGGATTAAGCTGGGAGTTTCT
MAOA_150_F2	TAGCAGGGCCTTGAATCTGT
MAOA_150_R2	GATAGTGCCCAGAGTCACCA
STAG2_150_F1	GGAGAAGAAGACACAGTTGGATG
STAG2_150_R1	TTCTGTGAGGCATTTAGGGAAAA
STAG2_150_F2	CCTATGCTCGCACAACTATGAG
STAG2_150_R2	GGAAGCCACACATCCTCTCT
CASD1_150_F1	ACCTGGAAACCCTATGCTCAA
CASD1_150_R1	TGCAGCTATACATGCCAAC
LOC_150_F1	TCGTCTGCTTCATCCTCCTC
LOC_150_R1	GCCTAACATGCTTGGACCAC
MAOA_250_F1	TGCAAGTCTTAGGTTGGTTGC
MAOA_250_R1	TCAGTAATGGGTCATGTGCAA
MAOA_250_F2	AAGACATGTAGGTTGGGGC
MAOA_250_R2	CAGAACACCCTGCTCTAACCT
STAG2_250_F1	GACTCTAAGGCCAGGTCAGG
STAG2_250_R1	GGAGGTGAGTTGTGGTGTCT
STAG2_250_F2	GCCTAATCATTCTCCCTGACCT
STAG2_250_R2	TGGTGTCAAATCCATTCCCTC
CASD1_250_F1	GGTTAGAGGAAGACAAAAGTGGA
CASD1_250_R1	CCTCAGTCCACACTTTGATACAC
LOC_250_F1	AGCTTACCTCTTTGTCTCTTCT
LOC_250_R1	CAACCTCAAAGTATCACGTGGA
MAOA_350_F1	TTCCCTTCAGAAATTGAATCCTTG
MAOA_350_R1	CCTGGGAGAAAGCAAAATCA
MAOA_350_F2	TCCCGGAGTATCAGCAAAAG

MAOA_350_R2	CATGAGAGACCCCCAAACAC
STAG2_350_F1	TCCGAATATTTTTGGTGCATT
STAG2_350_R1	CAGAGCCTTGATGAGTGCTG
STAG2_350_F2	TCTGAAGGAATGCTATGGTATGAA
STAG2_350_R2	TTGTCAAGGGTCATAGACACAA
CASD1_350_F1	CTTTGGGAAGCTTTGCGTAAAA
CASD1_350_R1	CGATTCAGGAAGATGTAAGCCA
LOC_350_F1	TCAGGAATGATGGTCTACGTGA
LOC_350_R1	TCTCAGCTCTATTCCGTGAGT

Table S3. Primers used for amplification of KDM6A. Number = amplicon number, F = forward primer, R = reverse primer. Sequence includes Fluidigm CS adapters.

Primer	Sequence (5' -> 3')
1_F	ACACTGACGACATGGTTCTACACGCTTTCCGGTGATGAGGAAA
1_R	TACGGTAGCAGAGACTTGGTCTCCGTACCTGTCCAGTCCG
2_F	ACACTGACGACATGGTTCTACATCTTTCAGGGCAATTAAGCATT
2_R	TACGGTAGCAGAGACTTGGTCTACAACCTACCTTTAAACTAGACTCA
3_F	ACACTGACGACATGGTTCTACAGTACAATTGGACCATGGCCA
3_R	TACGGTAGCAGAGACTTGGTCTAGTGCAGAGGTATTACTACAACCT
4_F	ACACTGACGACATGGTTCTACACAGGATGCCATTAAATGCTACTT
4_R	TACGGTAGCAGAGACTTGGTCTTCTGGGGAAATATGTGGCTTT
5_F	ACACTGACGACATGGTTCTACAATGCTGTGTACATCCTCCA
5_R	TACGGTAGCAGAGACTTGGTCTACTTGTTTGCTACCTCTACTCCT
6_F	ACACTGACGACATGGTTCTACATGACAGATGAGACCAACAGGA
6_R	TACGGTAGCAGAGACTTGGTCTCAGGCTGAGAGACGCTAGG
7_F	ACACTGACGACATGGTTCTACACTGCCTACAACTCAGTCTCTG
7_R	TACGGTAGCAGAGACTTGGTCTCAGAAAAGGGTCCATTGGCC
8_F	ACACTGACGACATGGTTCTACATAACCGCACAAACCTGACCA
8_R	TACGGTAGCAGAGACTTGGTCTTCTCTCAAAGTGATAAAACCCAGT

9_F	ACACTGACGACATGGTTCTACACGACCTCTCTCTTCCACTGG
9_R	TACGGTAGCAGAGACTTGGTCTAATGCCTTGTTGTCCACCTG
10_F	ACACTGACGACATGGTTCTACAGGCTGCTCTCAATCACCTCT
10_R	TACGGTAGCAGAGACTTGGTCTGCAGTGCTGTTAGGTGTCTC
11_F	ACACTGACGACATGGTTCTACAGAGACACCTAACAGCACTGC
11_R	TACGGTAGCAGAGACTTGGTCTTCCCATCAACAAGGCAGAGA
12_F	ACACTGACGACATGGTTCTACAGCCATTTCAACAGCAACACC
12_R	TACGGTAGCAGAGACTTGGTCTGGGGCTCTGAGATTCTTCCA
13_F	ACACTGACGACATGGTTCTACAGGAAGAATCTCAGAGCCCCA
13_R	TACGGTAGCAGAGACTTGGTCTCACACTAACCTGCATGCCTT
14_F	ACACTGACGACATGGTTCTACAATGGACTTGTGCAAATGCCTAGTAA
14_R	TACGGTAGCAGAGACTTGGTCTTGGAGGTGGACATTTATCCAACAA
15_F	ACACTGACGACATGGTTCTACATGTTTTCTGAGATCTAACCACA
15_R	TACGGTAGCAGAGACTTGGTCTCAAGGCCACGTATTACTGTAACA
16_F	ACACTGACGACATGGTTCTACATGTAGAACAATAACTAGACTGCT
16_R	TACGGTAGCAGAGACTTGGTCTACACAGTATTAGAAACATGCCTTTT
17_F	ACACTGACGACATGGTTCTACAGTTCTGGGAGGAGGAGGAAA
17_R	TACGGTAGCAGAGACTTGGTCTAGCACAGGATAACTCTTTGCA
18_F	ACACTGACGACATGGTTCTACAAAATTCCACAGGTATTTGTAGC
18_R	TACGGTAGCAGAGACTTGGTCTCCAACATGGCTTAGAAGATTTCC
19_F	ACACTGACGACATGGTTCTACAGTGAAGTTGCAGCTACATGA
19_R	TACGGTAGCAGAGACTTGGTCTTGCTCCCTGGAACCTTTCATG
20_F	ACACTGACGACATGGTTCTACAACCGTGTGCTAACCAATTGC
20_R	TACGGTAGCAGAGACTTGGTCTACAAACCATTACAGTCACCT
21_F	ACACTGACGACATGGTTCTACAGGAGCTTCTTAATGTAGTTGATCC
21_R	TACGGTAGCAGAGACTTGGTCTGCTGAATAAACCTATACACTGGAAC
22_F	ACACTGACGACATGGTTCTACACTAATGGGTTCTTGGTGGCC

22_R	TACGGTAGCAGAGACTTGGTCTTGAACCCAATGAACAGTGCC
23_F	ACACTGACGACATGGTTCTACAGCTGGTCACAAATAATTTCTCCC
23_R	TACGGTAGCAGAGACTTGGTCTTGAGCTGGTTCTTCTTTGTCC
24_F	ACACTGACGACATGGTTCTACAACCTTGAAAACCTTTGTGGTGCT
24_R	TACGGTAGCAGAGACTTGGTCTCACTGCTGCTTCATAACCCA

Journal Pre-proof

Table S4. Primers used for amplification of area around KRAS codons 12 and 13 as well as the mimic gene PITPNM2. Mimic amplicons contained the sequence context of KRAS codons 12 and 13, including 5 preceding and 3 subsequent nucleotides (total synchronous sequence: GAGCTGGTGGC GTA) at the same position within the amplicon.

Number = amplicon number, F = forward primer, R = reverse primer. Sequence includes Fluidigm CS adapters.

Primer	Sequence (5' -> 3')
KRAS_1_F	ACACTGACGACATGGTTCTACATAAGGCCTGCTGAAAATGACT
KRAS_1_R	TACGGTAGCAGAGACTTGGTCTATGGTCCTGCACCAGTAATATG
MIMIC_1_F	ACACTGACGACATGGTTCTACATAGCACCCAGCCAGCTTG
MIMIC_1_R	TACGGTAGCAGAGACTTGGTCTATGACCACCCATGAAATATGAGCT
KRAS_2_F	ACACTGACGACATGGTTCTACAGGTGGAGTATTTGATAGTGTATTAAC C
KRAS_2_R	TACGGTAGCAGAGACTTGGTCTTAGCTGTATCGTCAAGGCAC
MIMIC_2_F	ACACTGACGACATGGTTCTACACCTGCTGTTCCCTACAAAGCTG
MIMIC_2_R	TACGGTAGCAGAGACTTGGTCTAGGCTTCTCCCGTCTAAGGA

Table S5 PCR reaction components. For KDM6A, pre-amplification was performed in multiplex groups (group 1: primers 1,4,7...group 2: 2,5,8... group 3: 3,6,9...). For KRAS, each sample was amplified in two independent duplex PCR reactions containing a KRAS and corresponding mimic primer pair.

Gene	Primers	dNTPs	5X Phusion® HF Reaction Buffer (New England BioLabs),	Phusion® High-Fidelity DNA Polymerase	Water
KDM6A	1 μ M	0.5 mM	5 μ l	1 U	To 25 μ l
KRAS	1.2 μ M pair 1 0.8 μ M pair 2	0.5 mM	5 μ l	1 U	To 25 μ l

Table S6 PCR cycling conditions used for amplification of KDM6A and KRAS. PCR was followed by ExoSAP-IT enzyme treatment (2 μ l of enzyme for 5 μ l of sample, ThermoFisher) at 37 °C for 15 min and 15 min inactivation at 80 °C and 1:10 dilution in DNA Suspension Buffer (Teknova). For KDM6A, samples were further amplified using the Fluidigm Access Array™ according to the supplier's protocol.

Step	Temperature	Time	Cycles
Initial denaturation	95 °C	2 min	1
Denaturation	95 °C	10 s	35
Annealing	60 °C	10 s	
Elongation	72 °C	15 s	
Final Elongation	72 °C	5 min	1

Table S7. Summary of mutations identified in KDM6A⁺ patches.

Ref = nucleotide in reference genome, freq = frequency, Alt = alternative nucleotide -> this is the mutation, Change = predicted consequence of the mutation. Frequencies derived from frequency of mutant reads in samples. Of note, the mutation found in intron 18 was present in two independent patches. Furthermore, the mutations S1154* and W1193* have previously been found in cancer samples (COSMIC database).

Gender	Sample	Genomic coordinate	Exon	Ref	Alt	Alt freq	Maximum alt freq	Change
Male	1A	X:45078391	intron 18	A	G	85.8	100	Intronic
Male	1B	X:45078391	intron 18	A	G	72.9	100	Intronic
Male	2A	X:45078391	intron 18	A	G	82.9	100	Intronic
Male	2B	X:45078391	intron 18	A	G	85.3	100	Intronic
Male	3A	X:45085892	24	C	A	51	100	S1154>STOP
Male	3B	X:45085892	24	C	A	0	100	N/A
female	4A	X: 45089773	25	G	A	15.8	50	W1193>STOP
female	4B	X: 45089773	25	G	A	10.4	50	W1193>STOP

Table S8. Sequence context used to extract mutant reads from sequencing data. For each variant, the mutant allele frequency was calculated by dividing by the total read number.

Context	Nucleotide change	Amino acid change
GAGCTGGTGGCGTA	WT	WT
GAGCTGATGGCGTA	G>A	G12D
GAGCTGCTGGCGTA	G>C	G12A
GAGCTGTTGGCGTA	G>T	G12V
GAGCTAGTGGCGTA	G>A	G12S
GAGCTCGTGGCGTA	G>C	G12R
GAGCTTGTGGCGTA	G>T	G12C
GAGCTGGTGACGTA	G>A	G13D
GAGCTGGTGCCGTA	G>C	G13A
GAGCTGGTGTCGTA	G>T	G13V
GAGCTGGTAGCGTA	G>A	G13S
GAGCTGGTCGCGTA	G>C	G13R
GAGCTGGTTGCGTA	G>T	G13C
GAGCTGGAGGCGTA	T>A	WT
GAGCTGGCGGCGTA	T>C	WT
GAGCTGGGGGCGTA	T>G	WT
GAGCTGGTGGAGTA	G>T	WT
GAGCTGGTGGGGTA	G>C	WT
GAGCTGGTGGTGTA	T>C	WT

Mathematical Background

Calculating the crypt fusion rate

For individual crypts, fusion/fission events occur at a rate ρ and have a duration $\Delta\tau$. If we take a snapshot of a piece of tissue at a time t_0 we see all fusion/fission events that occurred in the window $[t_0 - \Delta\tau, t_0]$. Calculating the average number of events per crypt, X , in a time $\Delta\tau$ over many snapshots is the same as calculating the probability of an event for a single crypt in the window $\Delta\tau$ (as we can only have a single event in any time window equal to the event duration). The number of events for a single crypt follows a Poisson distribution,

$$X_1 \sim \text{Poi}(\rho\Delta\tau). \quad (1)$$

We want to observe events on the edge of mutant patches such that we can differentiate fission events from fusion events. For a patch with edge length N (that is, N crypts define the patch perimeter, each with at least one wild-type crypt as a neighbour), the number of crypts undergoing fusion or fission is distributed as

$$X_N \sim \text{Poi}(N\rho\Delta\tau). \quad (2)$$

For a given patch with edge length N , then, the probability of zero events in a window $\Delta\tau$ is

$$p\{X_N = 0\} = e^{-N\rho\Delta\tau} \sim 1 - N\rho\Delta\tau + \mathcal{O}(N^2\rho^2\Delta\tau^2), \quad (3)$$

where $N\rho$ is considered small compared with $\Delta\tau$ such that we may define a parameter $\varepsilon = N\rho\Delta\tau$ where $\varepsilon \ll 1$. Correspondingly, the probability of seeing at least one event in a window $\Delta\tau$ is

$$p\{X_N \geq 1\} = 1 - p_0 \sim N\rho\Delta\tau + \mathcal{O}(\varepsilon^2). \quad (4)$$

This equation can be applied to either fusion events or fission events separately by changing the event rate ρ to ρ_{fu} or ρ_{fi} , the event rates of fusion and fission, respectively, assuming that the event duration $\Delta\tau$ is approximately equal for fission and fusion.

Calculating the fusion rate

Let the number of partially mutant (partial) and fully mutant (monoclonal) FUF1 events observed on the edge of mutant patches be n_p (termed M/W in main text) and n_m (termed M/M in main text), respectively. These numbers are combined

over many different mutant patches and tissue samples, with a total patch edge length of N . To calculate the fusion rate ρ_{fu} given the fission rate ρ_{fi} , we use the following observations and assumptions:

1. All fission events are monoclonal.
2. Not all monoclonal events are fissions.
3. All partial events are fusions.
4. Not all fusions are partials.

The first and third assumptions stem from the belief that the timescale over which monoclonal conversion occurs in a crypt is short compared to the time between fusion/fission events. The second and fourth observations are alternative statements of the fact that fusion at the patch edge can happen inwards: a mutant crypt on the patch edge can fuse with a mutant crypt within the patch, hence creating a monoclonal event. We define the parameter χ to be the proportion of fusion events that are M/M. Then the ratio n_p/n_m may be written as

$$\frac{n_p}{n_m} = \frac{2n_{fu}(1 - \chi)}{n_{fi} + 2n_{fu}\chi}, \quad (5)$$

where n_{fu} and n_{fi} are the number of fusion and fission events, respectively. The factor of two accompanying each instance of n_{fu} in (5) comes from the hypothesis that fusion can be initiated by either of the participating crypts, so the number of events associated with the fusion rate of any individual crypt should be half the number observed. We do not know n_{fu} and n_{fi} a priori, however.

We may recast the probability $p\{X_N \geq 1\}$ from (4) as the number of observed events over sample size, n_{events}/N , for fusion and fission, we get

$$\frac{n_{fu}}{N} \sim N\rho_{fu}\Delta\tau, \quad (6)$$

and

$$\frac{n_{fi}}{N} \sim N\rho_{fi}\Delta\tau, \quad (7)$$

where we have assumed the duration of a fusion event is approximately equal to that of a fission event. Thus, we find the approximate equivalence

$$\frac{n_{fi}}{n_{fu}} \sim \frac{\rho_{fi}}{\rho_{fu}} \quad (8)$$

between the ratios of numbers and rates of events. Using this, we may rewrite (5) as

$$\frac{n_p}{n_m} = \frac{2(1 - \chi)}{\frac{\rho_{fi}}{\rho_{fu}} + 2\chi}, \quad (9)$$

and subsequently find an expression for the fusion rate:

$$\rho_{\text{fu}} = \frac{\rho_{\text{fi}}}{2 \frac{n_m}{n_p} (1 - \chi) - 2\chi}. \quad (10)$$

The simplest model for the parameter χ is to assume unbiased (isotropic) fusion, such that the proportion of fusions that are monoclonal is simply

$$\chi = \frac{N_t - N_w}{N_t}, \quad (11)$$

where N_t and N_w are the total number of neighbours and number of wild-type neighbours of a given fusion event, respectively. To get a bulk measure of χ for each clonal mark, N_t and N_w were averaged over all observed M/M events.

Diffusion model of tissue reorganisation

Below we lay out the theoretical framework and statistical methods used for understanding tissue rearrangement due to clonal expansion in the gut as a diffusion process.

Parameterisation and derivation

We will approach the idea of crypt packing by defining a quantity γ that represents the local stromal fraction of the tissue (we will also refer to this as the “white space” fraction) - then, the crypt area per unit area of mucosa is given by $1-\gamma$. If you look at a small region of tissue in cross-section, γ is the fraction of that region that is taken up by stroma rather than epithelial cells (i.e. that fraction that is not part of a crypt). It is useful to think of the crypts as a density that is moving in the “free space” of the stroma. Then, we can define another quantity ψ that represents this density in such a way that $\psi \equiv 1/\gamma$. This density ψ tells us the number of units of area we would need to observe to see one unit of area of white space. This is a convenient definition as it allows the density to be expressed as a function unbounded in the positive real numbers whereas the local crypt fraction $1-\gamma$ is bounded in $[0,1]$.

In intestinal tissue, we assume there is a patient-specific homeostatic degree of crypt packing that can be represented by “ambient” values γ_a , ψ_a for the stromal fraction and crypt density, respectively. Near to a region of clonal expansion (a fission-driven mass source), the tissue is perturbed and the crypt density is altered such that

$$\psi(\mathbf{r}, t) = \psi_a + \tilde{\psi}(\mathbf{r}, t), \quad (12)$$

where the spatiotemporal variation in the crypt density is contained in the perturbation term $\tilde{\psi}(r, t)$. By centring our polar coordinate system $r = (r, \theta)$ at the initiation point of the clonal expansion we can state our far-field condition: $\tilde{\psi} \rightarrow 0$ as $r \rightarrow \infty$, meaning that we expect the tissue to remain in its ambient structure far from any perturbation. We choose to model the density perturbation $\tilde{\psi}$ as undergoing diffusive dynamics governed by the 2D diffusion equation

$$\frac{\partial \tilde{\psi}}{\partial t} = \nabla \cdot (D \nabla \tilde{\psi}), \quad (13)$$

where the coefficient of diffusion D quantifies the speed with which the tissue can react to new mass being created by fission by rearranging to accommodate it. We assume D is isotropic and homogeneous such that (13) simplifies to

$$\frac{\partial \tilde{\psi}}{\partial t} = D \nabla^2 \tilde{\psi}. \quad (14)$$

We want to use (14) to understand the dynamical process underlying observed patches of clonally-expanded mutant tissue; we note that while we know the initial size (a single crypt) and the current size (n mutant crypts) of the clonal expansion we do not know the total age of the mutant patch nor when the individual fission events driving the expansion occurred. We first show how to solve the system in the case of an instantaneous injection of mass at time $t=0$ before showing how to use this solution to build a more realistic model of dynamic fission events.

We approach (14) by taking a spatial Fourier transform such that the transformed density

$$\hat{\psi}(k_x, k_y, t) = \int_{-\infty}^{\infty} \int_{-\infty}^{\infty} \tilde{\psi}(x, y, t) e^{-ik_x x} e^{-ik_y y} dx dy, \quad (17)$$

is governed by

$$\frac{\partial \hat{\psi}}{\partial t} = -D(k_x^2 + k_y^2) \hat{\psi}, \quad (18)$$

where $k = (k_x, k_y)$ is the wave vector in a Cartesian coordinate system (x, y) with its origin at the initiation point of clonal expansion. Equation (18) can be solved by integrating with respect to time and applying the initial condition $\hat{\psi}(0) = F [M \delta(r)]$, where M is the extra crypt area introduced by the injection of mass. We find

$$\hat{\psi}(\mathbf{k}, t) = M e^{-D|\mathbf{k}|^2 t}. \quad (19)$$

We proceed by inverting the Fourier transform to find the crypt density in terms of the spatial coordinates x and y . First, note that the inversion can be separated as follows:

$$\tilde{\psi}(x, y, t) = M \left(\frac{1}{2\pi} \right)^2 \left(\int_{-\infty}^{\infty} e^{-Dk_x^2 t + ik_x x} dk_x \right) \left(\int_{-\infty}^{\infty} e^{-Dk_y^2 t + ik_y y} dk_y \right). \quad (20)$$

Completing the square in the exponent of the x integrand we can recast the integral as

$$\int_{-\infty}^{\infty} e^{-Dk_x^2 t + ik_x x} dk_x = e^{-\frac{x^2}{4Dt}} \int_{u(-\infty)}^{u(\infty)} e^{-Dtu^2} du, \quad (21)$$

where $u = k_x + ix/2Dt$ and the integral on the right hand side of (21) can be evaluated:

$$\int_{u(-\infty)}^{u(\infty)} e^{-Dtu^2} du = \sqrt{\frac{\pi}{Dt}}. \quad (22)$$

By symmetry the full solution is found to be

$$\tilde{\psi}(\mathbf{r}, t) = \frac{M}{4\pi Dt} e^{-\frac{r^2}{4Dt}}, \quad (23)$$

where $r^2 = x^2 + y^2$ is the radial distance from the centre of the clone. The stromal fraction near to a mutant patch may be expressed using (23) as

$$\gamma(\mathbf{r}, t) = \frac{1}{\psi_a + \tilde{\psi}(\mathbf{r}, t)} = \frac{\gamma_a}{1 + \frac{M\gamma_a}{4\pi Dt} E_d(r)}, \quad (24)$$

where for notational ease we have defined the exponential function

$$E_d(x) = e^{-\frac{x^2}{4Dt}}. \quad (25)$$

Diffusion with a stochastically-firing point source

To investigate the temporal aspect of clonal expansion the diffusion model was extended to accommodate growth over time due to stochastic crypt fission at the patch centre. One can intuitively think of this as overlaying identical diffusion processes in space with different initiation times. Mathematically this can be achieved by breaking the solution space into chunks separated by each fission event time. If the Fourier-space density $\hat{\psi}_i(t)$ is the solution of (18) in a time

interval $[t_0, t_1)$, achieving a value $\psi_1(t_1)$ at the end of this period, then the solution $\psi_2(t)$ for the next period $[t_1, t_2)$, where a fission event occurs at t_1 , is found by solving (18) with the initial condition $\psi_2(t_1) = \psi_1(t_1) + F[a_m \delta(r)]$ where a_m is the area of the new mutant crypt. Performing this process iteratively produces, with initial area perturbation $A_0 = a_m - a_w$ generated by the mutational hit, the compound diffusion solution

$$\hat{\psi}(\mathbf{k}, t) = A_0 e^{-D|\mathbf{k}|^2 t} + \sum_{i=1}^{n_f} a_m e^{-D|\mathbf{k}|^2 \tau_i}, \quad (26)$$

where $\tau_i = t - \sum_{j=1}^i t_j$ for $i \in [1, n_f]$ with t_k the event times of n_f crypt fissions. Inverting the Fourier transform gives the full spatial solution for the density perturbation:

$$\tilde{\psi}(r, t) = \frac{A_0}{4\pi D t} e^{-\frac{r^2}{4Dt}} + \sum_{i=1}^{n_f} \frac{a_m}{4\pi D \tau_i} e^{-\frac{r^2}{4D\tau_i}}. \quad (27)$$

The formulation (27) supposes that we do not know how large a mutant patch will grow in a given amount of time t , but that we can generate fission times t_k and take those events with $t_k < t$ to define our solution up to the desired time t . We can so generate fission times given a fission rate ρ by assuming exponential waiting times (between events generated by a Poisson process) and using

$$t_n = -\frac{\ln(1 - u_{01})}{\rho n}, \quad (28)$$

where n is the current patch size, t_n is the time of the n th fission event and u_{01} is a random draw from the unit uniform distribution $U(0, 1)$. This method can also be used to generate mutation times using the mutation rate α (9.3×10^{-7} for KDM6A; 1.7×10^{-6} for STAG2), the monoclonal accumulation rate ΔC (6.0×10^{-6} for KDM6A; 2.1×10^{-5} for STAG2), the number of stem cells per crypt undergoing neutral drift N_{stem} (7) and the total number of crypt in the gut N_{crypts} ($\sim 10 \times 10^6$). So given a mutation that confers an expansion bias in terms of an increased fission rate over wild type epithelium, we can simulate the distribution of theoretical clonal expansion dynamics by generating a mutation time and a sequence of fission event times using (28) and calculate the evolution of the packing density over time using (27). The full theoretical white space fraction is given by inserting (28) into

$$\gamma(\mathbf{r}, t) = \frac{1}{1/\gamma_a + \tilde{\psi}(r, t)}. \quad (29)$$

Comparing theory to experiment

While (29) fully describes the theoretical diffusion process we posit as an explanation for the alleviation of crypt packing in the gut in lieu of mass crypt fusion, we must do more work to form a quantity suitable for comparison with experimental measurements. The data we have are measurements of the total

area of patches of n crypts (including their “share” of the stromal space bordering the patch) and the area of the individual crypts making up each patch. Thus we can calculate the total white space Γ in a patch by subtracting the summed crypt areas from the total patch area. We can get a comparable theoretical quantity Γ_{th} by integrating the theoretical white space fraction (29) over the area A occupied by a patch P of n crypts:

$$\Gamma_{\text{th}} = \iint_{P_A} \gamma(\mathbf{r}, t) d\mathbf{A}. \quad (30)$$

The integral (30) is non-trivial for an arbitrary patch geometry. To simplify the problem we transform the geometry of the patch into a subsector of a circle centred at the coordinate origin while conserving the patch area.

To do this, three quantities must be found: the angle θ_s subtended by the subsector, its inner radius R_{in} and its outer radius R_{out} . To find θ_s the distance d between the centroid of the patch and the centroid of the mutant source patch (the coordinate origin) is first calculated. Then,

$$\theta_s = \begin{cases} 2 \operatorname{atan} \frac{R_w}{d}, & \text{if } d > 0, \\ 2\pi, & \text{if } d = 0, \end{cases} \quad (31)$$

where R_w is the radius of the patch being transformed (and where “radius” means the radius that would produce the area of the patch if the patch were a circle). Now, the area of a subsector is given by

$$A_{\text{sec}} = \frac{\theta_s}{2} (R_{\text{out}}^2 - R_{\text{in}}^2), \quad (32)$$

and area conservation enforces the equality $A_{\text{sec}} = \pi R_w^2$. If $d > 0$ we may use the approximation $R_{\text{in}} = d - cR_w$ and $R_{\text{out}} = d + cR_w$ for some small $c > 0$ and substitute into (32) to find

$$c = \frac{\pi R_w}{2d\theta_s}. \quad (33)$$

Using (31) to fix the value for R in as

$$R_{\text{in}} = \begin{cases} d - \frac{\pi R_w^2}{2d\theta_s}, & \text{if } d > 0, \\ 0, & \text{if } d = 0, \end{cases} \quad (34)$$

we may then invoke area conservation once more to find

$$R_{\text{out}} = \sqrt{R_{\text{in}}^2 + \frac{2\pi R_w^2}{\theta_s}}. \quad (35)$$

We can now approximate the integral (30) with

$$\Gamma_{th} \approx \int_0^{\theta_s} \int_{R_{in}}^{R_{out}} \gamma(\mathbf{r}, t) r dr d\theta, \quad (36)$$

which we evaluate numerically. The theoretical value for the total patch white space defined in (36) can then be used to fit the diffusion model given a data set of patch measurements.

Statistical model for inferring the diffusion coefficient

To infer the parameters defining the tissue-intrinsic diffusion process we define the likelihood as

$$\Gamma^{(pq)} \sim \mathcal{N} \left(\Gamma_{th}^{(pq)}(D, \gamma_a^{(p)}, t^{(p)}, M^{(p)}, L^{(pq)}), \sigma_\Gamma \right), \quad (37)$$

where $\Gamma^{(pq)}$ and Γ_{th} are respectively the observed and theoretical total white space in patch q of the neighbourhood of the p th mutant patch (as defined in (36)). The parameters defining $\Gamma_{th}^{(pq)}$ are the single tissue-intrinsic diffusion coefficient D , the ambient stromal fraction γ_a , sequence of event times (mutation and subsequent fissions) $t^{(p)}$, and input areas $M^{(p)}$ (mutant and wild type crypt areas a_m, a_w) of the p th mutant patch, and the location parameters $L^{(pq)}$ which define the transformed inner and outer radii and angle subtended by the patch q of the neighbourhood of the p th mutant patch. We simultaneously infer the coefficient of diffusion D and the local ambient white spaces γ_a .

We use a hierarchical model to constrain γ_a such that each value is drawn from a population distribution

$$\gamma_a^{(p)} \sim \text{Beta}(\alpha_{\text{pop}}, \beta_{\text{pop}}), \quad (38)$$

with hyperpriors

$$\alpha_{\text{pop}} \sim \text{Gamma}(10, 1), \quad \beta_{\text{pop}} \sim \text{Gamma}(10, 1), \quad (39)$$

chosen to be uninformative around an unbiased mean value $\gamma_a^{\text{pop}} = 1/2$. Standard normal distributions bounded to the positive real line are used as prior distributions for the diffusion coefficient and the standard deviation σ_Γ about the theoretical total white space,

$$D \sim \mathcal{N}^{(+)}(0, 1), \quad \sigma_\Gamma \sim \mathcal{N}^{(+)}(0, 1). \quad (40)$$

Inference for the full model defined by eqs. (37)–(40) was performed by MCMC sampling using the Stan probabilistic programming language. The sequence of

event times $t^{(p)}$ an input to the model, generated using (28). For each clone 1000 potential sequences (trajectories) were generated and the inference was run 250 times with a random sample of the potential trajectories used each time. This allowed us to be sure that the resulting model parameters accounted for the large variation in the temporal development of the patches due to the stochastic nature of the mutational hit and the fissions themselves. From the resulting distributions, “most likely” trajectories were selected by fixing the diffusion coefficient D and ambient stromal fraction of each neighbourhood γ_a to their median values and evaluating the likelihood of the data under the model for each of the 1000 potential trajectories per clone. For each clone, the 25 most likely trajectories were selected and averaged to give an approximation of the likely age of each patch.

To test whether we are justified in imposing the form of a diffusion process on the data we performed the inference above for a null model wherein each neighbourhood around a mutant clone would be explained by a constant stromal fraction. This involved inferring γ_a for each patch and setting $\gamma(r) = \gamma_a$, and then calculating $\Gamma_{null}^{(pq)}$ and using it in (37) to evaluate the likelihood of the data under the null model. To compare the diffusion model to the null model, the full set of 1000 potential trajectories for each clone were used as input to calculate a distribution of model likelihoods given the inferred population median diffusion coefficient and the per-clone median ambient stromal fraction. The results show that there is more evidence to support the hypothesis of identifying the mutant patch as the source of clonal expansion causing a diffusion-like radial dependence in the local stromal fraction.

Polyp initiation

Here we quantify when the biological process might break down due to physical constraints on crypt density. In the theoretical scheme defined above, as crypt density $\psi \rightarrow \infty$ the stromal fraction $\gamma \rightarrow 0$. Below some local value of γ , there will not be enough space for a crypt to fission. We posit that this may be a mechanism for outward growth, or polyp formation. A useful threshold to set on the available white space can be borrowed from the mathematics of optimal packing; identical circles may be optimally hexagonally packed to fill a fraction $\pi/\sqrt{12}$ of the space. Thus, we set the lower bound on the stromal fraction $\gamma_b = 1 - \pi/\sqrt{12}$. A mutant patch that creates mass through fission at such a rate that the tissue-intrinsic diffusion cannot act to fully accommodate new crypts will have a decrease over time of the available stromal fraction as the patch grows exponentially. We claim that if the available white space dips below γ_b then there the patch has a finite chance of initiating outgrowth.

We can quantify this more concretely by simulating an ensemble of mutant patches with a given fission rate. At each time point we can find the radial extent r_i of each instance i of the mutant patch by constraining the integral over the non-stromal fraction to equal the total area of the n_i mutant crypts in the patch,

$$\int_0^{2\pi} \int_0^{r_i} (1 - \gamma(r)) r dr d\theta = n_i a_m, \quad (41)$$

where the mutant crypts have area a_m . To approximate the effective local stromal fraction throughout the patch, the cumulative average of $\gamma(r)$, $\bar{\gamma}(r)$ is calculated starting from the patch centre $r = 0$. For each patch area πr_i^2 we may then calculate the fraction p_f of this area for which $\bar{\gamma} < \gamma_b$. This gives us an idea of the portion of the patch that is at risk of initiating a polyp with the next fission event. Averaging p_f over the whole ensemble, we find an estimate for the probability of a clonal expansion developing into a polyp for a given time t after the initial mutation.

Journal Pre-proof